CONCEPTUAL MINE DESIGN AND CHALLENGES OF MINING ASSISTED HEAVY OIL PRODUCTION OF BATI RAMAN OIL FIELD

A THESIS SUBMITTED TO
THE GRADUATE SCHOOL OF NATURAL AND APPLIED SCIENCES
OF
MIDDLE EAST TECHNICAL UNIVERSITY

BY

VOLKAN SATAR

IN PARTIAL FULFILLMENT OF THE REQUIREMENTS
FOR
THE DEGREE OF MASTER OF SCIENCE
IN
MINING ENGINEERING

JUNE 2023

Approval of the thesis:

CONCEPTUAL MINE DESIGN AND CHALLENGES OF MINING ASSISTED HEAVY OIL PRODUCTION OF BATI RAMAN OIL FIELD

submitted by **VOLKAN SATAR** in partial fulfillment of the requirements for the degree of **Master of Science** i**n Mining Engineering, Middle East Technical University** by,

Prof. Dr. Halil Kalıpçılar
Dean, Graduate School of **Natural and Applied Sciences** _____

Prof. Dr. Naci Emre Altun
Head of the Department, **Mining Engineering Dept.** _____

Prof. Dr. Hasan Öztürk
Supervisor, Mining Engineering**, Mining Engineering Dept.** _____

Examining Committee Members:

Assoc. Prof. Dr. Onur Gölbaşı
Mining Engineering Dept., METU _____

Prof. Dr. Hasan Öztürk
Mining Engineering Dept., METU _____

Prof. Dr. Güzin Gülsev Uyar Aksoy
Mining Engineering Dept., Hacettepe University _____

Date: 19.06.2023

I hereby declare that all information in this document has been obtained and presented in accordance with academic rules and ethical conduct. I also declare that, as required by these rules and conduct, I have fully cited and referenced all material and results that are not original to this work.

Name Last name : Volkan Satar

Signature :

ABSTRACT

CONCEPTUAL MINE DESIGN AND CHALLENGES OF MINING ASSISTED HEAVY OIL PRODUCTION OF BATI RAMAN OIL FIELD

Satar, Volkan
Master of Science, Mining Engineering
Supervisor : Prof. Dr. Hasan Öztürk

June 2023, 164 pages

Bati Raman Oil Field is Turkey's largest oil reserve (1.85 billion barrels). It is situated at an average depth of 1450 m, producing 12° API heavy oil (very viscous) from a 60m thick calcareous reservoir rock. The recovery by primary oil production method and even with different Enhanced Oil Recovery (EOR) techniques (water flooding, steam flooding, and CO_2 injection) has been limited to 9%. One of the plans for the production of Bati Raman oil is to use Mining-Assisted Heavy oil Production (MAHOP). In this method, multiple shafts and declines are excavated from the surface to the reservoir and a series of excavations (galleries) continue along the bottom of the reservoir. Fan-shaped steam injection and production holes are drilled in the reservoir from the crown of the galleries for the use of conventional Steam-Assisted Gravity Drainage (SAGD) for oil production. This research aims to design the mine conceptually using the Micromine Software package, evaluate the challenges; such as tunneling practice, steam supply, ventilation, and tailing disposal, and create an economic model of the mine. For a production rate of 250K barrels of oil /day, the NPV and IRR of the project are found to be 6.5 billion $ and 23%, respectively. Operating cost is estimated to be 32.32 $ per barrel of oil while initial capital investment is estimated to be 5.36 B $. The sensitivity analysis showed

that the project is most sensitive to the oil price which is assumed to be 70 $ per barrel oil for the base case.

Keywords: Heavy Oil, Mining, Tunnelling, Ventilation, Economic Model

ÖZ

BATI RAMAN PETROL SAHASININ MADENCİLİĞE DAYALI AĞIR PETROL ÜRETİMİNİN KAVRAMSAL MADEN TASARIMI VE ZORLUKLARI

Satar, Volkan
Yüksek Lisans, Maden Mühendisliği
Tez Yöneticisi: Prof. Dr. Hasan Öztürk

Haziran 2023, 164 sayfa

Bati Raman Petrol Sahası, Türkiye'nin en büyük petrol rezervidir (1,85 milyar varil). Ortalama 1450 m derinlikte yer alır ve 60 m kalınlığındaki kalkerli bir rezervuar kayasından 12 ° API ağır petrol (çok viskoz) üretir. Birincil petrol üretim yöntemiyle ve hatta farklı Geliştirilmiş Petrol Geri Kazanımı (PGK) teknikleriyle (su basması, buharla taşma ve CO_2 enjeksiyonu) geri kazanım % 9 ile sınırlıdır. Bati Raman petrolünün üretim planlarından biri de Madencilik Destekli Ağır Petrol Üretimi (MDAPÜ) kullanmaktır. Bu yöntemde, yüzeyden rezervuara çok sayıda kuyu ve desandre kazılır ve rezervuarın dibinde bir dizi kazı (galeri) devam eder. Petrol üretimi için geleneksel Buhar Destekli Yerçekimi Drenajının (BDYD) kullanılması için rezervuarda galerilerin tepesinden fan şeklindeki buhar enjeksiyonu ve üretim delikleri açılır. Bu tez, madeni Micromine Yazılım paketini kullanarak kavramsal olarak tasarlamayı, tünel açma uygulaması, buhar temini, havalandırma ve atık bertarafı gibi konularda zorlukları değerlendirmeyi ve madenin ekonomik modelini oluşturmayı amaçlamaktadır. 250.000 varil petrol/gün üretim oranı için projenin NBD'si 24 milyar $ ve IRR'si %23 olarak bulunmuştur. İşletme maliyetinin varil petrol başına 32.32 $, ilk sermaye yatırımının ise 5,36 milyar $ olacağı tahmin

edilmektedir. Duyarlılık analizi, projenin baz durum için varil petrol başına 70 $ olduğu varsayılan petrol fiyatına en duyarlı olduğunu göstermiştir.

Anahtar Kelimeler: Ağır Petrol, Madencilik, Tünel Açma, Havalandırma, Ekonomik Model

To My Family

ACKNOWLEDGMENTS

The author wishes to express his deepest gratitude to his supervisor Prof. Dr. Hasan Öztürk for his guidance, advice, criticism, encouragement, and insight throughout the research.

The author would also like to thank Prof. Dr. Güzin Gülsev Uyar Aksoy and Assoc. Prof. Dr. Onur Gölbaşı for their suggestions and comments.

TABLE OF CONTENTS

LIST OF TABLES

TABLES

LIST OF FIGURES

FIGURES

LIST OF ABBREVIATIONS

ABBREVIATIONS

AOSTRA – The Alberta Oil Sands Technology and Research Authority

BAC – Bulk Air Cooling

CAPEX – Capital Expenditures

D&B – Drilling and Blasting

EOR – Enhanced Oil Recovery

IRR – Internal Rate of Return

MAHOP – Mining Assisted Heavy Oil Production

NPV – Net Present Value

OPEX – Operational Expenditures

SAGD – Steam-Assisted Gravity Drainage

SCF – Standard Cubic Feet

SOR – Steam Oil Ratio

TBM – Tunnel Boring Machine

TPAO – Türkiye Petrolleri Anonim Ortaklığı (Turkish Petroleum Corporation)

UCS – Uniaxial Compressive Strength

WOR – Water Oil Ratio

CHAPTER 1

INTRODUCTION

Energy is one of the greatest needs that turned out to be for humankind with the development of technologies in every industry, and the production of energy in history mostly started with non-renewable energy sources such as fossil fuels. However, today, the trend of using renewable energy increased its popularity, yet the energy demand in the world increased gradually. Petroleum is one of the non-renewable energy sources which is close to its end, especially with the conventional oil production methods. Therefore, the production of heavy oil or depleted Oil Fields with Enhanced Oil Recovery (EOR) methods has crucial importance for energy production. However, because of the depth, geologic, and reservoir properties, some of the oil reservoirs cannot be produced by even EOR techniques. Production of petroleum from these types of reservoirs requires a multidisciplinary solution such as the implementation of underground mining for oil production. This type of approach to oil production started at the beginning of the 20^{th} century. However, the application of mining in the oil industry was not the first option even today.

The importance of oil production is undeniable not only in terms of energy demand but also in economic benefits. Countries like Türkiye, which cannot produce a sufficient amount of petroleum from its resources are heavily dependent on foreign contraries in terms of fuel oil. Therefore, the importance of the production of petroleum from depleted or heavy oil such as the Bati Raman Oil Field is even more than anticipated. Bati Raman Oil Field is Türkiye's largest oil reservoir yet the production of oil did not reach an acceptable level because of the reasons which is mentioned since its discovery.

As the low production of the Bati Raman with conventional oil production and EOR techniques, a new method that implements underground mining has been discussed.

This method called Mining Assisted Heavy Oil Production (MAHOP) is a new approach to Steam Assisted Gravity Drainage (SAGD) developed for possible application in the Bati Raman Oil Field. Steam injection and production will take place underground unlike the SAGD process but the collection of low viscous oil will be similar. Unlike the SAGD, steam injection, and the oil production boreholes will be drilled vertically at the roof of the galleries with fan-shaped aligned, and steam that is injected into the reservoir through these boreholes will create a steam chamber, and with the temperature, oil viscosity will be decreased. The oil that viscosity had decreased will flow through the cracks to the perforated boreholes with the help of gravity and be collected. Except for the oil production method, the design of the underground openings will be similar to the underground mining methods. However, due to the nature of the oil production, openings are expected to be longer than in any other mine. Thus, with the development of the Tunnel Boring Machine (TBM) technology, openings are planned to be opened with TBMs and placed to cover almost all of the reservoir.

While MAHOP is a new and unique oil production method assisted by underground mining, the design of this type of underground mining has not been done before. Thus, this research mainly focuses on the conceptual design and evaluation of the challenges of MAHOP to the Bati Raman Oil Field.

1.1 General Remarks and Definitions

In this study, with the MAHOP method, other types of especially EOR techniques are mentioned. However, these methods are used mostly for comparison between MAHOP and will not be detailly investigated. In addition, parameters that will be used for the design of the underground mine will be operational based and any rock mechanics model will not be used in this research. Nevertheless, mining design and rock mechanics are intertwined so, in the placement of the production galleries basic rules for the stability of the openings are used.

Production openings, production galleries, and galleries are used interchangeably for most of the study. Oil production will be held only from the galleries which will be opened in the reservoir and this means that these terms are the same.

1.2 Problem Statement

Like the Bati Raman Oil Field, there are a lot of depleted reservoirs that cannot be extracted through the conventional oil production method or with the EOR techniques because of the high viscosity, depth, and lithology of the area. The aforementioned reservoirs constitute a large part of the oil reservoirs that have already been discovered and even though the trend of usage of fossil fuels is decreasing, the application of the MAHOP and production of these potentially recoverable reservoirs with this method has great importance. Also, MAHOP is a new method that did not use any other reservoirs. Thus, the underground design of the method should be detailly investigated in terms of challenges that can be faced such as tunneling, recovery, ventilation, heat, etc.

1.3 Research Objective and Scope of the Study

The main objective of this study is to conceptually design an underground mine by using mining software according to the MAHOP method for Bati Raman Oil Field and evaluate the operational challenges that can be faced in the mine. Also, an economic evaluation of the mine will be planned to be done at the end of the study.

The objectives of the research are described as follows;

1. Designing a conceptual underground mine of Bati Raman Oil Field
2. Evaluating probable challenges; tunneling, recovery, hauling, and tailing disposal
3. Creating a ventilation network for the mine
4. Cooling the mine to an acceptable temperature level by using heat simulation

5. Estimating capital and operational expenditure of the mine
6. Economically evaluating the mine for a production rate of 250,000 barrels of oil per day

1.4 Research Methodology

The methodology of this study includes the following steps;

1. Creating and verifying a solid model of the Bati Raman Oil Field reservoir
2. Deciding the proper equipment for the gallery excavation (Continuous Miner or TBM)
3. Deciding production gallery dimensions
4. Deciding the optimum working level for MAHOP
5. Placing and connecting the production galleries on Micromine (Micromine Pty Ltd., 2022)
6. Dividing the reservoir into “panels” according to the production schedule
7. Implementing design to the Ventsim (Howden Group Limited, 2019)
8. Calculating required air amount and simulation on software
9. Cooling the mine to an acceptable level
10. Calculation and Evaluation of the Economics of the project

1.5 Thesis Outline

This research is composed of six chapters. In the introduction, the outline of the study and problem statement of the research will be in the first chapter with the objective and scope. In Chapter 2, a summary of the Bati Raman Oil Field, similar case studies, and the challenges that can be faced in the literature will be investigated. Detailed design of the field such as defining working-level, cross-cut, and steam boiler locations, and production schedule will be provided in Chapter 3. In Chapter 4, ventilation network construction, cooling pocket locations, and heat and ventilation simulation results of the mine will be examined. An economic evaluation of the mine, capital and operational

cost estimations, and economic sensitivity analysis will be in Chapter 5. In the final chapter, the result of the feasibility study of the mine will be discussed and recommendations based on the conceptual design and ventilation will be listed.

CHAPTER 2

LITERATURE REVIEW

In this chapter, the Bati Raman Oil Field will be introduced briefly. Then, similar cases of mining implemented oil production will be discussed similarities and differences and challenges that can be faced in the production faces will be included.

2.1 Bati Raman Oil Field

The Bati Raman field is Türkiye's largest proven oil reservoir with approximately 1.85 billion barrels of oil, discovered in 1961. It is located in southeast Türkiye Batman province and it is 76 km away from the Syrian border (Figure 1). Bati Raman field is located at an average depth of 1450 m and the reservoir has a length, width, and average thickness of approximately 15.5 km, 2.5 km, and 60 m, respectively. The reservoir is located in a cracked limestone with low pressure, low gravity with 12^{o} API (Table 1), and heavy oil viscosity of 450-1000 cp with average porosity of 20% (Canbolat et al., 2022; Kantar et al., 1985).

Table 1 API Gravity Classification (Al-Dahhan & Mahmood, 2019)

Type	Degrees API
Light Crudes	Higher than 40
Medium Crudes	Between 30 and 40
Heavy Crudes	Between 10 and 30
Very Heavy Crudes	Below 10.0

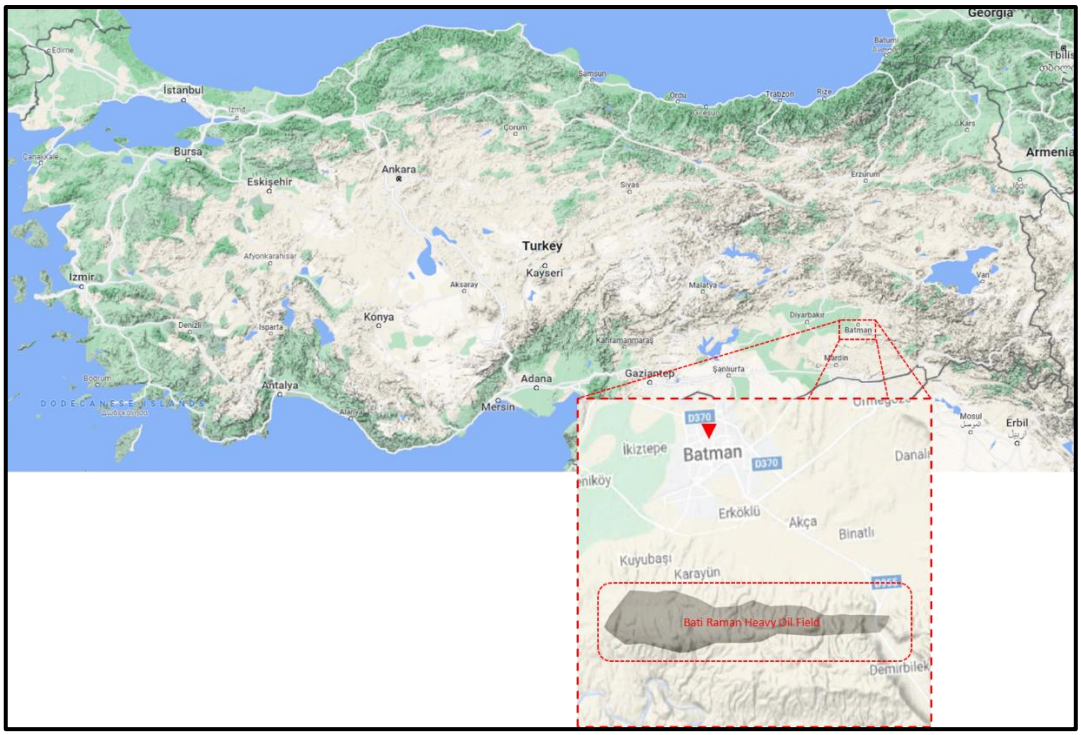

Figure 1 Location of Bati Raman Oil Field

The reservoir is located in a formation called the Garzan formation. The formation topography is mostly affected by the anticlinal folds which contain narrow valleys between parallel rolling mountains. The Garzan formation mostly consists of highly fractured bioclastic limestones in which grain size and fossil content change laterally towards the east-west direction. Also, grain size and the lithology of the formation change with the thickness of the formation and it affects the porosity in the reservoir. In the thin part of the reservoir formation, more calcareous shale and marlstone were observed in the content. For the structural geology of the field, the major structure is the almost 25 km long anticline which trends N 65^{o} W with a 15^{o} dipping angle. Besides the anticline, a thrust fault that is almost parallel to the anticline is dipping 55^{o} towards to northeast direction. However, except for this fault which is located south of the reservoir, there is a lot of faulting in the region (Sanlav et al., 1963). In addition, with the evidence of water flushing, the presence of the water is expected

to be in the Mardin formation that is underlying the Garzan formation (Ala & Moss, 1979). The formations in the regions are depicted in Figure 2.

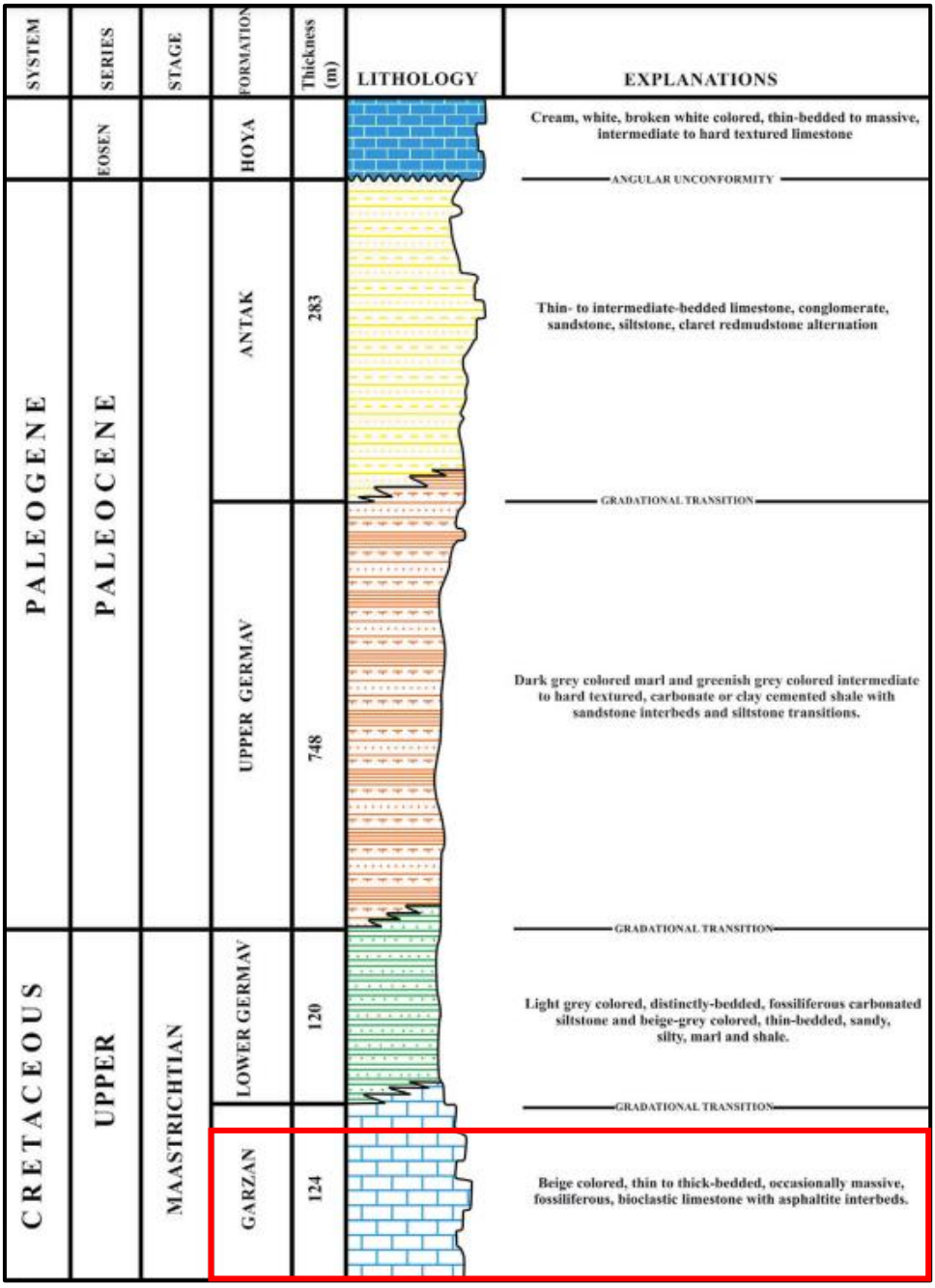

Figure 2 Stratigraphic log plot of Bati Raman (Sinanoğlu, 2021)

Production of the Bati Raman Oil Field started in 1961 with the conventional oil production method and it reached its peak at 9000 barrels/day in 1969. However,

with the production, reservoir pressure decreased gradually, and eventually, production rates decreased to insufficient levels. In 1986, with the exploration of the CO_2-rich Dodan field, CO_2 injection started in the field to increase production by increasing the reservoir pressure. Nevertheless, only 6% of the oil in the reservoir just recovered and it is expected to reach only 10 percent with the CO_2 injection. Except from these two production methods, other different EOR methods have been tested such as CO_2 /Foam and steam injection. Although at the beginning these methods are promising, each implemented method did not meet the required production values with sufficient recoveries because of the depth, operational challenges, and the high naturally fractured and vuggy structure result of heterogeneity in the reservoir (Sahin et al., 2012, 2014).

2.2 Similar Cases of Oil Mining

Theoretical studies and practical applications of MAHOP need to be investigated carefully to understand the possibilities and be aware of the operational challenges. However, there is a few examples of the combination of mining and conventional oil production methods. Therefore, previous mining integrated oil production methods or oil mining methods are mostly reviewed in the literature.

The first mining implementation in oil production started actually at the beginning 1900s yet, it was never used in a widespread manner. These types of applications were mostly similar to the conventional mining methods which are mechanical extraction of very heavy oil (tar sand) with both underground and surface mining methods. These methods were categorized as direct stopping and block caving for underground mining methods and terrace pit, strip mining, and open pits for surface mining methods (Borg, 1982). However, especially in the underground stopping type of production, operational difficulties according to the probable hazard and risks compel the application. To be able to implement the methods of production requires some safety measures to decrease the risks in the working area. However, some of the precautions such as degasification, result in a loss of energy in the reservoir

(Borg, 1982). Therefore, oil production by underground stopping was not commonly used and these types of operational difficulties forced to use of enhanced oil recovery methods in the underground.

One of the first underground EOR applications is the placement of steel coils in a sump at the bottom of an inclined shaft located in a reservoir in California. Those steel coils were used to heat the oil sand to increase production. This was firstly successful but production dropped rapidly. Even though there were few examples of the usage of EOR in the underground at that time, especially in the USA, the interest in the implementation of these methods on the depleted reservoirs was increased after Pechelbronn and Wietze mines successfully produced oil with underground EOR methods (Hutchins et al., 1978).

Among these two mines, the Wietze mine application in the 1930s is the most similar method to MAHOP used. Wietze oil reservoir which was located in Hannover, Germany has 4 different beddings with a dip angle of 30-45^{o} and these beddings showed different viscosity and permeability based on their positions. Production was mostly done by extracting oil sand underground with the pneumatic hammer picks and then the broken material was hoisted to the surface process facility. The hot-water separation process is used on the broken material for extracting heavy oil. However, on the fourth bed because of its viscosity, an EOR process is planned with diagonally placed 4 boreholes with a vertical borehole placed at the center (Figure 3), and a different type of fan-shaped borehole pattern was used. On the other hand, water flooding and solution injections are used to increase reservoir pressure, unlike the MAHOP. With these methods of production, yearly production increased over the years and reached its peak at 795,000 barrels/year in 1909, and total production reached 14 million barrels until the reservoir is depleted. Unfortunately, Rice did not mention any recovery value for the Wietze mine production in his book (Rice, 1932; Streeter et al., 1991).

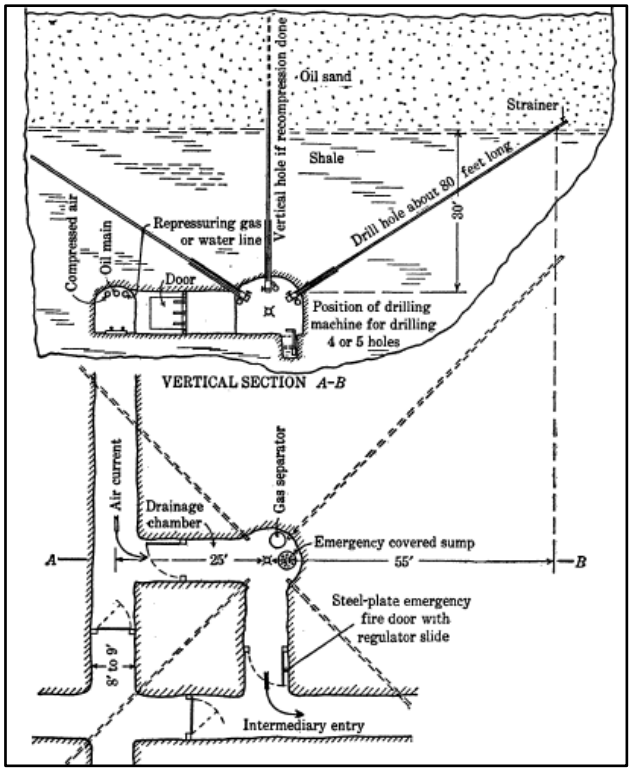

Figure 3 Wietze Mine fan-shaped borehole and layout illustration (Rice, 1932)

In those years, different oil production with EOR methods was developed with Leo Ranney's horizontal well patent, and several similar methods were tested across the USA. Firstly, 250-meter-long horizontal wells used in an outcropping reservoir in Ohio with perforated tubing, and vacuum were used to increase the production on the site. Then, horizontal wells were tested in Pennsylvania in the early 1940s. A 130-meter shaft sunk in a hydrocarbon formation, and at the bottom of the shaft, 760-meter-long inclined horizontal wells were drilled and explosives were used in oil production (Hutchins et al., 1978; Miller, 1946). In addition, the above-mentioned methods were mostly found to be economically infeasible, thus the usage of those methods was not used in a widespread manner.

A more recent operation, which underground mining used to assist oil production is the Yarega Oil Field which is located in the Komi Republic near the Ukhta River. The field was discovered in 1932 and until today mining involved oil production methods are tested in the field. These methods are called one-level system, two-

level system, and lastly, surface/underground thermal oil development method which is used now. The difference between these methods is mostly based on the steam injection and tunneling locations. For the one-level system which is also tested in the Athabasca Oil Field in 1977, wells that are drilled from the production galleries below the formation, are used for steam injection. On the other hand, in the two-level system, steam injection is done by highly dense drilled injectors which are located below the reservoir. Lastly, the surface/underground thermal oil-mining development method can be differentiated from all other existing methods from its surface-located steam injection wells. Recovery of these production methods varies, but the highest recovery is achieved with the surface/underground method which is 60% with a 2.7 Steam Oil Ratio (SOR). The mine layout of the Yarega Oil Field can be seen below (Figure 4). Lastly, Yarega Oil Mine has faced extensive temperatures in the working areas as we expected in the Bati Raman Oil field, yet details of cooling operations are not mentioned (Chertenkov et al., 2012).

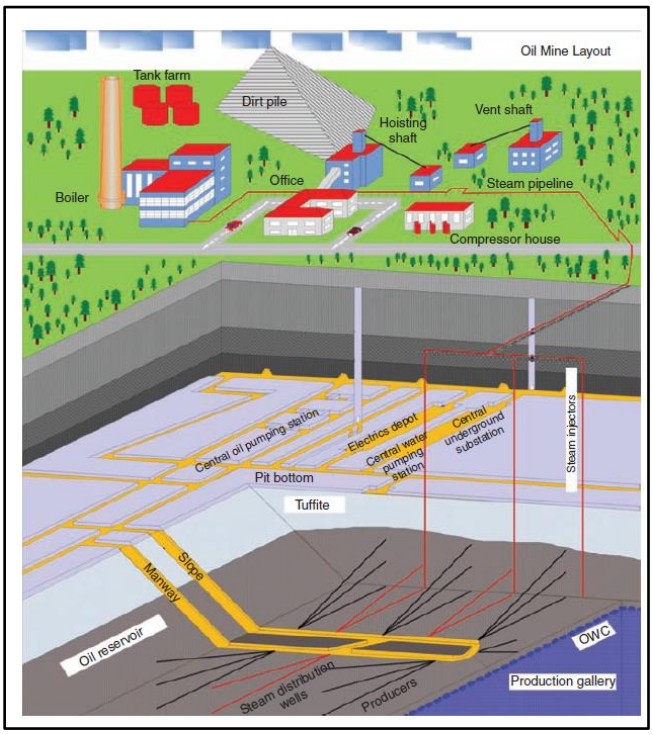

Figure 4 Yarega Oil Field Mine Layout (Chertenkov et al., 2012).

The Alberta Oil Sands Technology and Research Authority (AOSTRA) was the other main source of in situ advancements. AOSTRA relied on (Butler, 1982; Komery et al., 1999) work and adaptations of Russian thermal mining techniques for its underground recovery advancements. Despite encountering a lack of interest by the petroleum industry, the government-sponsored agency took a big financial risk by funding a project called the Underground Test Facility (UTF) in early 1983. AOSTRA tested underground oil sands mining theory—at a depth beyond that which conventional surface mining methods were productive in Alberta. The UTF opened in 1987, 60 km north of Fort McMurray, with an innovative design. The two vertical shafts (4m diameter) were opened up over 200 m deep. The Phase A pilot involved three horizontal well pairs 70 m in length, each with 40-50 m of exposure to oil sands within the McMurray formation. It was proved that the underground SAGD system was working. It was decided to drive tunnels within the more stable limestone formation beneath the oil sands and then drill upwards into the reservoir. Phase B went ahead over several years of experimentation. It involved another three horizontal well pairs, each pair 70 m apart. AOSTRA originally anticipated it would achieve about 30% to 45% bitumen recovery, but eventual results exceeded expectations at 65% (Komery et al. 1993).

It should be noted that the above-mentioned methods are different from the MAHOP method. So, in these examples, problems that can be faced while constructing the conceptual design are taken into account.

In addition, current studies about the production and recovery of MAHOP have also been studied. In their research (Canbolat et al., 2022), constructed a laboratory-scale model and investigated the recovery values of reservoirs with different types of characteristics related to different steam temperatures. He proved that the oil recovery reaches 70% with a MAHOP which is carried on 5 fan-shaped holes at 100^0C steam injection.

Except for the laboratory-scale model, an economic evaluation has been done. In that study, capital costs have been calculated as 2.75 billion USD and 1.97 billion USD

for both 60% and 80% recoveries, respectively. Also, the operational expense is estimated at 12 USD/barrel. On the other hand, according to (Nguyen et al., 2014), the operational cost of SAGD for shallower reservoirs is $ 12. With the depth considerations, the oil production rate between the two production methods, capital, and operational expenses are expected to be relatively lower than a conventional Steam Assisted Gravity Drainage (SAGD) Because of the increase in the quality of the steam and decrease in the steam loss. Thus, the MAHOP method was found to be more economical than the SAGD process in terms of both initial investment and operating expense (Canbolat et al., 2020).

2.3 Literature Research About Challenges

In this section, challenges and their possible solutions which can be seen in a probable MAHOP project are investigated in detail in three parts, Tunnelling, Mine ventilation, and Mine cooling.

2.3.1 Tunneling

Tunneling is one of the common research interests for both mining and civil industries. Thus, the development of tunneling technology to improve productivity and safety from an economic perspective was inevitable with the technological advances. Before the first modern TBM application, mostly underground excavations were conducted with conventional drill and blast (D&B). After the success of modern TBMs, D&B, and TBM excavation methods become the two main choices in tunneling and until today more than 10,000 TBM applications took place on sewage, traffic, and underground storage projects (Maidl et al., 2008).

Other than civil engineering projects, TBMs also used in mining engineering sectors. One of the first applications of TBM in mining started at the beginning of the 1970s, with a German coal mine. After that, again a coal mine which is located in the USA used TBM in mine development (Handewith, 1983). White (1978) investigated a

5.1-meter diameter TBM application on a decline construction for a coal mine in the southern coalfields of New South Wales. Boldt and Hennek (1981), studied Rheinland and Friedrich Heinrich mines which opened 13 km long tunnels with 6-meter TBMs. Cigla et al. (2001) investigated two successful implementations of TBMs in metal mines, San Manual Copper and Stillwater Platinum mines. Other than these examples, the use of TBMs in mining has been reviewed in several different studies (Brox, 2013; Handewith, 1980; Home & Askilsrud, 2011; Robbins, 1984; Stack, 1982; Taylor et al., 1978; Zheng et al., 2016).

As stated above, both tunneling method is widely used. However, the selection of the method is not straightforward. In the past, multiple studies showed that both methods have pros and cons related to productivity, cost, safety, and flexibility. On the other hand, the literature covered mostly case studies and subjective conclusions.

In the literature, Nord and Stille (1988), studied factors that can affect the method selection by investigating two hybrid cases that used both methods. Further studies from Nord (2006) underlined that a common guideline cannot be established and each project should be evaluated in terms of excavation rate, risk assessment, and supporting. Unlike Nord, Barton (2000) defended the method selection are dependent on the ground conditions (Q-value), and later on suggested a hybrid method according to ground condition knowledge of projects (Barton, 2013). Like Barton, Suorineni et al. (2008), used just one parameter to determine the method of excavation. According to his study, if the required advance rate is bigger than 23 m/day, TBM is a more profitable method to use on the project. Similar to Suorineni, Cinar, and Feridunoglu (1994), defined the method selection with a “cost per meter vs length of tunnel” graph and showed that when the tunnel length is greater than 5 km, the TBM excavation method is economically feasible. In a more recent study, Macias and Bruland (2014), recommended a more qualitative method by including multiple different parameters such as project design considerations advance rate, risk, ground conditions, etc. (Zare et al., 2016).

According to the above-mentioned method selection literature, the excavation method selection of the Bati Raman field should be defined to assess the possible challenges. Thus, the advance rate, tunnel length, and a simple field identification were taken into account.

Within the nature of the production method of MAHOP, production galleries (tunnels) must have covered the reservoir as much as possible to increase production recovery. Also, considering the size of the field, enormous excavation lengths up to a couple of hundred km were foreseen. As reported by, Cinar and Feridunoglu (1994) if the excavations are done in a limestone stratum over 5-6 km long, the TBM application seems to be more profitable. In addition, due to the excavation length of the project, the advance rate of the tunnel has great importance economically. Even though multiple excavation operations would have been done simultaneously in the field, the required advance rate was expected to be higher than 25 m. Therefore, as Suorineni et al. (2008) stated, TBM appeared to be more suitable for this project.

Besides the advance rate and the tunnel length restrictions, a safe environment should be taken into account while selecting the excavation method. Consequently, the possible working environment of the project is investigated. The previous similar underground oil mining cases indicated that the working environment was expected to be similar to the underground coal mines in terms of ventilation (Hutchins et al., 1978). Thus, the usage of a blasting agent for the D&B method could impose danger because of the possible high methane concentration in the air. On the other hand, permissible blasting agents are also used in coal mines. However, the advance rates of those types of explosives are really limited especially in hard rock conditions (Yilmaz, 2023).

Despite the TBM's higher productivity and safety, usage of TBM's on mining projects is very limited compared to civil engineering projects. Reasons for that problem are related to the challenges such as ground conditions, high in-situ stresses, groundwater conditions, etc.

2.3.1.1 Main Reasons for TBM Tunneling Challenges

In this part, the main reasons for the problems that occurred in the TBM application will be separated into 3 subgroups called, Mixed ground conditions, Fractured rock masses, and High in-situ stress similar to Gong et al. (2016).

2.3.1.1.1 Mixed Ground Conditions

The presence of multiple geologic formations with significantly different properties such as geomechanics, geology, and hydrogeology, or the same geologic formation with different weathering degrees is referred to as mixed ground conditions. This condition results in the non-homogeneous distribution of stress on the cutterhead and cutters and is related to the abnormal wear of cutters. While this type of ground condition mostly faced during tunneling in civil engineering projects took place in mountainous areas and underground excavations close to urban areas (Gong et al., 2016; Steingrimsson et al., 2002; Tóth et al., 2013; Zhao et al., 2007), for mining projects, the origin of this problem, especially in underground metal mines. This is mostly related to the ore genesis processes and tectonic activities. While these processes are the causes of the high alteration between the host rock and the ore, it mostly creates a complex geological condition (Zheng et al., 2016) which may lead to mixed ground conditions. Fortunately, the probability of facing the disadvantages that occurred in the metal mining TBM applications is small due to the sedimentary structure along the Bati Raman Oil Field (Alsharhan & Nairn, 1997). Also, a great amount of the excavation will be done in the reservoir. Thus, the only change in the geologic structure is most probably in the fault zones and transition between the reservoir and the host rock.

2.3.1.1.2 Fractured Rock Mass Conditions

In reality, rock masses are mostly fractured and their degree of fracturing is defined by different rock mass classifications. The GSI (Hoek, 1994), used 4 categories for the fractured rock masses, blocky, very blocky, seamy, and crushed. A similar approach was applied to difficulties that can be faced on a TBM application by Gong et al. (2016). The blocky rock masses, result in rough surfaces for the TBM cutter head. Highly fractured (very blocky) rock masses which are related to the highly fractured and closely jointed more than 4 joint sets, may result in rock fall-out or even jamming of the TBM. Lastly and most crucial one for this project is fault and shear zones. This type of rock masses may show mixed face conditions, loose and soft material, and also heavy water inflows.

Unfortunately, because of a lack of geological information about the site, whether the above-mentioned structures (blocky or highly fractured) are in the reservoir or not is unknown. However, according to Türkiye Petrolleri Anonim Ortaklığı (TPAO) site maps, there are multiple fault zones in the reservoir. The geological structural map with the production holes is depicted below (Figure 5). In Figure 5, bold and random grey lines are anticipated to represent faults.

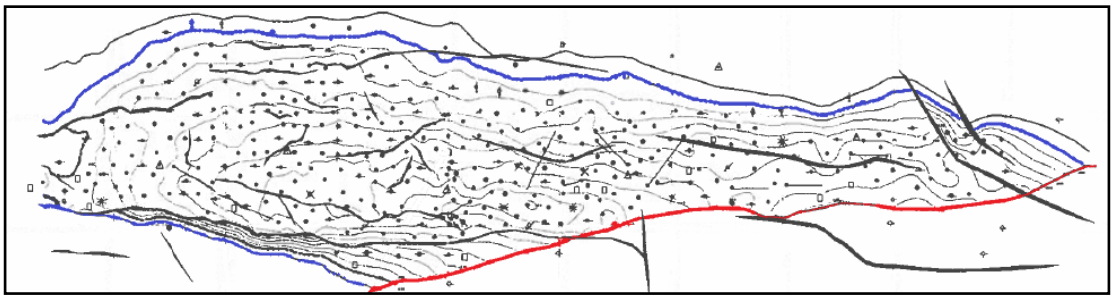

Figure 5 Structural Contour Map of Bati Raman (TPAO, personal communication, November 23, 2020)

As can be seen in the above figure, due to the high density of faults in the region, challenges related to the faults should be detailly investigated.

2.3.1.1.3 High In-situ Stress Conditions

Generally, the in-situ stress on an underground excavation is mostly related to the overburden amount. Therefore, in-situ stresses are expected to be high in deep underground excavation. This condition consequently affects deep TBM tunneling in 3 ways. These are;

1. rockburst occurrence due to excessive in-situ stress
2. Failures related to the high in-situ stress
3. Problems related to the high in-situ stress without failure

These 3 categories not only cause safety issues but also causes a decrease in advancement rate for multiple reasons. To emphasize the indirect effect of rock burst, muck removal, and gripper problems could be specified. Also, high in-situ stress results in high confining pressures on the tunnel face, thus, with the increased strength, the advancement rate decreases even without the failure. In addition, the number of joints could increase due to failures related to the high in-situ stresses. In that case, the boreability of the TBM could be affected negatively (Gong et al., 2016).

2.3.1.1.4 Gassy Rock Mass Conditions

Excavation in a gassy environment is a well-developed research area, especially for mining engineering for decades. However, TBM usage in a gassy environment is limited to mostly case studies (Ayhan et al., 2019; Bandini et al., 2017; Belle & Foulstone, 2015; Bilgin et al., 2016; Copur et al., 2011; Doyle, 2001; Grandori, 2006; Rodríguez & Lombardía, 2010, etc.). Although the details related to the methane explosion will be investigated in the Mine ventilation and cooling part, TBM applications in a gassy environment should be discussed. As known, gasses can be categorized for their harmful impact, and the main problem for the TBM application is explosive gasses. While these gasses could be spontaneous combustion around the excavation, it may cause mine fire and equipment and even human losses. In addition, among these explosive gasses, natural gasses such as methane, butane, and

hexane are expected to exist in the Bati Raman reservoir. Therefore, precautions according to the environment of the reservoir should be done for TBM application. These precautions and solutions will be discussed in the Problems and Solutions part below.

2.3.1.2 Problems and Solutions

In this part, probable problems can be encountered in deep TBM applications in fault zones like Bati Raman Oil Field. These problems can be categorized into 4 groups; stress-induced brittle failures, plastic shear failures and squeezing of weak rock, instability of the tunnel walls and face, and heavy water inflows and heads (Barla et al., 2011; Loew et al., 2010). Problems related to these categories and their solutions will be discussed. In addition, precautions related to the gassy environment TBM application will be briefly investigated.

According to Barla et al., (2011), stress-induced brittle failures can be specified as spalling and rock bursting. These two problems are mostly observed in many cases, especially in deep hard rock tunnel excavation.

Spalling is a failure in which rock is fractured into parallel slaps on the tunnel wall in a mostly symmetrical pattern. Slaps that are formed because of anisotropic high in-situ stress can vary in thickness and can form a V-shaped notch on the unsupported tunnel walls (Martin et al., 1998). In this failure type, the spalling that occurred in front of the grippers may lead to the grippers pad not being seated on the side walls of the tunnel and this condition can even lead to the jam of the TBM. In some extreme cases, spalling results in rock bursts (Barla et al., 2011).

Another brittle stress-induced failure rock burst can be defined as high-velocity rock ejection from the tunnel surfaces (Stacey et al., 1994). In multiple studies, (Li et al., 2007; Tang, 2000), rock bursts are categorized into different groups such as strain burst, bulking, face crush, shear rupture, and fault slip type of rock burst. However, Board (1994) explained the mechanism of this failure with brittle failure of intact

rock due to high in-situ stress and the slip along a weak plane such as faults in his thesis. Whereas, the type of rock burst changes related to their mechanism, mostly the problems caused by TBM application are similar. These are mostly, muck removal and gripper problems similar to the spalling failures in addition to the health and safety of the workers (Gong et al., 2016).

Both of the brittle failures in the deep TBM excavation examples are depicted in Figure 6. In the first and second pictures (a and b) tip of the v shape of the spalling and spalling failure of the full tunnel face of Bedretto Adit can be seen. In the second picture, a severe rock burst in a deep South African gold mine is shown.

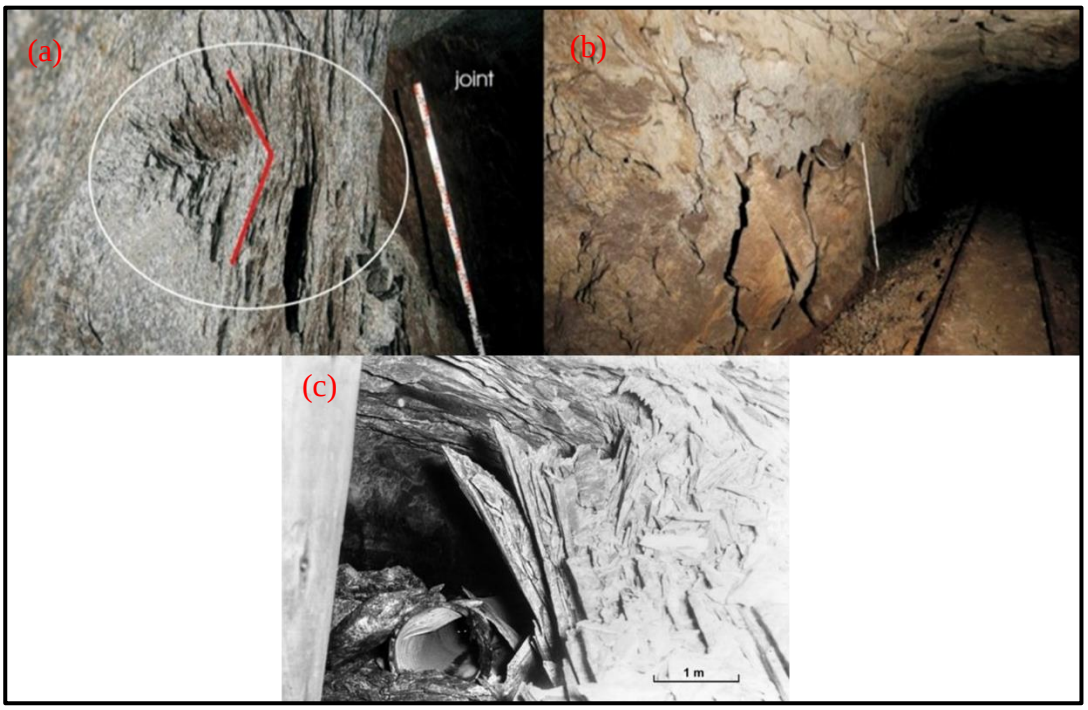

Figure 6 Bedretto Adit spalling failure, V-shaped notch tip (a), spalling along full tunnel face (b) (Huber, 2004); Rock burst in a deep South African Gold Mine (c) (Hoek & Martin, 2014)

Although, the restricted knowledge about the rock mass that will be excavated in this project, one of the simple field identifications called Uniaxial Compressive Strength

(UCS) test have done by Emci and Ozturk (2021). The UCS of the reservoir was found as 6.4 MPa and according to ISRM (1981), the strength of the reservoir is classified as weak rock. Thus, problems that can be observed in TBM application in weak rock, should be investigated.

One of the major problems faced in weak rock is squeezing. Squeezing is basically the convergence of the cross-section due to the large plastic deformations of the tunnel in time. These failures are mostly related to high in-situ stresses associated with creeping and a high amount of shear stress which is higher than the shear strength of rock (Barla et al., 2011; Gong et al., 2016). This type of failure mostly results in TBM jamming and decreases the productivity of the excavation.

Lastly, as mentioned above, high-density fault systems are predicted. Thus, problems related to the faults described by (Barla & Pelizza, 2000; Barton, 2000; Gong et al., 2016; Paltrinieri et al., 2016) is listed below,

- Instable excavation faces due to loosen material along the fault and shear zones
- Overbreak of the tunnel contour
- Excessive deformation
- Field stress changes because of the faults
- Large water inflows

In addition to the specific problems which is observed in TBM excavation, instability of the faces and walls has a major setback in TBM tunneling like most underground excavations. While this is a general geotechnical problem, the reasons are similar to almost all underground excavations such as insufficient pillar length, rock mass characteristics, etc.

For the solution of these stability problems, the correct estimation of the rock mass to be excavated is very crucial. Thus, Barton (2004) describes and advised the

geological logging, rock mass characterization, hydraulic test, and seismic profiles between holes and probe drilling for deep TBM excavation as part of the solution.

After the proper estimation of the rock mass, changing the direction or the location of the tunnels is the easiest solution. However, when there is no chance to implement this solution, increasing the strength of the rock mass is another way to overcome the stability problems. This can be done with pre-grouting which is a ground conditioning method. Grout or similar material is injected ahead of the tunnel face to increase the rock quality (Barton, 2004). Except for pre-grouting, an umbrella-shaped rock bolting is another option to increase stability. In this method, bolts are placed in the direction of the advancement with an umbrella arch shape (Barla & Pelizza, 2000; Gong et al., 2016).

While these examples increase the stability, especially on the face of the excavation, side wall stability should not be underestimated. Problems such as squeezing, rockburst, and sapling can also be observed in the sidewalls. Thus, immediate supports after the cutterhead with shotcrete, steel arching, etc. can be used to stabilize (Gong et al., 2016). Furthermore, opening the pilot tunnels ahead of the TBM as a preconditioning method is another option. In this method, a pilot tunnel ahead of the tunnel is excavated with the conventional D&B method to maximize the rock mass disturbance to change the failure mode and destress the environment (Zhang et al., 2012). Although this method is decreasing the risk of the rockburst in deep TBM excavation, it cannot be implemented in this project because using the D&B method.

In fault zones, stability is not the only problem as stated before. High water inflows and water head can be expected even though the predicted water table level is located at the bottom of the reservoir. Thus, precautions that could be implemented in the field should be discussed.

There are multiple ways to deal with adverse groundwater conditions. Injections used in rock consolidation such as PU resin, cement grout, and organo-mineral foam can also be used to deal with the groundwater problem. Pre-injection of those materials in a highly fractured with an expected heavy inflow could be very effective. Other

than this method, modifying TBM with the PU-injected pre-vault, drilling drainage holes to decrease the groundwater pressure, and Ground freezing can be implemented to overcome groundwater problems that can affect the TBM application (Barla & Pelizza, 2000; Laughton, 2005; Paltrinieri et al., 2016).

Lastly, solutions and safety procedures for the TBM application in a gassy environment are another part of this study that should be discussed. Bandini et al. (2017) offered 5 precautions and safety procedures to overcome the methane problem. Those are;

- Compartmentalization of TBM for gassy rock masses
- Usage of explosion-proof equipment
- Well-designed forced ventilation system to dilute gas mixture
- Usage of continuous monitoring tools with alarm systems
- Particular procedures for excavating, carrying out maintenance tasks, and conducting specific activities, such as accessing the excavation chamber for maintenance and drilling operations at the tunnel face

In addition, blowing-type ventilation systems are better at diluting methane from the face of the tunnel. However, a low airflow zone can be created with the blowing type ventilation (Kissel, 2006). Therefore, face ventilation with auxiliary will be detailed in the Mine ventilation and cooling section.

Even though the problems stated above have a crucial impact on the TBM application in Bati Raman Heavy Oil Field, these adverse conditions were observed in different successful cases. Therefore, with the possible precautions and technical solutions, the TBM excavation method in the MAHOP project is believed to be possible.

2.3.2 Mine Ventilation and Cooling

This part of the study is separated into two groups; Mine ventilation and Mine Cooling, and according to both of the subjects similar mines and their challenges and

the solutions to overcome these problems are investigated for probable MAHOP implementation in Bati Raman Oil Field.

2.3.2.1 Mine Ventilation

In this part of the research, possible MAHOP implementation in Bati Raman Oil Field will be studied in terms of ventilation design. The main purpose of underground mine ventilation is to provide oxygen for humans and internal-combustion engines, remove or dilute harmful gasses created from the mining operation or the geological strata of the mine to create a safe working environment, and lastly, provide adequate temperature and humidity for human and the machinery.

To begin with, the working environment cannot be specified due to a lack of knowledge but similar ventilation systems are important to investigate beforehand. Thus, similar oil mining cases and a general feasibility study the petroleum mining were investigated. The report which is published by the US Bureau of Mines stated that underground petroleum mining logically would be treated as coal mining in terms of ventilation (Hutchins et al., 1978). This means that the regulations and the challenges that can be faced in such a project could be similar to the deep coal mining cases too. Therefore, firstly underground coal mining methods will be discussed in detail in terms of the ventilation system. Then probable challenges and problems which are observed in the underground coal mines will be studied.

2.3.2.1.1 Required Fresh Air in an Underground Mine

While stating the underground mine ventilation purposes, methods or calculations that are used to estimate the required fresh air should be assessed. To start this section, the required fresh air for a human in order to work properly should be calculated. To estimate the fresh air income, first the number of people that are going to work and their inhalation rate (McPherson et al., 1993). Based on the work by

Forbes and Grove (1954), the inhalation rate table according to the n activity is depicted below (Table 2).

Table 2 Inhalation Rate

Activity	**Breaths (per min)**	**Inhalation rate (liters/s)**	**O_2 Consumption (liters/s)**	**CO_2 produced (liters/s)**
At rest	12-18	0.08-0.2	0.005	0.004
Moderate work	30	0.8-1.0	0.03	0.027
Vigorous work	40	1.6	0.05	0.05

According to the above information, the required fresh air can be calculated by using a basic equation that evaluates the oxygen and carbon dioxide concentration in a closed system by using oxygen consumption and carbon dioxide production by humans. An example equation (Hartman et al., 1997) for the oxygen concentration calculation can be seen below.

$$(O_2\ concentration\ in\ intake\ air)Q_{intake} - (Amount\ of\ O_2\ Consumped) = (O_2\ concentration\ in\ return\ air)Q_{intake}$$

In addition, a similar approach should be applied on the carbon dioxide to consider the maximum allowable concentration of carbon dioxide. After both calculations are completed, the higher value should be selected as the required fresh air for breathing.

As Hartman et al. (1997) stated, mine ventilation is also used to control the physical and the chemical quality of air together the supplying fresh air the humans. Therefore, the dilution of harmful gasses, dust, blasting agents, and fresh air required for a diesel engine to work properly should be estimated to create a workable environment.

The fresh air required to dilute harmful gasses for steady-state situations is calculated by De Souza and Katsabanis (1991) with the equation that follows:

$$Q_{intake} = Q_{gas} \frac{(1 - MAC)}{(MAC - B)} \quad (1)$$

Where Q_{gas} is the gas inflow rate (m^3/s), MAC is the Maximum allowable concentration and B is the gas concentration in the intake air.

Similar to the harmful gas dilution, an equation for the required fresh air quantity to dilute dust in the mine atmosphere for steady-state situations is stated by Hartman et al. (1997).

$$Q_{intake} = \frac{G}{(TLV - B)} \quad (2)$$

Where G is the dust generation in mass per second (mg/s), TLV is the threshold limit value and B is the dust concentration in the intake air.

As can be seen in both equations, the dilution of gas or dust in a steady state is very similar. Thus, these formulations can be used for the fumes that are created after the blasting (De Souza & Katsabanis, 1991).

Lastly, the fresh air required for diesel-powered equipment should be estimated. Generally, diesel is the fuel for the internal combustion engines. This states that the oxygen concentration in the atmosphere should be sufficient to create combustion inside the engine. To calculate the required fresh air, overall engine power in kilowatts is multiplied by the unit airflow requirement in m^3/s per kilowatts which is defined by the local mining occupational health and safety regulations (Halim, 2016).

$$Q_{intake} = qxG \quad (3)$$

Where q is the required air for each kilowatt (m^3/s per kilowatts) and G is the total power in kilowatts.

Additionally, prediction of CO_2 emission to the mine environment may be required for fresh air calculations. Although there is no direct CO_2 emission estimation in the literature, different gas emission prediction methods used for methane can be implemented to predict CO_2 emission through underground excavation. According to (Rodríguez & Lombardía, 2010), the specific gas emission can be found with the gas concentration in strata and production and ventilation rate.

$$S = \frac{C}{100}\, x \frac{Q}{P} \qquad (4)$$

Where the S is specific gas emission, C is the gas concentration in strata (%), Q is the ventilation rate of the face (m^3/day) and P is the daily excavation amount (tonnes/day).

From this equation 4, the expected gas emission from the face is calculated by using the daily excavation rate.

$$q(P) = P\, x\, S(P) \qquad (5)$$

Where the S(P) is the average specific emission related to the daily excavation.

In most cases, the production rate is varied from day to day. To predict the average gas emission, a specific gas emission related to the maximum and minimum excavation is required. Thus, in equation 5 the specific gas emission is defined as a function.

2.3.2.1.2 Mine Ventilation System

In this part, systems that could be used to ventilate the Bati Raman Oil Field will be discussed. Ventilation systems will be separated into two groups, face and modular section ventilation part. In the face ventilation part, methods that could be used in face ventilation in tunneling and auxiliary ventilation of the face for methane dilution

will be investigated. For the modular section ventilation, a district ventilation system will be detailed.

2.3.2.1.2.1 Tunnel Face Ventilation

Ventilation systems that are used in the tunnel face mostly named auxiliary ventilation systems and there are only 3 major ventilation types used in auxiliary ventilation systems: forced, exhaust, and mixed which is illustrated below (Fang et al., 2016). In principle, forced-type ventilation systems are widely used in tunneling and it is better for the dilution of methane and more efficient than the exhaust type of ventilation (Kissel, 2006; Toraño et al., 2009).

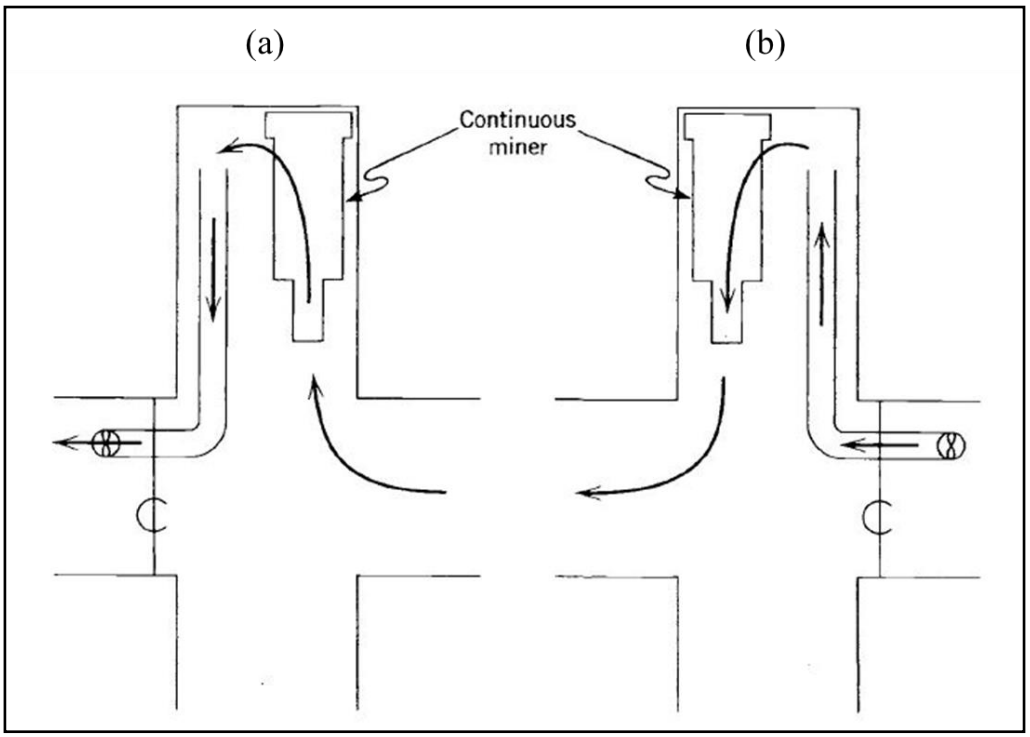

Figure 7 Exhaust (a) and Blower (Forced) (b) type auxiliary ventilation systems (Hartman et al., 1997)

In Figure 7, two types of auxiliary ventilation systems are illustrated in a continuous mining operation. Although TBM usage and continuous miner usage in excavations

have slight differences, the main idea behind the ventilation system is the same. Fresh air will be forced to the face of the TBM to provide adequate oxygen and dilute the harmful gases. Then the contaminated air will be ejected from the working area.

While this type of ventilation system is efficient, there are some setbacks to implementing this system into the MAHOP project. For example, in some instances where one ventilation duct is used to force fresh air onto the face and the other one is used to carry the contaminated air, a low airflow zone can be created. In such a system, gases like methane, and carbon dioxide could accumulate there. Therefore, another setup which is proposed by Kissel (2006) should be used (Figure 8). Other than this setup, the simulation of face ventilation and the details will be discussed in Chapter 4.

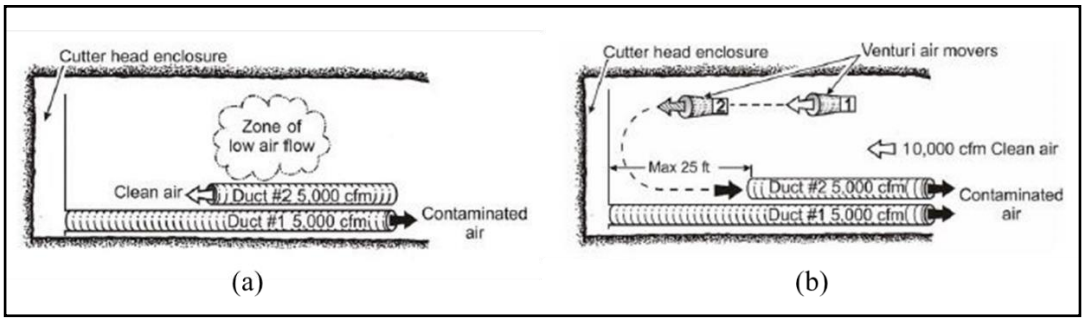

Figure 8 TBM face ventilation with low airflow zone (a) and TBM face ventilation with secondary exhaust duct (b) (Kissel, 2006)

2.3.2.1.2.2 Modular Section Ventilation

As Hutchins et al. (1978) stated, the ventilation system of oil mining is similar to underground coal mining in many aspects. However, the nature of coal mining extraction of the coal defines the ventilation system. For one of the underground mining methods, longwall mining, distinct ventilation systems are separated into two groups U-tube and through-flow ventilation. In the U-tube method, fresh air is directed through the working area from the intake gallery, then returns to the

openings that are parallel to the intake gallery. On the other hand, the through-flow method, intakes, and returns are separated geographically. While intake air goes through the working area, exhaust air is directed to the return gallery which is located at the other side of the stopping. With this method, the number of leakage paths is reduced by reducing the air crossing and stoppings (Hartman et al., 1997).

For the room and pillar mining method, a bi-directional (W) system and a uni-directional (U-tube) system are used to ventilate the underground method (Figure 9). Fresh air is connected to the two exhaust airways on both sides as it passes through the central airways in a bi-directional system. On the other hand, intake and return air are located on opposite sides of the coal panel. In both methods, return, and intake air are separated from each with stoppings called air brattice curtains, but the main disadvantage between these two methods is the number of stoppings used. In the bi-directional, the number of stopping used to separate intake and return air is doubled, hence the leakage paths are doubled consequently.

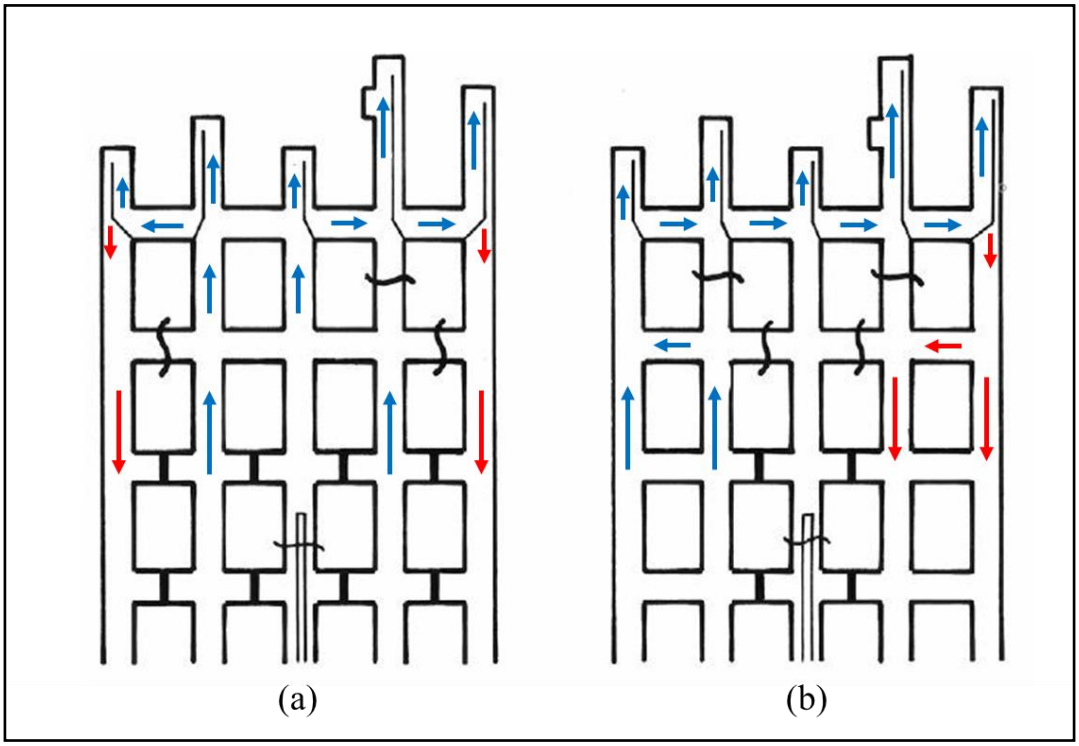

Figure 9 Bi-directional (W) system (a) and Uni-directional (U-tube) system (b) for underground room and pillar coal mine (Hartman et al., 1997)

Among these two-mining methods, the mine layout of the MAHOP which will be illustrated in Chapter 3 is close to the room and pillar mining method. Therefore, between Bi-directional and Uni-directional ventilation systems, a Uni-directional (U-tube) ventilation system will be implemented in the MAHOP project because of the reduced number of stopping and leakage paths.

2.3.2.1.3 Challenges in Underground Mine Ventilation

As in the mine ventilation system part, challenges that are observed in underground coal mines are investigated, and the parameters like the depth of the mine, the complexity of the design, harmful gasses, and respirable dust are found to be a significant challenge to ventilation design (Hardcastle et al., 2004). Thus, in this section, the depth and the complexity of underground mines and harmful gases including dust are taken into account in two different sub-groups.

2.3.2.1.3.1 Depth and Complexity of Underground Mines

The main problem in the deep mine ventilation design is the length of the underground openings. While the length of the opening increased, the friction force to be overcome by fresh air also increases. As can be seen in the Atkinson formulae (1), resistance and the length of the tunnel are directly proportional to each other (McPherson et al., 1993).

$$R = kL\frac{per}{A^3}\frac{\rho}{1.2} \qquad (6)$$

Where R represents resistance, k is the Atkinson Friction factor, L is the length of the openings, per is the perimeter, A is the cross-sectional area, and ρ is the density of fresh air.

As the resistance increases, the pressure that is required to push the fresh air to the working faces also increases. In the second formula (2), the relation between the pressure and the resistance can be seen and the P, R, and Q parameters in the equation represent pressure, resistance, and airflow, respectively. Thus, the expected resistance for the MAHOP implementation is high due to the average depth of the reservoir which is 1450 m.

$$P = RQ^2 \qquad (7)$$

As the main fan pressure increases, leakage of the system increases according to that. To compensate for the leakage, the cost of ventilation will be proportionally increased. In such cases, the usage of booster fans is one of the effective solutions to overcome this problem. In a properly designed ventilation system, booster fans can maintain adequate airflow in the areas where the pressure of the fresh air is not sufficient and redistribute the pressure pattern to minimize leakage (McPherson et al., 1993).

Another problem that is observed in the deep underground mine ventilation is the complexity of the system. As the ventilation system is getting complex, supplying sufficient airflow to the working faces becomes harder. To deal with the complex ventilation system and related problems such as mine fires, separating the mines into modular ventilation sections is one of the solutions. Especially in a hydrocarbon reservoir such as Bati Raman Oil Field, mine fire is always a risk that should be considered. In such a case, part of the mine that the fire has started can be closed and

separated from the rest of the mine. Also, separating the mine into modular sections will result in a decrease in the length of the opening to be ventilated. While the pressure decreases, the ventilation system will be simplified (Hutchins et al., 1978).

2.3.2.1.3.2 Harmful gasses

Thirdly, and most important expected problem is the harmful gases and respirable dust, and their removal or dilution. As mentioned above, Bati Raman is a hydrocarbon reservoir that is an organic-rich geological stratum and it is similar to underground coal mines. Although gases that can be observed in an underground coal mine are expected to be in the Bati Raman Oil Field, respirable dust problems and spontaneous combustion of these dust are not expected to be in the environment due to the limestone structure. However, excessive dust problems may be observable related to the excavation. Thus, dust dilution will be discussed in the next chapters and primary sources, threshold values, and properties of the harmful gasses will be discussed in this part.

In an underground mine, gases can be categorized into five categories; toxic, explosive, Asphyxiant (suffocating), nontoxic, and radioactive (Hartman et al., 1997). The first gas that comes to mind is methane which is an explosive gas, especially in underground coal mines. However, other than methane, nitrogen, and carbon dioxide (asphyxiant), hydrogen sulfide (toxic), and other natural gases such as ethane, ether, gasoline, and kerosene (explosive) can be observed in an underground coal mine.

To start with, methane is an odorless, colorless tasteless, non-toxic but highly flammable gas, and it is lighter than air. This gas is generally associated with coal-bearing strata but also exists on the organic-rich strata and even in some metallic mines together with other natural gases such as butanes, hexanes, etc. While these other natural gases may affect the methane's explosive range, the range between 4.5% to 14.5% is taken as the explosive range for only methane. In addition, the

strongest explosions take place when the methane concentration reaches 9.5% (Hartman et al., 1997; Kissel, 2006).

Nitrogen, on the other hand, occurs in normal air inertly and has a simple suffocating effect. However, some of the oxides of nitrogen are highly toxic and dangerous. These gases such as nitrogen dioxide and nitric oxide can be formed from internal combustion engines and blasting. The acceptable short-term exposure to these gasses is 0.0005% (Anon., 1972; Hartman et al., 1997).

Another suffocating gas, Carbon dioxide can be formed from fire, internal combustion engines, breathing, and strata like methane. This colorless, odorless, and noncombustible gas is heavier than air and mostly accumulated near the floor. In normal air, the percentage of carbon dioxide is 0.3% but as carbon dioxide, in the air increases breathing requirement for humans increases gradually, and around 18% suffocation occurs. The short-term exposure level for carbon dioxide is 5% (Anon., 1972; Hartman et al., 1997).

Toxic and explosive gases that can be observed in a coal mine are carbon monoxide and hydrogen sulfide. While carbon monoxide is colorless, tasteless, and odorless, hydrogen sulfide has a rotten egg odor and acid taste. The primary source of carbon monoxide is mine fires, explosion, oxidation, and internal combustion engines. On the other hand, strata, groundwater, and blasting can be expressed as primary sources of hydrogen sulfide. The threshold value for carbon monoxide and hydrogen sulfide is 0.04% and 0.0015%, respectively (Anon., 1972; Hartman et al., 1997).

Among the natural gases, ethane is explosive and asphyxiant similar to methane. However, the concentration of this gas could reach only 2% in very deep coal mines. Therefore, mostly in the mine ventilation literature, ethane cannot be found in detail. Other gasses such as propane and butane, can be observed in a trace amount in coal mines, and sources mostly are leakage of natural gas piping close to the mine (Thakur, 2019). However, these types of gases should be considered because of the reservoir characteristic of the Bati Raman Oil Field. The table contains the upper and lower explosion limit for some natural gases at 20^{o}C and atmospheric pressure

depicted below. Additionally, the threshold values of the harmful gasses and oxygen are tabulated (Table 4) below according to the Turkish Occupational Health and Safety Regulations for Mines (*Maden İşyerlerinde İş Sağlığı ve Güvenliği Yönetmeliği*, 2013).

Table 3 Upper and Lower Limit for Natural Gasses and Fuels (Engineering ToolBox, 2003)

Natural Gas and Fuels	**Lower Explosive Limit (LEL)(%)**	**Upper Explosive Limit (UEL)(%)**
Butane (n-Butane)	1.86	8.41
Ethane	3	12.4
Gasoline	1.4	7.6
Hexane (n-Hexane)	1.25	7
Kerosene Jet A-1	0.7	5
Propane	2.1	10.1

Table 4 Threshold Values of Oxygen and Harmful Gasses

Gases	**Threshold Values (%)**
O_2	19.000
CO_2	0.500
CH_4	2.000
H_2S	0.002

Above mentioned gases could form in a possible MAHOP project, hence their removal and dilution are vital. One of the first steps to ensure the mine atmosphere to be safe is gas detection and monitoring and 3 matters should be discussed in this matter. Firstly, the threshold values of the harmful gases which are mentioned above should be acceptable. Secondly, measurement instruments should be suitable for the detection of tasses. Lastly, measurement location and frequency should be decided

(McPherson et al., 1993). Then, the ventilation system can be adjusted to dilute or remove the gases in the perimeter by providing the required amount of fresh air.

Except for these two sub-groups, there is another major challenge that is expected in the MAHOP project, called mine cooling. Due to the importance of this challenge in this research, this problem was investigated in another sub-topic called mine cooling.

2.3.2.2 Mine Cooling

This section will focus on the heat-related challenges encountered in deep underground mines and their sources. Additionally, potential solutions to address these challenges will be explored. Furthermore, the cooling mechanisms adopted by deep South African mines will be investigated.

2.3.2.2.1 Heat sources

Among the purposes of mine ventilation, providing adequate temperature and humidity for humans and machinery is another challenge for deep mines. Thus, the sources and the reasons for this problem should be assessed to overcome. McPherson et al. (1993) categorized the heat sources as; strata heat, auto-compression, mechanized equipment, fissure water and channel flow, oxidation, explosion, falling rock, and metabolic heat. Similar to McPherson, Hartman et al. (1997), listed the heat sources and added pipelines.

Strata heat exerted into mine is dependent on the parameters that Grave and Stroh (1972) stated in their research. These parameters are stopping length, advancement through face, air control and utilization, the temperature and the humidity of intake air, etc., mostly factors like depth of working area and virgin rock temperature are considered.

The relation between depth and virgin rock temperature can be explained by the thermal gradient. As the mine gets deeper and deeper, the temperature gets higher

due to the thermal gradient and the conductivity of the rock. This relation can be explained with a formula that McPherson et al. (1993) suggest.

$$\frac{d\theta}{dD} = \frac{0.06}{k} \qquad (8)$$

Where $d\theta/$dD is the geothermal gradient, θ is temperature, and k is thermal conductivity.

Generally, each stratum has a different thermal conductivity, hence calculating heat load for a specific depth could change with the rock type. In Table 5, thermal conductivity, and geothermal steps are given for certain rock types.

Table 5 Geothermal Step and Thermal Conductivity of Certain Rock Types (McPherson et al., 1993)

Rock Type	**Thermal Conductivity (W/m°C)**	***Geothermal Step (m/°C)**
Carboniferous	1.2-3.0	20 – 50
Clays	1.8	30
Limestone	3.3	55
Sandstone	2.0 - 3.6	30 – 60
Dolerite	2	33
Quartzite	4.0 - 7.0	65 - 120

* Geohermal Step = dD/ dθ

Even though the temperature of the virgin rock is estimated, without the calculation of heat transfer between wall rock and ventilation air is not represent the working environment temperature. Although there are some empirical approaches and numerical approaches to assess heat transfer, an exact mathematical solution is impossible. The complex nature of the air-rock interface, coupled with the presence of water, the irregular shape of underground openings and constantly changing temperature distribution make analyzing heat transfer very difficult. Also, Rock thermal property determination with accuracy is vital (Tucker, 1968; Vost, 1973). Therefore, simplification of the solution with assumptions is required for numerical

and graphical solutions. One of the most widely used a numerical solution is stated by Goch and Patterson (1940).

$$q = S\frac{k}{r_e}(t_r - t_d)\omega \qquad (9)$$

Where S is underground opening surface area in ft^2, k is thermal conductivity in Btu/h·ft·^oF, r_e is the hydraulic radius in ft, ω is Goch-Patterson heat flow coefficient, and t_r and t_d is the rock and dry bulb temperature of intake air in ^oF, respectively.

In order to find the Goch-Patterson heat flow coefficient, two different coefficients called rock thermal properties coefficient (ϵ) and thermal diffusivity (α) should be found first.

$$\alpha = \frac{k}{w_r c_r} \qquad (10)$$

$$\epsilon = \frac{\alpha\tau}{r_e^2} \qquad (11)$$

Where w_r is rock-specific weight in Ib/ft^3, c_r is rock-specific heat in Btu/Ib·^oF and τ is time in h. Additionally, the hydraulic radius of an opening can be calculated with the formula (7).

$$r_e = \sqrt{2}\frac{A}{O} \qquad (12)$$

A represents the cross-sectional area in ft^2 and O is the perimeter of the opening in ft.

Unfortunately, the virgin rock temperature of the Bati Raman oil field cannot be estimated within the scope of this project but the reservoir temperature is known as 65.5 ^oC (Sahin et al., 2012). Hence, the geothermal step can be adjusted to simulate the temperature of the reservoir.

Auto-compression is another heat resource that should be taken into account. Auto-compression is a heat transfer process consisting of the conversion of potential energy into enthalpy as a result of the downward movement of air or any fluid.

Converted enthalpy can be calculated with the formula stated by (McPherson et al., 1993).

$$\Delta H = \Delta Z g + q \qquad (13)$$

Where H represents enthalpy in J/kg, Z is height datum in m, g is gravitational acceleration in m/s^2 and q is heat added from surrounding rock in J/kg.

Due to the depth of the reservoir, the effect of auto-compression resultant heat transfer to the intake air is expected to be high. But unlike thermal gradient calculation, auto-compression integration into the ventilation simulation is expected to be done by software package. Therefore, heat flow related to the auto-compression will not be discussed in detail.

Heat flow from the broken rock is another source that affects the working environment. Excavated and hauled material's temperature will be close to the virgin rock temperature and heat transfer from loosened to the ventilation air will occur because of the temperature difference. The relation between the temperature difference and heat transfer can is depicted in equation 9 (McPherson et al., 1993).

$$\text{Heat load} = mC(\theta_r - \theta_a) \qquad (14)$$

Where m is the mass flow of rock, C is the specific heat of rock and θ represents rock and air temperatures. Although the mass flow rate will not be high in general in MAHOP, the temperature difference is expected to be high. It should be noted that, where the temperature difference between the rock and air is high, cooling requirements will increase and can reach up to 20% of all refrigeration requirements (Bluhm et al., 2014).

Another heat source that should be considered is mechanized equipment. In MAHOP, electrical loaders, drilling machines, and TBMs are expected to be used. In a TBM application, cutterhead and face interaction create heat together with fragmented rock and mucking process. On the other hand, an electrical drilling

machine or loader creates heat from the engines only. Hence, among this equipment, electrical loaders and drilling machines create heat relatively less than TBM. For example, in a deep underground mine case, the calculated heat created by TBM is almost 11 times higher. Although heat created from this equipment is known in this case, the equipment which will be used in the MAHOP project will not be the same. Therefore, estimations should be done according to the ratios stated above (von Glehn & Bluhm, 2000).

Lastly, other heat sources, such as groundwater, oxidation, explosion, falling rock, and metabolic heat affect the working environment temperature and are considered neglectable due to high reservoir temperature, high auto-compression effect, and lack of information about the groundwater properties.

2.3.2.2.2 Mine cooling methods

Artificial cooling started transporting ice blocks into mines with ore cars in the 1860s. However, the first usage of vapor compression refrigeration at the Morro Velho mine which is located 2400m below the surface in Brazil was in 1923 (McPherson et al., 1993). More advanced cooling systems such as high-pressure coil heat exchangers with chilled water implemented in the 1960s at Mount Isa in Australia. Nevertheless, the first surface cooling plant used a coal mine called Bowen Basin in Australia almost 3 decades ago (Belle & Biffi, 2010; Kamyar et al., 2016).

Nowadays, more advanced cooling systems are being implemented in deep underground mines all around the world. These cooling systems mostly consist of 3 phases according to Van Der Walt and Whillier (1978);

- Service water cooling
- Air cooling on main intake levels
- Air cooling on near stopes

However, Bluhm et al. (2014) separated the cooling systems as surface and underground refrigeration systems. Although these categorizations are different from

each other, the place of cooling of air in the mine is similar. In this research, the cooling systems are separated related to the refrigeration systems' location similar to Bluhm et al. (2014) study.

For the surface refrigeration systems which are commonly used nowadays, a central refrigeration plant room and refrigeration machines with a thermal store are used to cool down the air. Additionally, surface Bulk Air Cooling (BAC) at the downcast shaft to air cooling and service water refrigeration system to cool down service water is used (Bluhm et al., 2014). A typical surface BAC system is illustrated below (Kamyar et al., 2016) (Figure 10).

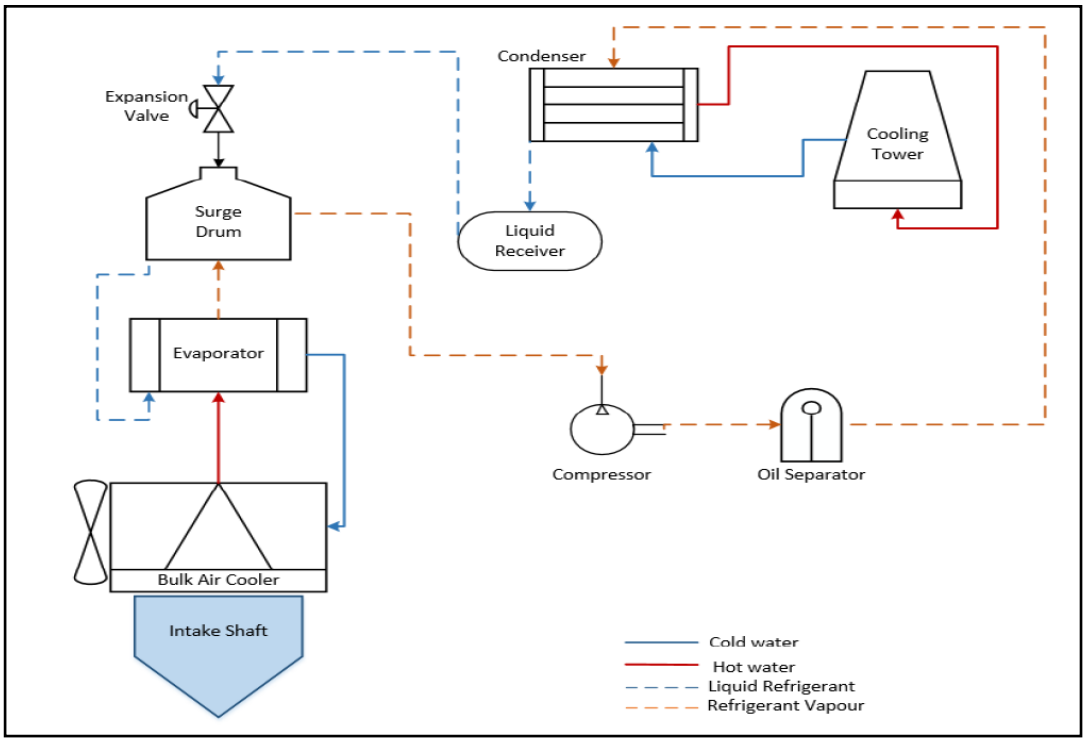

Figure 10 Typical BAC refrigeration plant located at the surface (Kamyar et al., 2016)

In a similar system, subzero glycol is utilized as a refrigerant for the main chilling operation. Then, chilled water, sprayed the intake air to cool down the intake air and reduce the auto-compression effect. Also, in such a system, chilled service water could be used for dust control and local cooling by spraying the fragmented rock or virgin rock.

On the other hand, an underground refrigeration system mostly consists of a central refrigeration plant with one or multiple refrigeration machines with a suitable distribution system and underground air coolers. For the multiple-machine arrangement, parallel-connected machines use R134a as a refrigerant to cool down the intake air to the places where the cooling is necessary (Bluhm et al., 2014).

Apart from these commonly used systems, different approaches have been tested in multiple deep and hot mines. One of the old applications is Withwaterand and Orange Free State Goldfields in South African mines. In this research, air-cooled with the chilled water spray method on the stopes right after the blasting operations. This system, shaft sinking and chilled water storage with suitable piping located close to the working faces are compared for mine ventilation and cooling process, and chilled water spray was found the more economical way to cool the stopes. However, the system was arranged to dilute the harmful gases created by the blasting, hence cooling process and dilution of harmful gases took 16 hours (Grave & Stroh, 1972).

Another different application is employed in Jinqu Gold Mine in China. In this mine, a downhole cooling system uses cold groundwater for the cooling process to decrease the overall ventilation cost. Although this method was successfully implemented in the mine, the application of the system is dependent on the groundwater conditions and temperature. In a case where the groundwater temperature is higher than the intake air, this method can be turned against the cooling process (Nie et al., 2018).

In another case that uses TBM for the excavation of faces below 3000 meters from the surface, utilize a heat exchanger which is placed on a TBM train. A ventilation duct system carried the intake air to the heat exchanger 300 meters behind the face, and the cooled air was forced to the working face with an auxiliary fan. However, this method was found to be relatively more expensive than the conventional type of cooled water spray method in the end (von Glehn & Bluhm, 2000).

In another case, small operational changes on commonly used cooling systems also test in the field. Among these changes cooling system, which is located in the

downcast shaft, is placed in the middle of the shaft to compensate for the heat created from the auto-compression and chilled services water usage on the mucked material to decrease the heat flow from the fragmented rock looked promised (Butterworth, 1999).

Lastly, Kamyar et al. (2016) study investigated current developments in the underground cooling system and described a new method implemented in the Bowen Basin mine. In that system, a heat exchanger is located in an opening parallel to the gallery which is hot intake goes through. Then, hot air re-directs to the heat exchanger with a ventilation door placed on the main gallery, and the cooling down process takes place in the opening. In this method, chilled water provided by the refrigeration facility located on the surface is used by the heat exchanger. In order to prevent chilled water from getting hot in the shaft, water cooled up to become a slurry of melting ice (Kidd, 1995). Although, Kamyar et al. (2016) stated that the long travel distance of the chilled water is costly and underground refrigeration systems are more economical, locating a refrigeration plant underground is disadvantageous because the heat rejection to the ambient air cannot be done underground (Ramsden et al., 2007). Therefore, using a hybrid system with both surface and underground refrigeration systems could be the most efficient way for mine cooling.

2.4 Cost Estimation

In this part of this study, capital and operational expenses for an underground mine project will be explained briefly. Then Estimation of both capital and operational cost estimation methods is investigated.

2.4.1 Mining Cost Structure

There are two distinct cost types for an underground mine project. Those are Capital cost and Operational cost. The sub-categories related to these major expenses could

be categorized according to cost occurrence time and variables that affect the amount of expense during production. The schematic that shows the structure of the expenses is depicted below (Figure 11). Capital investment is separated into two groups which are initial capital investment and working capital investment. In general, the difference between them is the timing of when the investment is required. Initial investment which is the investment required to start up the project mostly contains mine-site development, infrastructure, environmental compliance, license cost, etc. On the other hand, working capital investment is the investment required to continue the production non-stop after the project started, including equipment refurbishment of scrapped equipment, exploration cost, and mine-site development to reach the different parts of the orebody. Although operational cost seems similar to the working capital (stay-in-business), It should be noted that operational expenses are not covered by the working capital investment (Mohutsiwa & Musingwini, 2015; Rudenno, 2009).

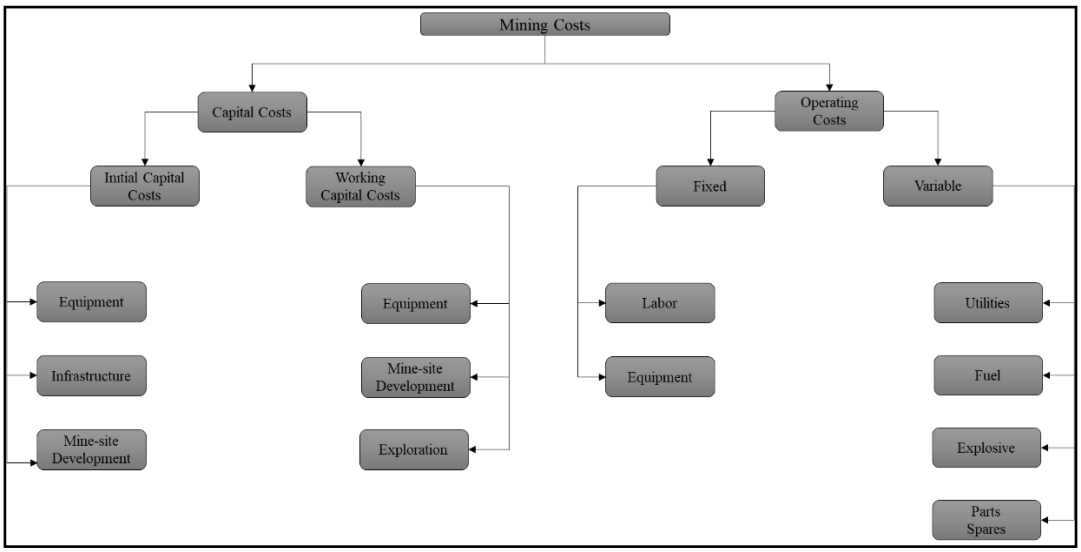

Figure 11 Mine Cost Structure (Mohutsiwa & Musingwini, 2015)

2.4.2 Cost Estimation Methods

In cost estimation methods, estimation methods will be separated into two groups: capital cost estimation and operational cost estimation. For each type of expense, methods used for mining projects will be explained.

2.4.2.1 Capital Cost Estimation Methods

The probable mine projects require capital and operational cost estimations to define whether the project is economically viable or not. However, the detail level of the estimation is depended on the stages of the operation. These stages can be defined as initial appraisal, preliminary feasibility study, etc. At each stage, the data required to estimate, and time spent on the study increases, while the error margin decreases between the estimated and real expenses.

The cost estimation methods for initial capital expenses which are related to the above-mentioned stages can be specified as, Order of Magnitude, Preliminary cost estimates, definitive cost estimates, and detailed cost estimates.

Order of Magnitude is a method mostly used for the initial appraisal stage, and the accuracy of the estimation is around -30 to +50%. In this method, cost capacity or cost capacity ratios are used to estimate the initial estimate. Preliminary Cost estimates accuracy is -15 to +30% and the details like the layout of the mine, equipment details, and flow sheets are used in this method. This method is mostly utilized in preliminary feasibility studies and the amount of time required to make such an estimation takes approximately several weeks. The definitive cost estimates error range changes between -5 to +15% and it takes months to finish. This method is in need of mine plans and layouts for the mining method, production capacity recovery, grade, dilution, process plan, all the equipment, etc. Lastly, Detailed cost estimates are the most accurate and time-consuming method of estimation. The error margin is expected to be between -2 to +10%. These estimates have been done

according to my finalized design of mine (Gentry & O'Neil, 1984; Turton et al., 2009).

In the early stages of the project, generally, the data required to estimate a project's initial capital investment is based on similar mining projects. However, the adjustments related to operation such as project site condition, mining method, and commodity prices should be implemented in the estimation (O'Hara & Suboleski, 1992). An example method uses a similar mining project proposed by O'Hara (1980). In this method, an exponential capacity factor of the project is multiplied by similar project expenses such as capital cost, equipment cost, stripping cost, etc.

In a more detailed method, called component cost ratio, capital cost items are estimated according to the detailly determined total installed equipment cost. On each item, cost coefficients are multiplied by the purchased equipment cost and summed at the end to estimate the initial capital cost. Different from that method of estimation, mathematical models like the parametric estimation technique could be used to estimate the cost of the projects. This model establishes a relationship between the physical or functional features of the projects and cost, making it a logical and predictable approach. This method could be helpful when there is a lack of information available and could be used in preliminary cost estimation (Mohutsiwa & Musingwini, 2015).

For projects that require more detailed investigation, capital cost items should be estimated separately. Sometimes, even the total expenditure of a project could be handled with different categories like Ostwald (1992). In his book, he separated the cost estimates into 4 sub-categories: Direct labor, direct material, and subcontract, facilities and equipment, and engineering. On each sub-category, the method of estimation could change according to the needs and the data availability. Those methods were comparison from another project, linear regression, historical quote, cost estimating relationship, etc.

Detailed methods like Ostwald proposed, could benefit from the cost estimation handbook published by an organization like AusIMM, CAPCOSTS, or CostMine.

These handbooks are mostly based on previous mine project data and estimate the expenses by using graphs and formulations (Shafiee & Topal, 2012).

More recently, with the development of artificial intelligence based on support regression models, new capital cost estimation methods are implemented in mining projects by Nourali and Osanloo (2019). This method utilizes 52 open-pit porphyry copper mines to estimate similar project capital estimation. However, one of the disadvantages of these types of methods is the requirement of available data and unfortunately, MAHOP is a unique project hence an ai-based estimation model cannot be implemented in this project.

For working capital cost, the estimation process is fairly different. This cost, as mentioned above, is the required amount of money other than the initial capital investment to keep the mining operation running after production is started. Unlike Mohutsiwa and Musingwini (2015), Gentry and O'Neil (1984) categorized the working capital investment into 4 groups cash on hand (payroll payment), accounts payable, accounts receivable, and inventories for spare parts, raw material, equipment refurbishment, etc. several methods are used to estimate these expenses, but the easiest methods are to take the 10-20% of initial investment as working capital or to observe the above-mentioned expenses for the first couple of months after the production started.

2.4.2.2 Operational Cost Estimation Methods

Operational cost estimation methods are similar to capital cost estimation methods in nature. Generally, while the cost items are different, methods used to estimate these expenses mostly change with the data availability and the project stages. Similar to the capital expenditures (CAPEX), early stages of the project, the estimations of operational expenditures (OPEX) highly are influenced by similar projects. The techniques known as the similar project method and cost-capacity relationship methods rely on the mining method, and commodity type, as well as the

geographical and geological characteristics of an already existing project. However, the reliability of these types of approaches is arguable and can be sometimes misleading. Thus, methods that are used for well-established mine plans, give more accurate results. For instance, the component cost method which relies on detailed mine planning utilizes the unit cost ($/ton) of the main development of a mine, overburden removal, and ore production to estimate the OPEX of a mining project. In a more detailed estimation, the mine plan should be finalized, and all of the components should be assessed in terms of labor and consumable consumption such as fuel, electricity, etc. Although this type of estimation requires more time and people, accurate OPEX estimation is expected (Blank & Tarquim, 1989).

Other than the above-mentioned techniques, using composite indexes and factor weights is another option to estimate both CAPEX and OPEX in the early stages of mine planning. The composite cost is a combination of various costs such as equipment, fuel, labor, etc. To update composite cost, an index is created from the weight factor. This factor indicates the relative importance of the cost item in the composite cost method. Cost figures are derived from similar mines and categorized into 15 different indexes. These percentages are utilized to calculate total expenses (Bullock, 2018).

In this chapter of this study, a detailed literature review was conducted about the Bati Raman Oil field, Similar oil mining cases, challenges related to tunneling, mine ventilation and cooling, and cost estimation. Bati Raman oil field location, reservoir properties, and geology of the area are discussed and previous oil mining cases which are located in Russia, Germany, and USA are investigated and similarities between the MAHOP project are evaluated. Then, challenges that are expected on a tunneling project and their solutions are taken into account. Similarly, problems related to mine ventilation and cooling, especially in deep underground mines are evaluated, and probable resolution to these problems is underlined. Lastly, the cost structure of a mining project is detailed, and multiple cost estimation methods are included.

CHAPTER 3

CONCEPTUAL DESIGN OF THE BATI RAMAN OIL FIELD

In this chapter, the production method of MAHOP will be explained in detail related to the implementation on the Bati Raman Oil field reservoir investigated according to reservoir properties, optimum working level, and applications to increase recovery. In addition, a simple production schedule and its details will be implemented in the research.

3.1 MAHOP

As mentioned above sections, MAHOP is a heavy oil production method that is assisted by the underground mining practice for the reservoirs that cannot be produced by any conventional production or EOR methods. This production technique uses the advantages of underground steam production to overcome the depth problem for heavy oil and/or depleted reservoirs such as Bati Raman Oil Field.

To start describing the main basics of the method, a similar approach that is used to planning conceptual design will be utilized. Firstly, the reservoir should be accessible from the surface in order to start the oil production with underground steam implementation. Similar to any other deep mining project, D&B, and continuous excavation operations are the options to reach the reservoir from the surface. However, due to the risk of the usage of blasting agents in possible methane-exposed openings drift, production gallery and declines excavation by continuous excavation machines like TBM is expected to be more suitable. In addition, for safety considerations and optimal production, multiple access into the reservoir is required. Although multiple surface access is required for such underground projects, the number of declines which is utilized to reach the surface is mostly dependent on the reservoir dimensions.

After the reservoir is accessible, steam is required to be distributed homogeneously to decrease the viscosity of the heavy oil within the whole reservoir. To distribute the steam within the reservoir, parallel drifts called production galleries should be excavated to cover almost all of the reservoir. The distance between these production galleries is dependent on the multiple variable stability of the openings, continuous excavator turning radius, maximum allowable angles at which fan-shaped boreholes can be driven, etc. In addition to the production gallery position alignment, the size of the opening may change according to the utilization of the production gallery except for the production of oil such as the dimensions of the largest equipment that will be transported, fan-tube diameter, conveyor belt dimensions, etc.

For the above-mentioned, fan-shaped aligned 30 cm diameter, 5 fan-shaped aligned boreholes will be drilled to heat the reservoir's upper parts and collect the low-viscosity oil. The borehole located at the center will be perpendicular to the tunnel roof, but the closest boreholes to the center of the roof and far-end boreholes' drilling angles are highly dependent on the distance between the production galleries and the reservoir. While the distance is increasing, the angles between horizontal and boreholes will be steeper. On the other hand, when production galleries are excavated in the reservoir gentler angles should be used to increase the range of steam which is reached into the reservoir. For Bati Raman Reservoir, after the optimum elevation for the production is calculated which will be detailly investigated later, the expected tunneling below the reservoir is 60%. Therefore, steep angles such as 70^{o} and 80^{o} between horizontal are illustrated in Figure 12. All these fan-shaped aligned boreholes will be perforated to protect the borehole structure and homogenously distribute the steam. Additionally, the distance between the two borehole sets will be 25 meters. Furthermore, all fan-shaped boreholes will not only be used to inject steam into the reservoir but also will be used to collect the more viscous oil from the reservoir. This indicates that the distance between steam injections will be 50 meters and one oil production borehole between them (Canbolat et al., 2022). Although, these preferences for boreholes are decided according to the Bati Raman Reservoir and can be applied for other depleted and/or heavy oil reservoirs, both the alignment

and the distance of boreholes may change in order to increase the recovery according to borehole length, project production rate, the viscosity of the reservoir, and steam quality. In addition, the steam pressure inside the steam injection boreholes is assumed to be sufficient to prevent oil leaking.

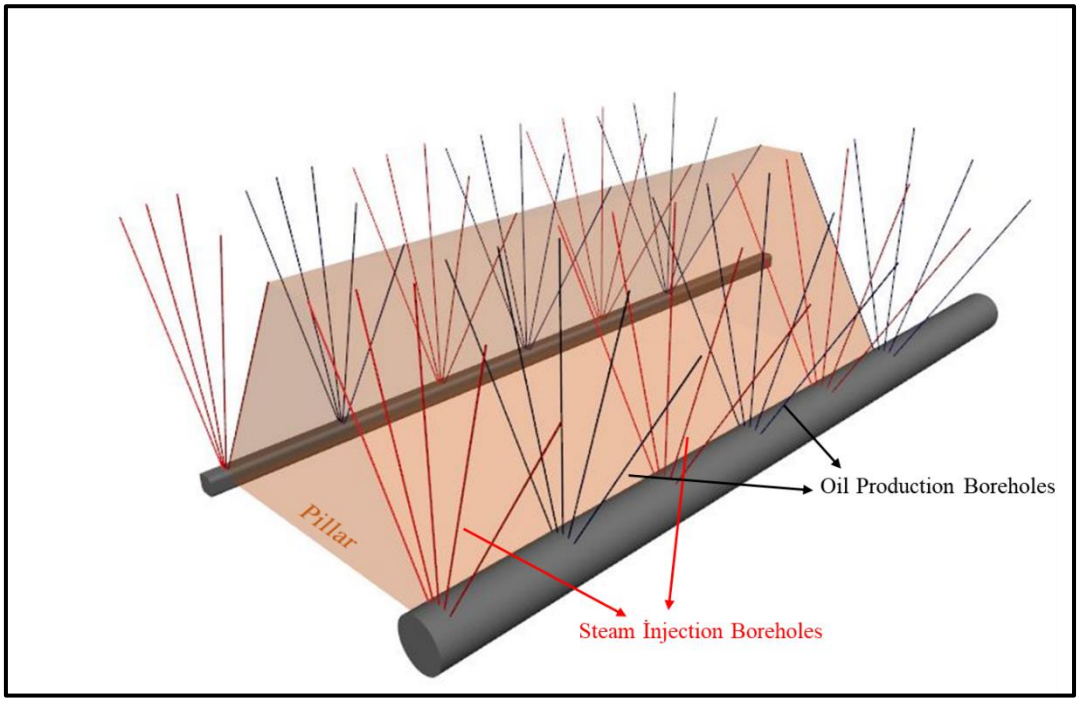

Figure 12 Fan-shaped aligned production boreholes

The steam which is used to decrease the viscosity of the oil will be produced by the steam generator within the reservoir to increase the steam quality. While the amount of steam that is going to be produced will only be related to the required daily productions, the location of the steam generator will be dependent on the distance to be traveled by steam from the steam generator. Because of the travel distance and the steam quality that is inversely proportionality, the position of the steam generator should be selected according to decrease the steam traveling distance to reach optimum steam quality.

After the steam injection started, a steam chamber will be formed within the reservoir, and decrease the viscosity of the oil with heat. Low viscous oil will be

collected through the oil production boreholes and directly send to the oil sumps. From these sumps, the oil will be pumped to the surface through high-capacity pumps that are used in the petroleum industry. Although, the oil viscosity will be decreased while transporting, the oil viscosity and the selected pumps are assumed to be sufficient to pump oil to the surface without choking the pipes.

Except for the MAHOP production, in those sites, there will be an auxiliary petroleum production will be done from the excavated material. As know from the above, some portion of the production galleries will be driven within the reservoir. This extracted oil-bearing rock could be processed to increase the overall recovery from the reservoir. In this method, the excavated rock will be transported to the surface processing facility by using both underground trucks and conveyor belts. Firstly, the excavated material will be loaded onto underground trucks with an internal conveyor to transport the materials to the conveyor belts which are located in declines. Then, the oil will be freed from the rock with the help of heat similar to the oil shale retorting method in the surface processing facility.

3.2 MAHOP Implementation on Bati Raman Reservoir

In this section, a conceptual design for Bati Raman oil production with the MAHOP method is detailly investigated by similar steps covered by designing the mine. Firstly, verification and construction of the 3D model of the reservoir. After that, the dimension of the production openings, the azimuth of the production openings, and the distance between the production opening selection will be included in the study.

3.2.1 3D Model of Bati Raman Reservoir

Similar to designing any underground mine, modeling the resource that is going to be extracted is one of the first things to do. In most cases, the creation of a resource 3D model required drill hole data comes from the field. Those data usually consist of the coordinates, depth, grade of each segment, and dip and dip direction of the

drillholes. However, in this case, only the depth and thickness of the reservoir data were available with the drillhole number. Therefore, the coordinates of drillholes are estimated by using the structural maps of Bati Raman which is depicted in Figure 13 (a). 133 drillholes are used to create the roof and floor planes of the reservoir. Then these planes are connected to create the 3D model of Bati Raman Reservoir. The verification of this model has been done by checking the location of the faults on both the structural map and the model. One of the comparisons between the map and model is illustrated in Figure 13 (b).

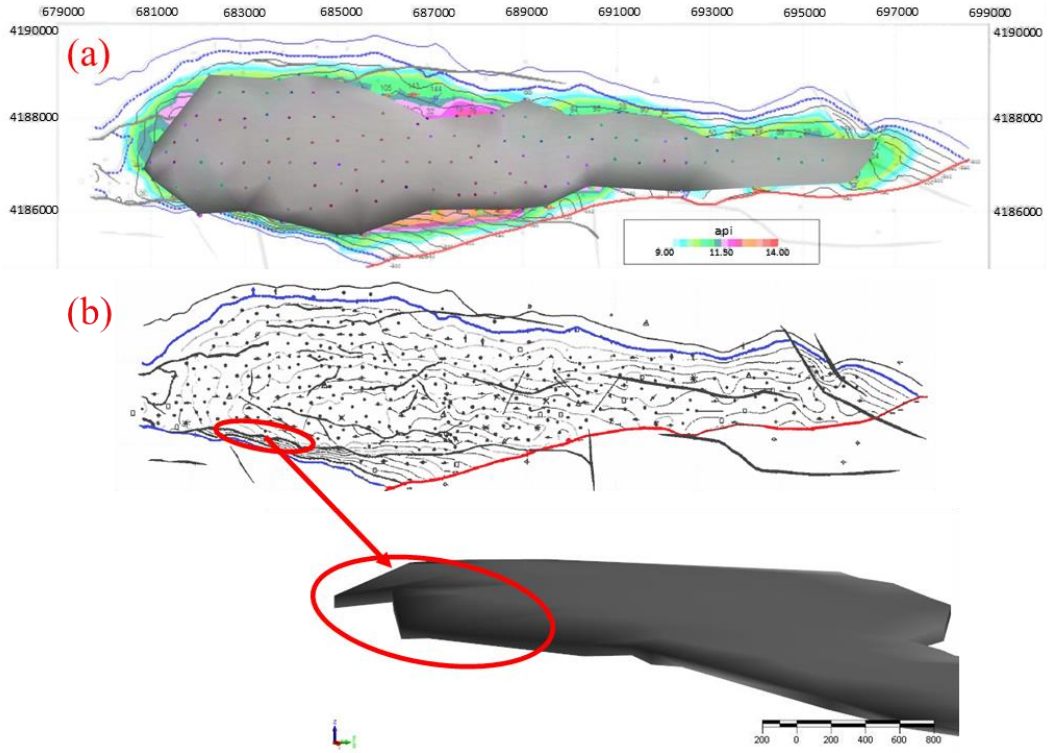

Figure 13 Structural Map of Bati Raman Reservoir and drillhole coordinates (a) (Sahin et al., 2012); Example Verification of 3D model with location of a fault (b)

3.2.2 Production Openings

After the construction of the 3D model, in the next phase of the implementation, dimensions, azimuth, elevation, and the distance between the production openings are detailly investigated.

Cross-sectional dimensions and tunnel profiles are restricted in drift excavations with the TBM. In addition, due to the nature of the TBM operating mechanism, the only tunnel profile available is a circular profile. Hence, the selection of diameter is the main aspect that should be considered. The diameter of the production galleries is mostly affected by the utilization of opening and rock mechanics. Because the rock mechanics are not the scope of this study, utilization of the openings is taken into account for selecting the diameter of production galleries. These openings will be used for the haulage of the excavated material, transportation of the equipment as well as oil production from the MAHOP. Therefore, the largest equipment which will be passed through should be estimated.

Although the equipment that is going to be selected was not certain, there are a few options, such as the underground trucks, raise borer, and steam generator parts. Among these machines or parts, steam generator parts are estimated to be the largest ones with 4.65-meter width. This parameter is found in the steam generator catalog provided by ICI Caldaie (*ICI Caldaie GX12 Bar Industrial Steam Generator Catalogue*, n.d.). An illustration of the production opening cross-section with the steam generator is illustrated below in Figure 14 and the radius is calculated as 10 meters according to the steam generator that is suitable for the daily production in Bati Raman (will be explained later). Detail of the calculations is depicted in Appendix – I.

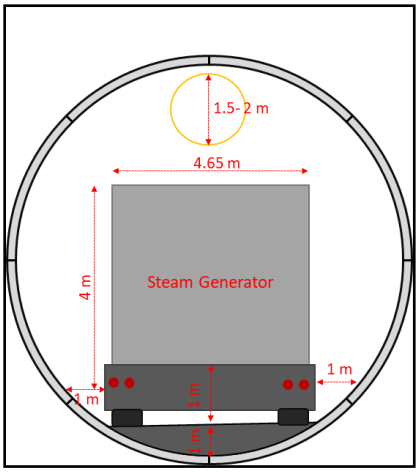

Figure 14 Cross-section illustration with steam generator

After selecting the tunnel diameter, the azimuth of the production galleries is decided according to the number of turns and the length of the possible production galleries. As stated in the literature review, one of the operational difficulties while excavating the openings with the TBMs is changing the excavation direction. Additionally, as the name implies these types of continuous excavation machines, cannot be moved or transported to another section of the mine without dismantling. Therefore, continuous production openings with a minimum number of turns are required to ease the excavation operations. So, azimuth of 90^{o} from the north which is the direction of the longest dimension of the reservoir leads to a minimum number of turns.

Another problem that possibly arises while designing the location of production galleries, is the selection of the distance between two parallel drifts. Generally, the TBM operations are not mobile as the D&B operations in mining, especially in terms of turning radius. Hence, the distance between the production galleries is determined by the turning radius of the TBM which are going to be used. Although 10-meter or higher diameter TBMs used in projects, the turning radius information is not available in the literature. Nevertheless, a turning radius estimation from the previous data can be done by using the smaller and the larger diameter TBM used in different

civil and mining projects. While, in some projects, an 8-meter diameter TBM's turning radius is 160 meters. On the other hand, for larger (12-meter diameter) TBMs turning radius is stated as 350 meters(TBM STAFF, 2017; TMRG, 2020). From this information, a 10-meter diameter TBM's turning radius is estimated as 250 meters.

However, a 500-meter distance between the two production openings results in another crucial problem for the oil production with MAHOP which is the recovery. While the distance between the drifts increases the fan-shaped borehole's length increases proportionally. Therefore, the steam that reaches the reservoir is getting cold and leads to steam being low-quality. To overcome this problem and to decrease the distance between the production openings, another continuous excavation equipment is selected to excavate the production openings between the two parallel TBM openings. These continuous miners have smaller diameter and length compared to the TBMs that is going to be used in this project which helps excavate closer production openings. Although, these continuous miners have a turning radius of 13 meters, the distance between openings is selected as 62 meters because of the previous rock mechanics studies related to the MAHOP (Emci & Ozturk, 2021). Furthermore, the openings that are going to be excavated by the continuous miners are planned to be served only for MAHOP oil production due to the dimension of the openings.

3.2.3 Optimum Production Level

In the early part of the project, production openings are planned to follow the base of the reservoir to increase the overall recovery of the project. However, one important part related to methane concentration changed the design of the production galleries. As stated in the literature review part, methane is a highly flammable gas, especially 9.5% concentration in the air and it is lighter than the air. Therefore, the accumulation of methane on the roof specifically poses a threat where the openings that have positive gradient change to negative gradients of the working environment. To eliminate this problem, production openings are designed to be flat on each part

of the reservoir. Nevertheless, this new design has created another problem related to the overall recovery.

Although the reservoir can be described as tabular, undulation on the base and roof and the fault zones are affecting TBM implementation. Even TBMs can excavate with a gradient, following the undulating base of the reservoir is not possible. Hence, an optimum flat operating level for production should be selected.

In order to define the optimum level for MAHOP production, it is necessary to identify key factors that affect recovery. There are several parameters that influence the production recovery such as steam quality, volume reached by the boreholes, length of the boreholes, oil properties within the reservoir, etc. However, two parameters have been identified as particularly effective for oil recovery. One of the parameters is the covering percentage of fan-shaped boreholes in the reservoir. This parameter can be described as follows: if the production openings get deeper the volume that is reached by the fan-shaped boreholes is increasing which is result in the increasing production recovery from MAHOP. The other parameter is the effectiveness of the boreholes that are going to be drilled at the roof of the production openings. To describe this parameter, while the borehole length increases the leakage of the steam increases gradually, and for the deeper openings the distance that steam travels in waste increases. To increase the efficiency of the borehole, the borehole length below the reservoir should be taken as low as possible. To select the optimum elevation for production, the highest recovery with the highest borehole efficiency should be chosen.

To calculate the covering percentage of boreholes, a series of volume calculations have been done on Micromine (Micromine Pty Ltd., 2022). These volume calculations started with the reservoir separation into two eastern and western parts and the details of this separation will be introduced in the mine layout part. Then, the top 5-meter portion of the reservoir which acts as a pillar, is deducted from the original volume to create the recoverable reservoir. From this volume, below the 13

different planes that represent the production levels are removed to calculate the producible reservoir for each production level.

On the other hand, to estimate the efficiency of the boreholes, fan-shaped boreholes are created on the planes that are utilized to calculate the producible reservoir. The total number of boreholes is decreased to one eight to ease the computational overburden resulting from the 3D volumes. After that, boreholes are trimmed with the base of the reservoir to calculate the distance driven into the reservoir, and the efficiency is founded by dividing the borehole length in the reservoir by to total borehole length (Equation 15).

$$Borehole\ efficiency\ (\%) = \frac{Borehole\ Length\ in\ the\ Reservoir\ (m)}{Total\ Borehole\ Length\ (m)}\ x\ 100 \quad (15)$$

From these calculations for both the eastern and western part of the reservoir, two curve which is recovery vs. borehole efficiency according to production levels has been created to find the optimum level from the junction of these curves.

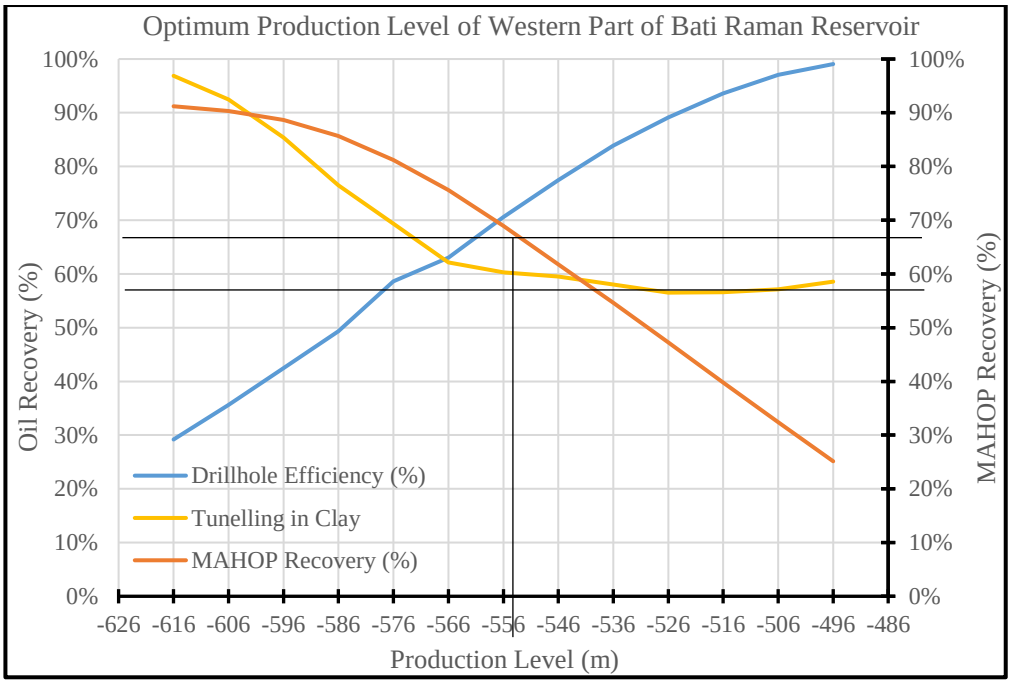

Figure 15 Optimum Level Calculation Curves for the Western Part of Bati Raman

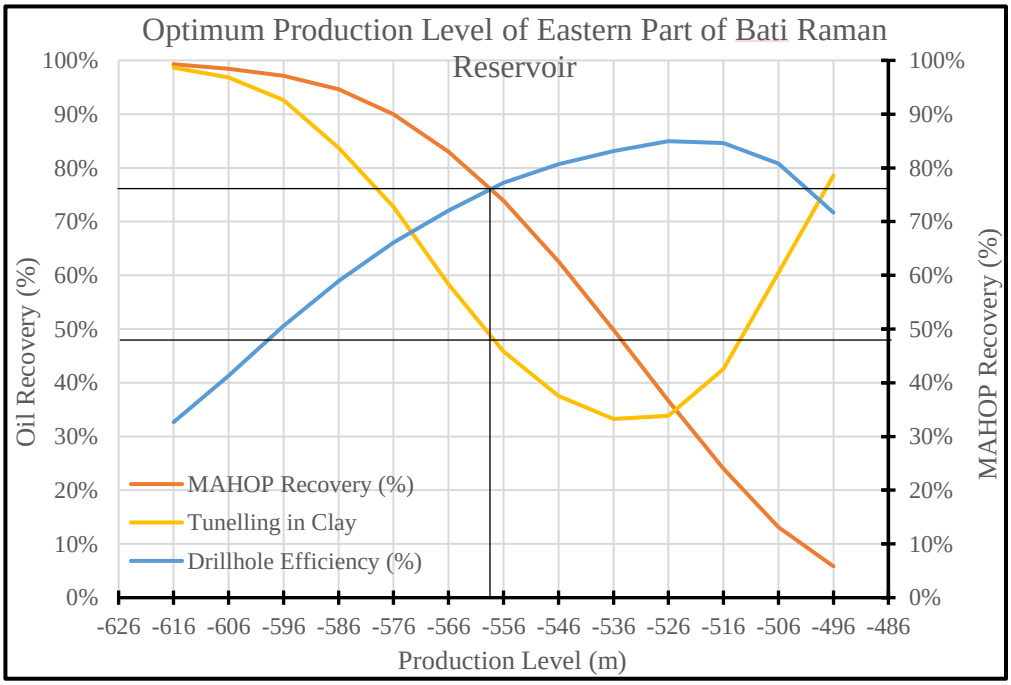

Figure 16 Optimum Level Calculation Curves for the Eastern Part of Bati Raman

According to Figure 15 and 16, optimum levels for both portions of the reservoir is almost the same at -558 meter. For the western part, 69.6 % recovery is attained with 69.6 % of borehole efficiency. On the other part of the reservoir, 76.2% recovery was achieved with the same percentage of borehole efficiency. Additionally, respective tunneling was created in 3D on the program to calculate the volume of excavations done into the reservoir. The volumes inside of the reservoir are trimmed and used to calculate the percentage of excavation done into the Bati Raman Reservoir. According to the results, 60.2% of the TBM excavation is done below the reservoir in the western part. For the western part, 48.4% of the excavation took place below the reservoir. The data used to create these graphs are available in Appendix I.

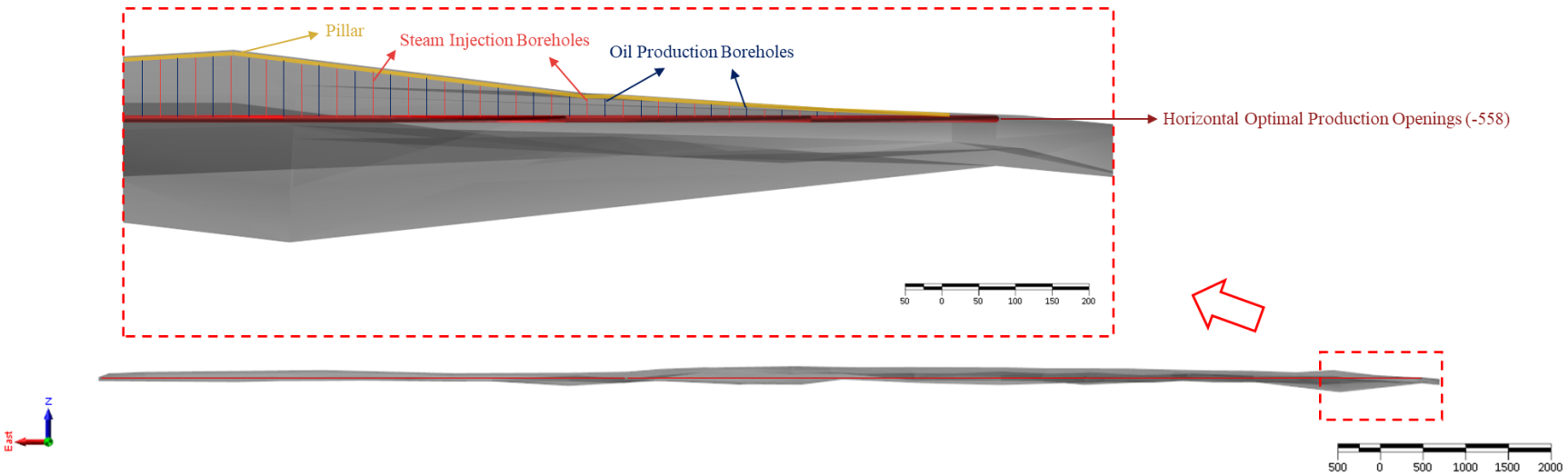

Figure 17 Optimal Production Opening and Boreholes Illustration (Side View)

3.2.4 Mine Layout

This section is separated into four main groups production galleries, declines, cross-cuts, and underground facilities such as TBM assembly stations and steam generators. In each part, processes that are used and problems which is expected while designing are discussed. Lastly, an overall mine layout will be introduced at the end of this part.

3.2.4.1 Production Galleries

After deciding the optimum working level concluded, the mine layout of MAHOP in Bati Raman is initiated with the position decision of the first production opening. Firstly, a production opening which is not smaller than 1 km is created at the northwest part of the reservoir. Then, parallel openings that are going to be excavated with TBMs are placed 250 meters south. Although the turning radius of a TBM is taken as 250 meters, two TBMs are expected to work simultaneously on the northwest part to decrease the excavation times. Because of this approach, nested production openings created a junction. A proper connection is required to provide good stability. Therefore, the location of junctions between the two openings was selected to be as straight as possible by connecting the two production galleries at the midpoint of the half-circle curve (Figure 18) Also while designing the connection between production openings, sequential and continuous excavation tried to be satisfied for each TBM.

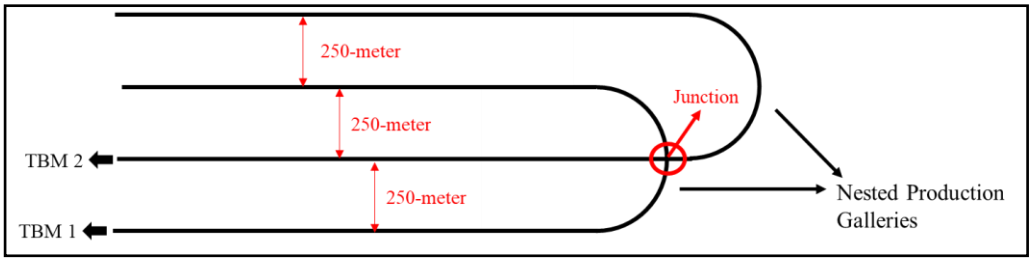

Figure 18 TBM Nested Production Galleries Excavation Layout

For the drifts that are going to be excavated by a continuous miner are planned to be driven between the two production openings 62.5 meters away from each other. Initiation of the excavations within the 10-meter diameter production galleries occurs after the TBM progressed for a couple of meters. Similar to the Production galleries opened with the TBMs, the connection between the openings is really important. There are several patterns are tried to connect the openings, but a pattern which can be seen below (Figure 19) is selected to be more suitable for this project without creating the number of junctions underground and using 3 continuous miners to decrease excavation time. In Figure 19, the first and the second layout from the top, excavation is done by 2 continuous miners and this restricts the production cycle in terms of the excavation rate. In addition, a junction would have been created in the first possible layout. Hence, the last layout which is excavation done by 3 different continuous miners is selected to be used in this study.

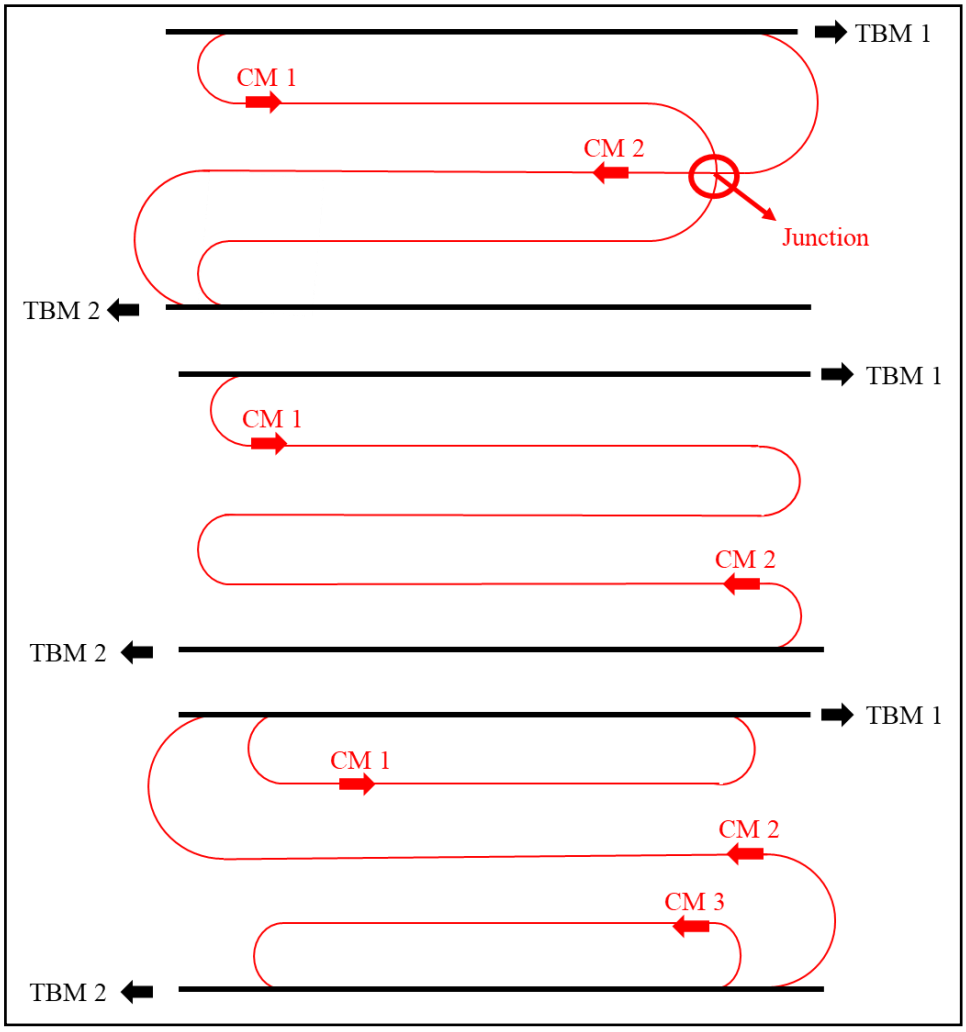

Figure 19 Continuous Miner Excavation Possible Layouts

3.2.4.2 Declines

After all the openings' locations and connections are planned, 6 different declines are created with a negative 15 percent from the surface. The number of declines is decided by the number of TBM that are going to excavate the production openings. Each of the 2 TBMs is grouped to create the nested production galleries and assigned to three different parts of the reserve according to the excavation length. Consequently, the western part of the reserve was excavated by two groups of TBMs, while the eastern part was planned to be excavated by only one group.

In addition to the decline design, the location where the declines reach the surface is called the portal. The portal location of the underground mine can state a problem, especially for the deep underground mine. The reasons for this can be stated as follow: the gradient of the declines is restricted by the equipment's maximum climb ability. Mostly the maximum grade that equipment can climb will restrict the declines to be excavated with gentle gradients. Hence, while the depth of the mine increases the horizontal distance of the excavation is increasing and may exceed the mine limits. Furthermore, the infrastructures and facilities above the surface may limit the construction of the portals in those areas. Therefore, for the Bati Raman Reservoir, these restrictions were taken into account and implemented for an average of 8.5 km long 6 declines.

3.2.4.3 Cross-cuts

As known before, because of the nature of the MAHOP production method, production galleries should cover the area of the reserve as much as possible to be able to increase the recovery of the heavy oil on the reserve so that, production openings will be longer than any usually underground mine. Thus, the transportation distance of the equipment and the excavated material can be excessive, especially in the middle portion of the western part of Bati Raman Reservoir. To overcome this problem and make the working environment in the reservoir safer, a cross-cut design was planned for the MAHOP implementation. These cross-cuts should be as large as the production galleries that are excavated by the TBM to transport the largest steam generator parts. Due to the reasons that are explained in the production opening's part and the dimensions of the openings, these cross-cuts are planned to be excavated with a 10-meter TBM similar to the production openings. Because these openings are opened with TBM, the sequential and continuous excavation leads to a similar approach to production openings. Unlike the production openings, the intersection of the cross-cuts and production openings are perpendicular, therefore different patterns were not tested. However, in some regions of the reservoir, the location of

the half-circle curvatures is adjusted according to the production openings to increase the overall recovery without decreasing the production gallery length. In addition, the initiation of the excavation by the TBM was another problem that needed to be overcome. There are two different ways is evaluated. Firstly, like the production openings, TBMs can start the excavation from the surface with the declines, but an excessive number of declines would have reached and the inactive declines could have been only an economic burden to this project. For the second approach, TBM assembly stations planned to be opened parallel to the midpoint of the half-circle in 3 different positions. From these stations, TBMs were planned to start to excavate cross-cuts continuously until all of the production galleries is accessible. The details of the TBM assembly stations are mentioned in the next part of this chapter.

Another specification that needs to be discussed is the distance between the two parallel cross-cuts. To decide the optimum distance, a series of haulage simulations from a random point has been done. In those cases, 250-meter, 500-meter, and 1000-meter distant cross-cuts are utilized for a haulage operation from the random point to the start of the decline, and the cycle time of the equipment is calculated. A representative figure of cycle paths is depicted below (Figure 20).

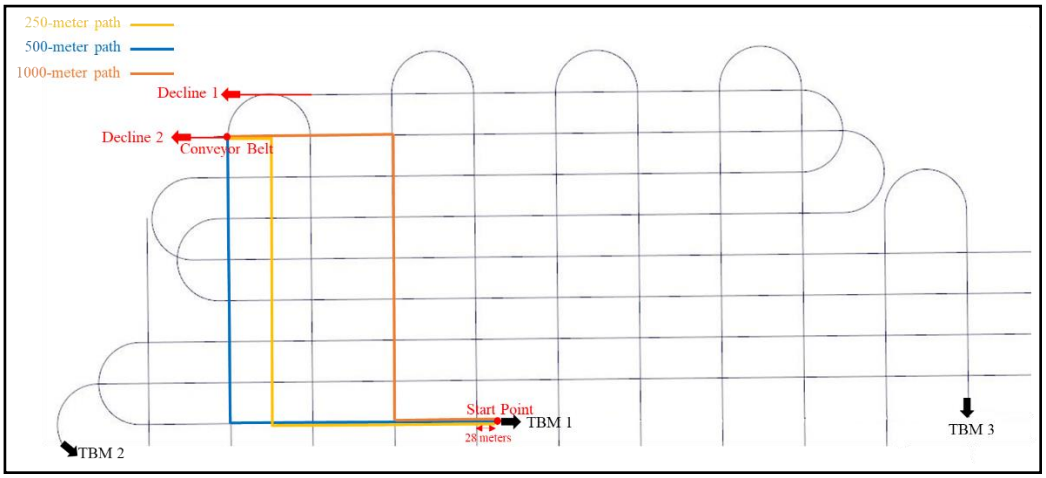

Figure 20 Path of a Truck in a representative cycle

Generally, the parameters that influence the cycle time are mostly the grade and distance of the haulage way, the driver experience, and the travel speed of trucks. The hauling distance calculations have been done for each case (Appendix I) and haulage distance for 250-meter, 500-meter, and 1000-meter distant cross-cuts is approximately 1965.5 meters for all options. For the other parameters Due to the design of the underground mine, the grade of the haulage way is the same for every opening as 0. To eliminate the experience of the driver and travel speed of trucks, spotting, maneuvering, and dumping time is taken as 200 seconds with the same travel speed for loaded and empty travel (Epiroc, 2020) for each case. With these assumptions, the cycle time of each case is calculated as 15.13 min. It can be deduced from these calculations that the importance of the distance between the conveyor belt and the cross-cuts is more vital than the distance between the cross-cuts. Hence, the location of the cross-cuts was arranged according to the decline position of the mine to reach optimum cycle times. Additionally, the distance between the cross-cuts is selected as 500 meters in order not to create nested cross-cuts and to decrease the distance required to travel in an emergency.

3.2.4.4 Underground Facilities

Other than the main layout of the mine, there are auxiliary facilities that are used for multiple purposes such as maintenance, ore crushing, or transportation. Unlike the common underground mines except for maintenance areas, other facilities will not be required. However, different type of facilities for different purposes is going to be used in Bati Raman Reservoir. One of the auxiliary facilities that is planned to be opened is the steam generators. These cubic openings will be placed at the center of each panel with a dimension of 30 meters on each side. The size of these openings is decided by an expert in steam generators who is working for the Akkaya Boilers company. The position of the steam generators was decided to be at the center of the panel to optimize the steam quality that reaches the reservoir while decreasing the travel length of the steam.

Another facility that is going to be discussed is TBM assembly stations. As with most equipment, TMBs have an operating life span. Although, the life span is dependent on multiple conditions like the strength and structure of the surrounding excavations, in the literature a general life span is stated as 10,000 hours or 4.5 km (Harding, 2019). When the excavation length is excessively similar to MAHOP implementation, several replacements of the TBMs are expected throughout the excavation operation. Therefore, stations that are going to be used to replace TBMs will be implemented in the mine layout. These stations can be separated into two TBM reassemble stations and TBM assemble stations for the TBMs that are going to be excavated cross-cuts. The design of these stations is taken from similar stations that are used in civil engineering projects and adapted to the TBMs will be used in the Bati Raman Reservoir. According to the assembly chamber used in the Gerede Water Tunnel, (Figure 21) that is created for a 5.6-meter diameter TBM, assembly stations in this project have a dimension of 25 meters in width, 20 meters in height, and 50 meters in length planned to be excavated.

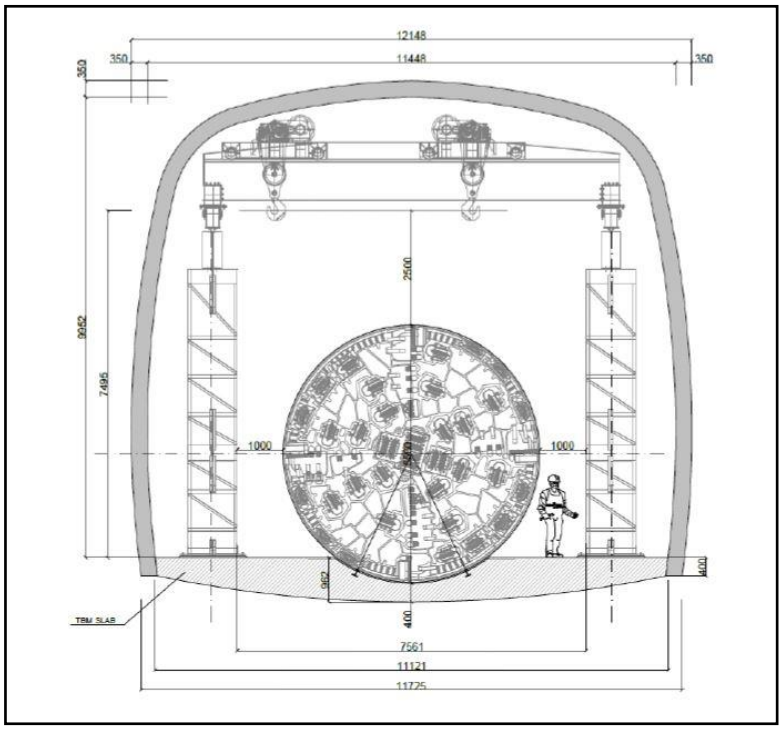

Figure 21 Gerede Water Tunnel TBM Assembly Chamber Plan (Grothen, 2018)

For the assembly stations that are utilized for the TBMs are going to be excavated in a similar manner that is used for reassembling stations. The main difference between these two types of openings is the width of the station openings. The width of the assembly station will be 50 meters because in the assembly station, two almost parallel TBM will be constructed within the openings and while one of the TBMs continues to excavate the production openings, the other one starts the excavation of the cross-cuts after the assembly. To evaluate the feasibility of this tunnel application underground, some of the civil engineering projects are evaluated and a similar junction is found in the Chicago Tunnel and Reservoir Plan (TARP)(Metropolitan Water Reclamation District of Greater Chicago, n.d.).

Both of the facilities that are discussed in this section are planned to be excavated and enlarged by the road headers. Even though the dimensions of this equipment will not be sufficient for the 20-meter and 30-meter heights of the openings, broken material will be left and arranged to use as leverage to reach higher elevations.

3.2.4.5 Overall Mine Layout

A combination of the above-mentioned designs created an overall design for the MAHPO implementation of Bati Raman Reservoir. Figure 22 depicts the production galleries together with the cross-cuts, declines, and underground facilities. According to this design, 6 TBMs are used to simultaneously excavate the first 73 km declines then nearly 115 km of production galleries, while 18 continuous miners are employed to drive 276 km of production galleries. Additionally, 73 km long cross-cuts are anticipated to be opened using 3 TBMs identical to those used for excavating the production galleries. Almost 464 km of openings without declines are required to implement MAHOP in the Bati Raman Oil Field, with approximately 58% of these openings being excavated below the reservoir base (Table 6).

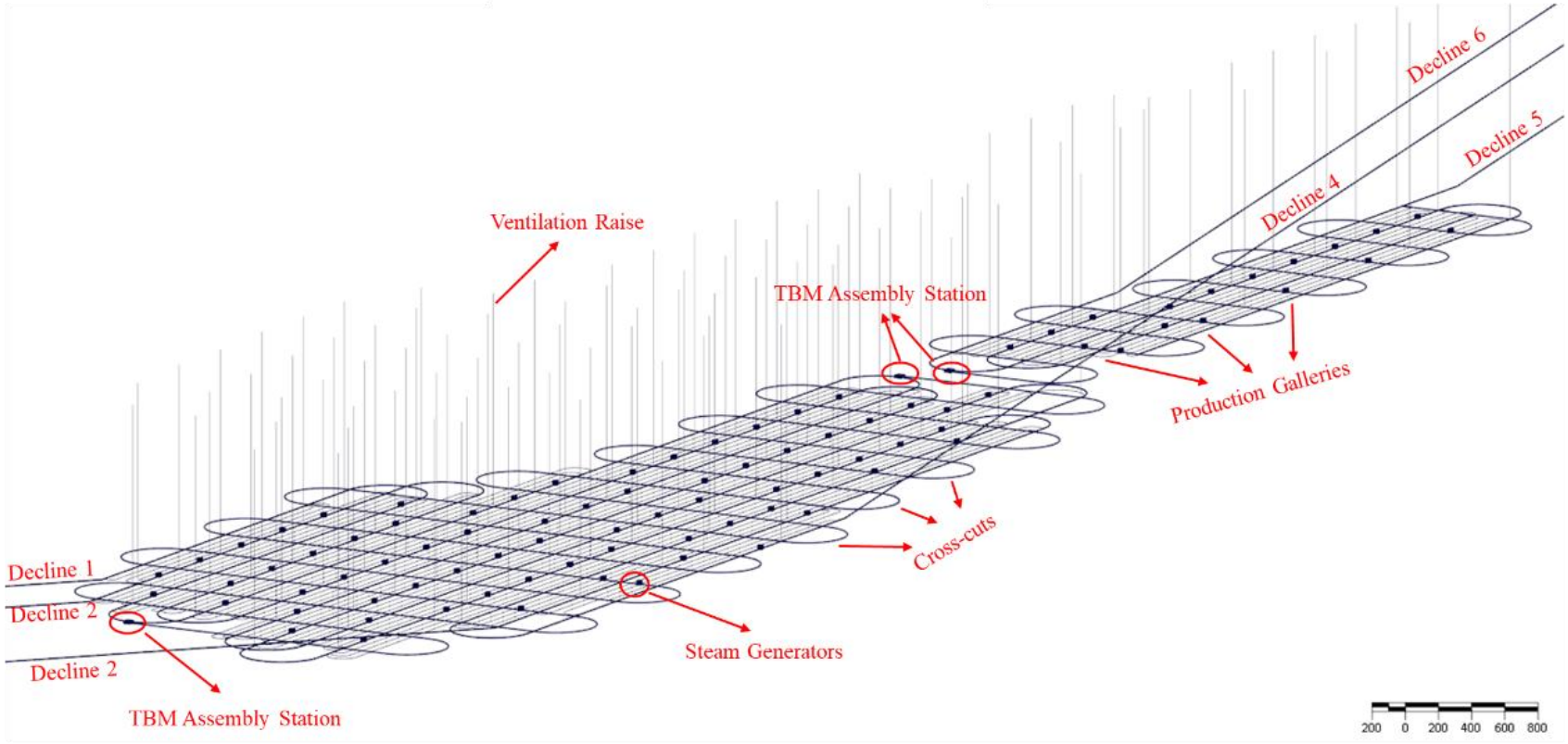

Figure 22 Overall Mine Layout of Bati Raman Reservoir

To initiate the cross-cut excavation 3 TBM assembly stations on the west and the middle of the reservoir were placed. In this layout, 88 steam generator locations can be seen in Figure 22. However, it should be noted that the 88 steam generator locations will not be operational throughout the mine life of the project.

Table 6 Underground Openings Details

Underground Openings	Length (m)	Width (m)	Height (m)	Inclination(°)
TBM Openings (Production Galleries)	114,705	10 (Circular)	x	0
Mobile Miner Openings	275,554	4	4	0
Cross-cuts	73,081	10 (Circular)	x	0
Declines	48,889	10 (Circular)	x	9.68
Fan-Shaped Aligned Boreholes	5-83	0.3 (Circular)	x	90-80-70
Panels	562.5	500	53.15	0
Steam Generators	30	30	30	0
TBM Assembly Stations	50	50	20	0
Ventilation Raise	1,250-1,600	1.5 (Circular)	x	90

3.3 Production of Bati Raman Heavy Oil Reservoir

In this part, a brief production schedule is studied to evaluate economically of this project in Chapter 5. Because of the complex structure of the excavation, exact production scheduling could not be done, but average oil production is estimated. The calculations and the parameters will be explained and an overview of production represented here.

3.3.1 MAHOP Production

To start with the production in Bati Raman Reservoir is divided into sectors and panels to ease the calculations and separate the ventilation system to supply the required amount of fresh air into the working environment.

Sectors are a small component of the production with a length of 50 meters (the area between two steam injection boreholes) that includes two sets of steam fan-shaped boreholes and one oil production borehole. On the other hand, the panels are the main production units for this project which is quite large compared to the sector. These panels are 500 meters long that include a total of 9 500-meter production galleries. The length of the production galleries is selected to ease the separation from each other with the cross-cuts Illustration of these two major components of the production is depicted in Figures 23, 24, and 25. As can be seen in Figures 23 and 24, 88 panels are predicted to be constructed with an almost identical area. 71 of them are located in the western part of the reservoir and the other 17 one is planned to be in the eastern section. In addition, it should be noted that the naming of the panels is not representing the production sequence.

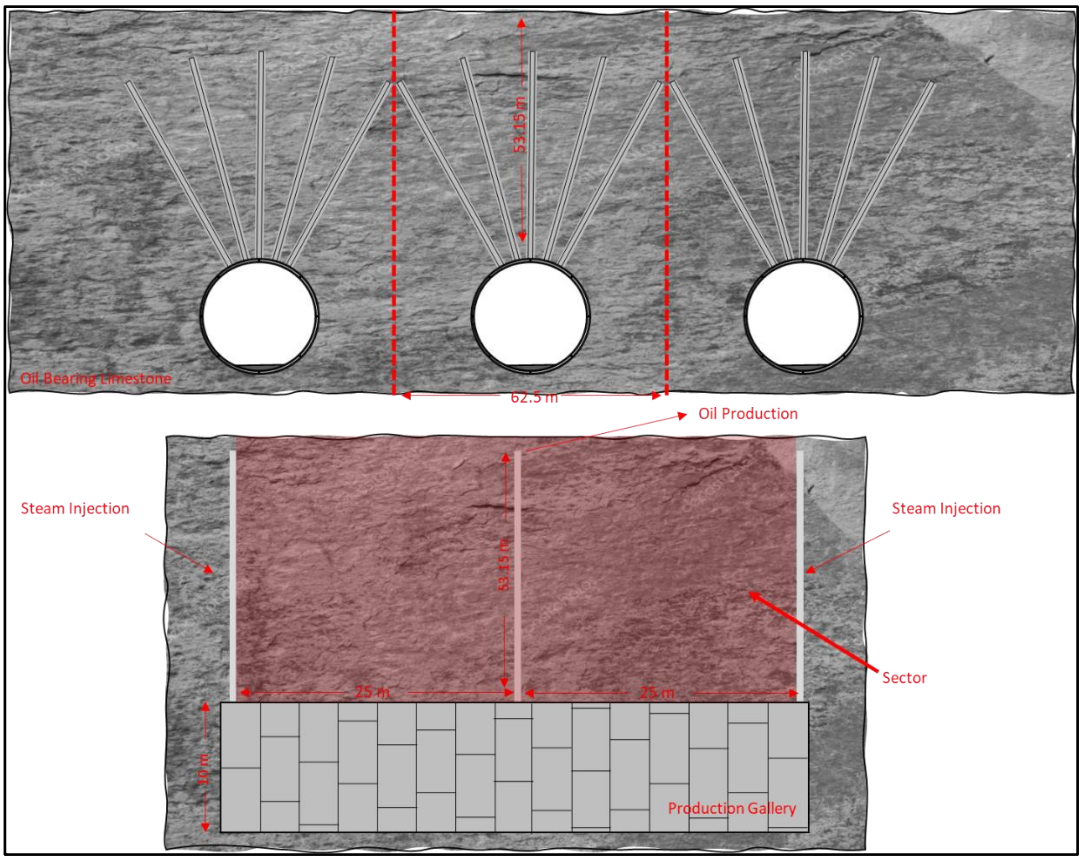

Figure 23 Sector representation of Bati Raman Reservoir

Figure 24 Panel Illustrations in the Western Part of Bati Raman Reservoir

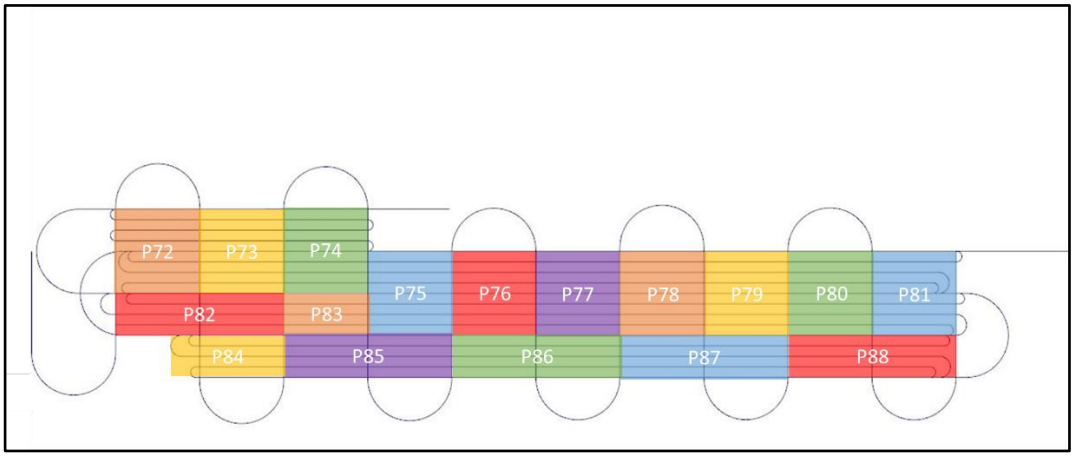

Figure 25 Panel Illustrations in the Eastern Part of Bati Raman Reservoir

After the panels are created the production amount from a panel and a sector can be calculated. The parameters that are used to calculate the producible amount from the production units are shown in Table 7. These parameters that are used are mostly taken from the experimental scaled model created by Canbolat et al. (2022).

Table 7 MAHOP Production Parameters

Parameters	
Daily Required prod. (Barrel /Day)	250,000
Porosity (%)	20
Oil in Pore (%)	75
SAGD on surface Oil Recovery (%)	70
MAHOP Recovery (%)	70
Steam Oil Ratio (SOR) MAHOP	9
Steam Generator Efficiency in UG (%)	50
Steam Generator Availability (%)	83
Steam Specific Volume at 130 Celsius and 4 bar (m^3/kg)	0.3475
Hourly Steam Production from one generator (kg/h)	20,000
Number of Mobile Miner	18
Number of TBM	9
TBM Daily Excavation Length (meters)	10
Mobile Miner Daily Excavation Length (meters)	7.5
Total MAHOP excavation Length without x-cuts (meters)	390,490
Total Tunneling below the reservoir (%)	57.82

To start with the daily production amount of Bati Raman Reserve, the predicted reservoir of Bati Raman (1.85 million barrels) is divided into 20 years of non-stop oil production. According to this simple calculation, the production amount is estimated to be 250,000 barrels/day. However, to justify this production from the experimental studies that have been done by Canbolat et al. (2023), a series of calculations are required. To be able to compare the production ratios between the experimental model and the possible field implementation, the ratio of daily oil production to steam chamber volume is taken directly proportional to the same ratio created by the field. According to the Experiment, 12,562.4 ccs of oil is produced from a steam chamber with a volume of 43,200 ccs (50x48x18 experiment dimensions). This will lead to the ratio of oil production to steam chamber volume to be as 0.29. If this same ratio is used to calculate daily production from the field steam chamber 2,982,930 barrels of oil should be produced. However, in these calculations, one of the major parameters that affect the production is ignored which is the steam injection amount and rate. To reach the daily production proportional to the experiment data, almost 70 tonnes of steam should be injected. To adjust the oil

production to 250,000 barrels/day, The Steam-Oil Ratio (SOR) that comes from the experiment will be used. The oil produced in cm^3 and rate together with Water Oil Ratio (WOR) in the MAHOP experiments is depicted below.

Table 8 MAHOP experiments at different wettability (Canbolat et al., 2023)

MAHOP Configuration	**Rate (cc/min)**	**Oil Recovery (cc)**	**Cumulative WOR (cc/cc)**
3 Fan Mixed-Wet	2.66	7084	12.79
3 Fan Oil-Wet	2.66	8453	11.11
3 Fan Water-Wet	2.66	9517	8.33

The steam injection rate of this experiment is 80 cm^3/min and the oil production at the end of the experiment which is 1000^{th} min is 9,517 cm^3. The ratio between oil production and total steam injection is calculated as 8.4. However, in this application, the SOR value is taken as 9.

Although the SOR ratio is implemented in the daily production calculation, expecting a uniform production of 250,000 barrels/day for every day will not be realistic for a panel. To explain the start of the oil production within a panel, firstly steam chamber should be formed to decrease the oil viscosity within this chamber. After the steam chamber is formed, oil production will gradually increase to a maximum level of production. To illustrate the expected production rate that is going to take place in Bati Raman, the cumulative oil production vs time graph from the MAHOP experiments can be seen below.

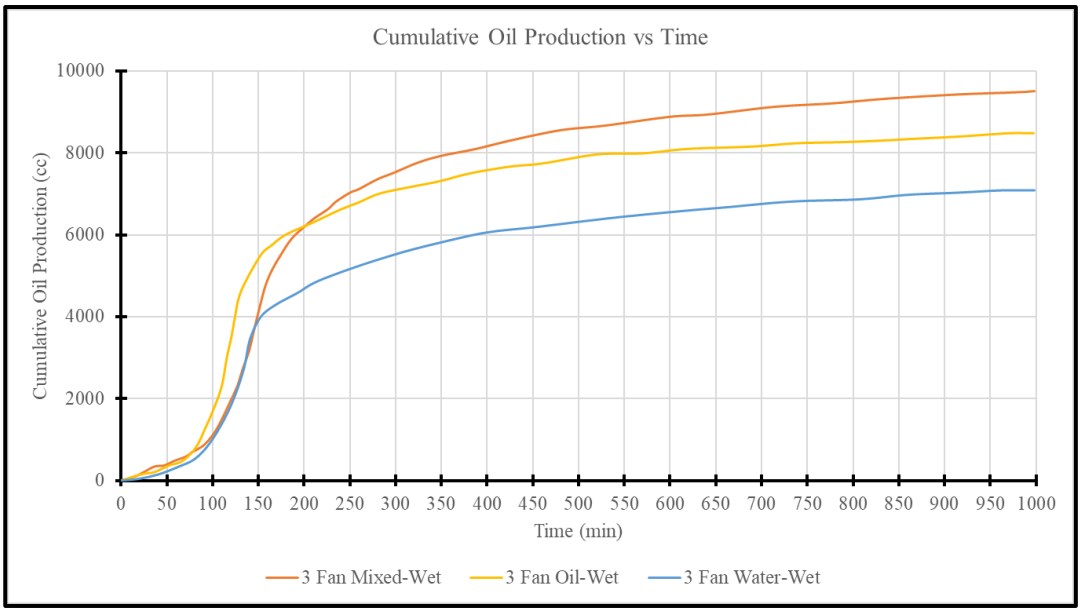

Figure 26 Cumulative Oil Production vs Time from MAHOP experiments

From this graph, the expected MAHOP production will start after 15% of the steam to produce the whole panel should be injected. When this ratio is applied to the production life of a panel according to 250,000 barrels daily production, the production starts approximately 35 days after the steam injection started. As can be seen on the graph, the production will continue to increase at some point, so a uniform production rate in a panel such as 250,000 barrels per day from numerous panels will not be possible, but the average production rate of these panels with a constant steam injection throughout the life of a panel will be 250,000 barrels/day. In this study to ease the calculations related to the production schedule the average oil production is taken into account.

After the required daily production of Bati Raman is decided, the detail of the production can be explained as follows: Although, the major part of the production is satisfied by the MAHOP a small portion of the production is supplied from the excavated material. Therefore, firstly the daily production coming from the excavated material is calculated and stated as follows: the surface area of the openings that are excavated by both continuous miner and TBM is multiplied by the daily advancement to calculate the excavated volume. Then, this volume is

multiplied by the average porosity, the percentage of oil in pores, and the recovery of the surface retorting process. It should be noted that almost 58% of the excavations are below the reservoir, hence while calculating the production from the surface retorting facility only 42% of the excavation should be taken into consideration. From this calculation, the average daily production coming from the excavation is calculated as 2,543 barrels/day. This result indicates that the daily production that comes from the MAHOP should be 247,457 barrels/day (39,346 m^3/day) to satisfy the required daily production.

From the daily production of MAHOP, the number of steam generators that are going to be used is decided by the required steam in kg/h from Steam Oil Ratio (SOR) which is estimated as 9 (Canbolat et al., 2022). Thus, 354,114 m^3/day steam at 130 ^oC and 4 bar is required. Nevertheless, similar to most equipment, steam generators have efficiency and availability that should be taken into account. The availability and the efficiency of the steam generators are assumed due to the lack of data as 83% and 50%, respectively. The efficiency of the steam generators cannot be known for the underground implementation but while selecting these percentages the worst cases are taken into account. After these percentages of the steam generators are taken into account, 99,355.73 kg/h steam production is estimated to satisfy the daily oil production in Bati Raman Reservoir. To compensate for the steam production 4 different steam generator with a 10,000 kg/h, 20,000 kg/h, 50,000 kg/h, and 100,000 kg/h capacity is evaluated and 5 steam generators with a capacity of 20,000kg/h are selected. The daily production of this steam generator is estimated as 48,562 barrels/day. This steam generator selection is based on both the average excavation time of a panel and the MAHOP production time of a panel to create a sequential production pattern. The details of these calculations will be explained in the production scheduling part.

In order to move on to the production scheduling part, the possible production amount of each panel and sector should be calculated. For the sector calculations, the average volume above the production galleries is estimated as 50 meters in length and 62.5 meters in width (Figure 23). However, for the volume estimation, the

average thickness that MAHOP is going to be implemented should be evaluated. This process is done by Micromine (Micromine Pty Ltd., 2022) to calculate the thickness between 10 meters above the production level and to 5-meter below the reservoir roof. According to this calculation, the average thickness is calculated as 53.15 meters. Then, the average oil volume in a sector is calculated by multiplying the volume of the sector by the porosity, the oil percentage in pores, and MAHOP efficiency and found as 13,952 m^3 (87,748 barrels). A very similar approach is utilized to find the possible production of a panel (Figure 27).

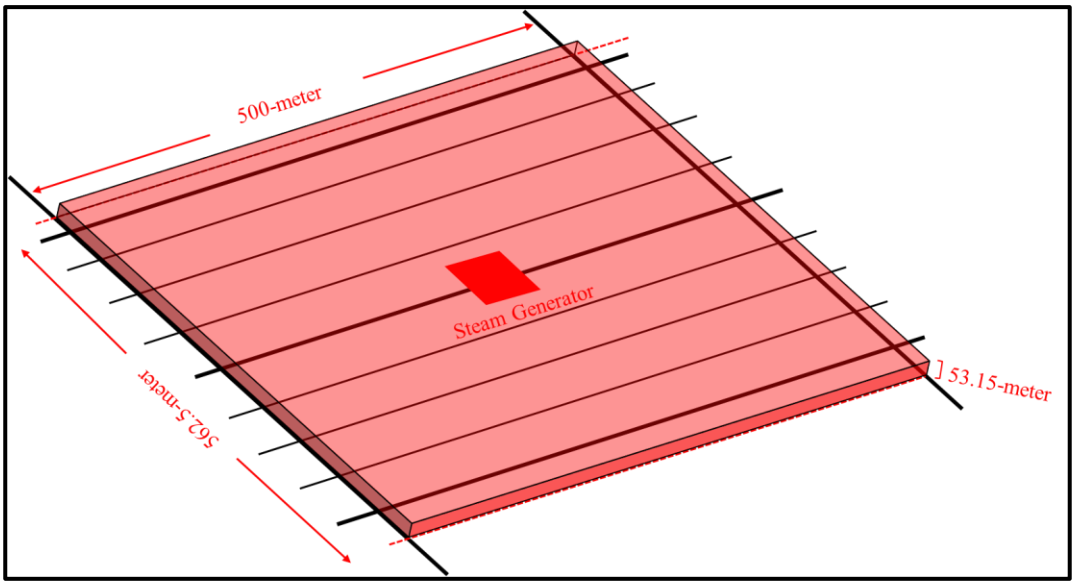

Figure 27 Panel Dimension of Bati Raman

Table 9 Average Panel Details

	Panel							
Number of Panels	Length (m)	Width (m)	Height (m)	Volume (m^3)	Porosity (%)	Oil in Porosity (%)	MAHOP recovery (%)	Oil Production (barrels)
1	563	500	53	14,948,438	20%	75%	70%	9,871,610
88				1,315,462,500	20%	75%	70%	868,701,651

On this calculation, by using the average thickness which is 53.15 meters, the volume of producible oil in a panel found as 1,793,813 m^3 (11,281,840 barrels). This

producible oil in a panel is utilized to estimate the whole production in Bati Raman according to the number of panels which is 87. From this estimation, the producible reservoir is calculated as almost 869 billion barrels.

Furthermore, the production time of a panel can be assessed by dividing the potential oil quantity of a panel by the daily production rate from a panel using a single steam generator. Using this method, it is estimated that it would take 232 days to complete the MAHOP production in a panel. A similar calculation can be done to determine the mine life of the Bati Raman Reservoir by dividing the total recoverable reserves by the daily production rate from five steam generators. Based on these calculations, the continuous operation of MAHOP production for 360 working days per year would yield a lifespan of approximately 12.3 years.

3.3.2 Production Scheduling

Production scheduling of MAHOP implementation is highly dependent on the excavation times of the production galleries. Therefore, while estimating the production in the Bati Raman Reservoir, the excavation sequence and its effects on production should be taken into account. To start with the effects of the excavation on to begin with MAHOP production firstly, two types of production opening excavation should be separately investigated due to the advance rate and starting times. The advancement rates of TBM and the continuous miner are assumed as 10 meters/day and 7.5 meters/day, respectively. The TBMs advancement rate is estimated by using a similar mixed-ground TBMs application that took place in 2018. From the weekly advancement data of the Gerede water tunnel project, an average advancement rate is calculated by including the down times (Grothen, 2018).

Except for the advancement rate of both types of equipment, excavation starting times are also other parameters that affect the scheduling, especially for the production openings that are going to be excavated by continuous miners. As know

from the previous part, continuous miners are going to begin the excavation into the production galleries that are driven by the TBMs. Therefore, TBMs should be completed a certain amount of excavation to initiate the excavation of other production openings by continuous miners. Although the length of the production galleries driven by the continuous miners is less than the others, finishing the openings of a panel will be longer than the other excavations due to the advancement rate and the dependency on the other excavations.

Additionally, cross-cut excavations will not influence the MAHOP production starting time, because all production and steam boreholes will be placed in the production galleries. However, the drilling of boreholes with a raise borer may affect the production starting date for each panel. Therefore, the required number of raise borers should be investigated. Firstly, the time to excavate a borehole is calculated by using the average excavation rate of 1.54 m/h (Mamaghani et al., 2016). Drilling a series of fan-shaped boreholes will be approximately 9 days (Appendix I). Therefore, the number of raise borers should be utilized in order not to delay the MAHOP production starting day.

With the above considerations, an average excavation time tried to be found for both the TBMs and continuous miners' excavations to calculate the mine life and steam generator capacity for this project. For the openings driven by the TBM, an average excavation time of a panel is evaluated for the first five consecutive panels which are closest to the first declines. To finish the excavation of a panel, TBM should excavate the 10-meter diameter production galleries which are located at the top and the bottom of the panel. Therefore, for the first panel (P5 in Figure 24) to start the production at the northwest of the reservoir, 4785.4 meters of production openings and a U-turn should be driven. This leads to the starting of the MAHOP production from the northwest part of the reservoir will start 478.5 days later the decline excavation concluded. After the first production started, a new panel excavation will be completed every 50 days until the first row of panel excavation is finished. According to the first row of panels excavation time the average excavation time of a panel can be assumed as 135 days in terms of TBM excavations. However, if the

number of panels that are going to be excavated is increased especially for the longer production galleries which are located at the center of the reservoir, the average excavation times are decreased because the number of U-turns per panel decreases for longer production openings. Hence, for a proper estimation, panels that are excavated by the TBM-1 path should be taken into consideration. After the calculations for the TBM-1 path are done, the average excavation time of a panel is decreased to 108 days. These calculations can be seen in Appendix I.

For the average excavation time calculations of a panel in terms of the continuous miners, a different series of calculations are used to include the waiting time of the equipment for the TBM-1 path. Firstly, the excavation starting times are calculated by evaluating the TBMs excavation sequence, then, the excavation time for the longest production galleries is added to the starting day. After the calculation of the excavation of the last panel, the results are divided by the number of panels that are excavated within the excavation sequence to find the average excavation time. It should be noted that excavation starting dates should be arranged according to the day after the finish date of the previous row of panels. Considering the above calculation, the average excavation time of a panel by the continuous miners is estimated as 118 days (Appendix I). Because both of the excavations are related, the average excavation time should be taken as 118 days for Bati Raman Reservoir.

To calculate the total excavation time, the average excavation time was multiplied by 88 panels and divided by 3 because of 3 simultaneous excavations. This rough estimation leads to approximately 10 years of production gallery excavation. After the calculation of the excavation time of the declines. Total excavations will conclude in 13 years.

As mentioned above, the steam generator capacity is selected according to the average excavation time of a panel in order not to delay production operations. Therefore, 20,000 kg/h capacity steam generators are selected for this project. To estimate the mine life of the Bati Raman Reservoir, the total producible oil is divided into the daily required production and found as 12.3 years. According to this

production schedule, the oil production of the Bati Raman Oil field will be ended in 15.8 years with almost 869 billion barrels of oil.

CHAPTER 4

VENTILATION AND MINE COOLING

In this chapter, the possible mine ventilation and cooling cases are discussed. These cases are selected according to the different project phases and locations in the mine. In each case, the required fresh air calculations and the implementation on the simulation program are explained. Additionally, similar to the ventilation simulations, heat that is created from a specific instance is calculated to overcome the heat problem of Bati Raman Underground Mine.

4.1 Bati Raman Underground Mine Ventilation

To start the required air calculations, firstly the ventilation cases should be defined according to the mining and production phases. Hence, for the first cases of ventilation and cooling part, excavation of declines is an early stage of the project.

As known from Chapter 3, there will be 6 different declines to reach the reservoir from the surface. These 6 openings will be identical in most aspects except the location and the length of these openings. Therefore, a single decline ventilation simulation to represent each decline is selected for the first case.

For the second and third cases, MAHOP production is taken into consideration with additional excavation operations. As explained in the literature research, dividing the mine ventilation for such projects into modular sections is recommended. Therefore, panels that each MAHOP production is taken place separately, and are chosen to be modular sections for ventilation. For the second case, a panel that is located at the edge of the reservoir that is close to one of the declines is selected to represent both productions in the eastern part of the reservoir and production which is close to the semi-circular U-turns created by the TBMs. On the other hand, for the third and last

case, two consecutive MAHOP panel production with TBMs and continuous excavation at the neighbor panel are simulated to create one of the worst cases.

After deciding the cases that are going to be evaluated, required fresh air calculations should be assessed for each case. Ventilation in an underground mine serve not only the supply air for humans but also to control the physical and chemical quality of the air (Hartman et al., 1997). Therefore, while calculating the required fresh air for each case breathing, dilution of harmful gasses, dilution of dust, and diesel engine fresh air requirements are taken into account. However, fumes that come from blasting agents will not be covered in this study because there will not be any D&B operations.

For the decline ventilation case, fresh air requirement is calculated for breathing and dust dilution. These excavations are held above the reservoir, so methane dissemination from the surrounding rocks is expected to be zero. Additionally, all of the equipment which is going to be used to excavate will be electrically powered. Therefore, in this case, fresh air requirements for both dilution of methane and diesel engines are not calculated. For the breathing calculations, 20 workers are estimated to working on the TBM with moderate activity. The result of this calculation showed that only 0.1251 m^3/s is required for breathing purposes. For the dust dilution calculation related to the TBM operation, the fresh air requirement is assumed from the study by Liu et al. (2019) as 75 m^3/s. This assumption and the details of the fresh air requirement can be seen in Appendix I.

The estimations related to one-panel ventilation are slightly complex compared to decline ventilation. In this case, diesel-powered engine oxygen requirements and methane dilution is included in the calculation. Almost 137 people are expected to be in the panel while the MAHOP production occurring. When the calculations are done breathing, the required fresh air in a panel for breathing is found as 0.87 m^3/s according to the carbon dioxide production. Dust production for the TBMs will be equal to the dust production rate in declines, but the number of TBM used to excavate close to the panel will be tripled. In addition to that, another continuous excavation

operation done by continuous miners will be held. Therefore, the required fresh air for the dust dilution is calculated as 300 m^3/s.

The oxygen requirement for diesel engines that is going to be working on one panel is listed below. According to Table 10, almost 263.7 m^3/s of air is required for diesel engines to work properly.

Table 10 Air Requirement for Diesel Engines

Equipment	**Number**	**kW**	**Utilization**	**Air Volume (m^3/s)**
Raise Borer	16	155	0.6	104.16
Scissor Lift	3	111	0.5	11.655
Cassette Carrier	3	54	0.5	5.67
Maintenance Vehicle	3	100	0.5	10.5
Heavy Duty Pick-up	3	100	0.5	10.5
Personnel Carrier	10	200	0.5	70
Transmixer	3	115	0.3	7.245
Ventilation Losses	0.2	-	-	43.946
			Total	263.676

The methane dilution in the reservoir could be needed because of the reasons stated in the literature review. Hence, the dilution of methane in a panel should be implemented in the calculations and simulations. Generally, methane exposure is dependent on multiple parameters, but exposure surface area is one of the important ones among them. In MAHOP all of the openings are going to be sealed with concrete supports of TBMs or shotcrete. The methane exposure from these surfaces is expected to be very small compared to excavation openings. Thus, the main methane concentration will be cumulated where the specific precautions took place. In order to find the methane exposure rate on excavations done by TBMs and continuous miners, a similar study about the TBM excavation in coal-bearing strata made by Belle and Foulstone (2015) is implemented in this study due to the lack of data in petroleum mining. According to this study, the methane spread to the working

environment from the TBM excavation is calculated as 40 l/s. This value is directly used in calculations for methane dilution equations as stated by Liu et al. (2019), and the required air for the dilutions is found as 24 m^3/s for one TBM. This leads to the overall fresh air requirement to dilute methane will be around 216 m^3/s.

Lastly, from 1986 to recent days, CO_2 injection through the Bati Raman reservoir is utilized to increase production (Sahin et al., 2012; TPAO, 2022). Until 2012, the average CO_2 injection is estimated by Sahin et al. (2012) as 1.8 billion scf (Standard Cubic Feet). As CO_2 injection started in 1986, CO_2 production occurred after two years. After 1989, the CO_2 in place changed from year to year. However, between 2012 to 2023 there is no additional information related to in-place CO_2. Hence, to predict the CO_2 emissions the highest in-place CO_2 amount is considered to be diluted. As can be seen from Figure 28, the highest in-place CO_2 took place in 1992 with 0.8 Billion scf.

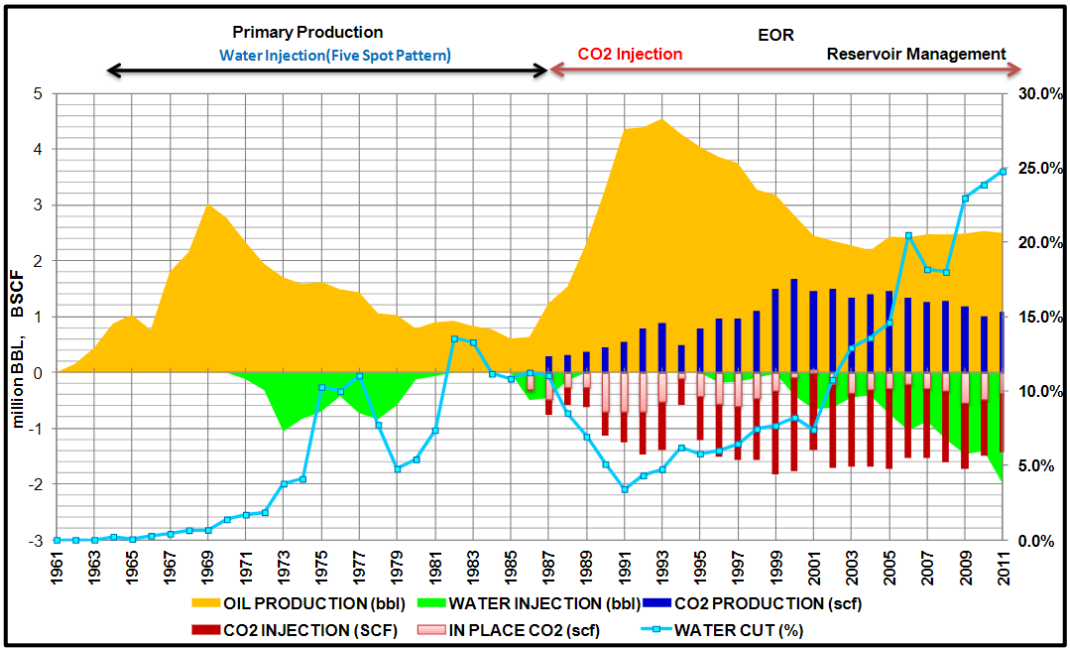

Figure 28 Bati Raman Injection History (Sahin et al., 2012)

To estimate the CO_2 concentration in strata, the ratio of pore volume in Bati Raman Reservoir to the CO_2 in place is taken and found as 6%. By using equations 4 and 5, the CO_2 emission for both TBM and the continuous miner is estimated as 4.43 m^3/s

and 1.48 m^3/s, respectively. Similar to methane dilution, gas emission rates are used to find the required fresh air to dilute CO_2. In accordance with this calculation, approximately 22.14 m^3/s of fresh air is found to be sufficient for CO_2 dilution (Appendix II). The fresh air requirement for the dilution of CO_2 is going to be equal for both one-panel and two-panel ventilation cases due to the similar number of excavations that are going to take place in the reservoir.

In the last case, where the two consecutive panels produce oil while excavation for the next panel continues, the required fresh air calculations are very similar to the second case. Although the required fresh air increased according to the increased number of people in the panel, the effect of these calculations is negligible. However, these calculations should be revised for the diesel engine oxygen requirements and dust dilution in the panels. In this case, the number of heavy-duty pick-ups and personnel carriers has increased to 6 and 12, respectively. Hence the required air for the diesel-powered engines is increased to 293 m^3/s.

The other change made in this case is the fresh air requirement for dust dilution. Because of the excavations done in the consecutive panel 6 continuous miners will be operated and each continuous miner required 25 m^3/s of fresh air for dust dilution, the air which will be directed from the surface is increased to 375 m^3/s.

After the fresh air requirement calculations are made, as can be seen from the calculations, the highest fresh air requirement in each case is dust dilution. Therefore, while designing the ventilation simulation, fresh air requirement is taken in accordance with dust dilution.

While implementing these cases to the mine ventilation program called Ventsim (Howden Group Limited, 2019) this sequence is used:

- Importing the 3D mine design of Bati Raman Underground Mine into the program
- Deciding the ventilation raises and door locations according to the design

- Adding fans and regulators to direct the fresh air to the excavation and production areas

In Figure 29, the 3D mine layouts that are used for the ventilation are represented.

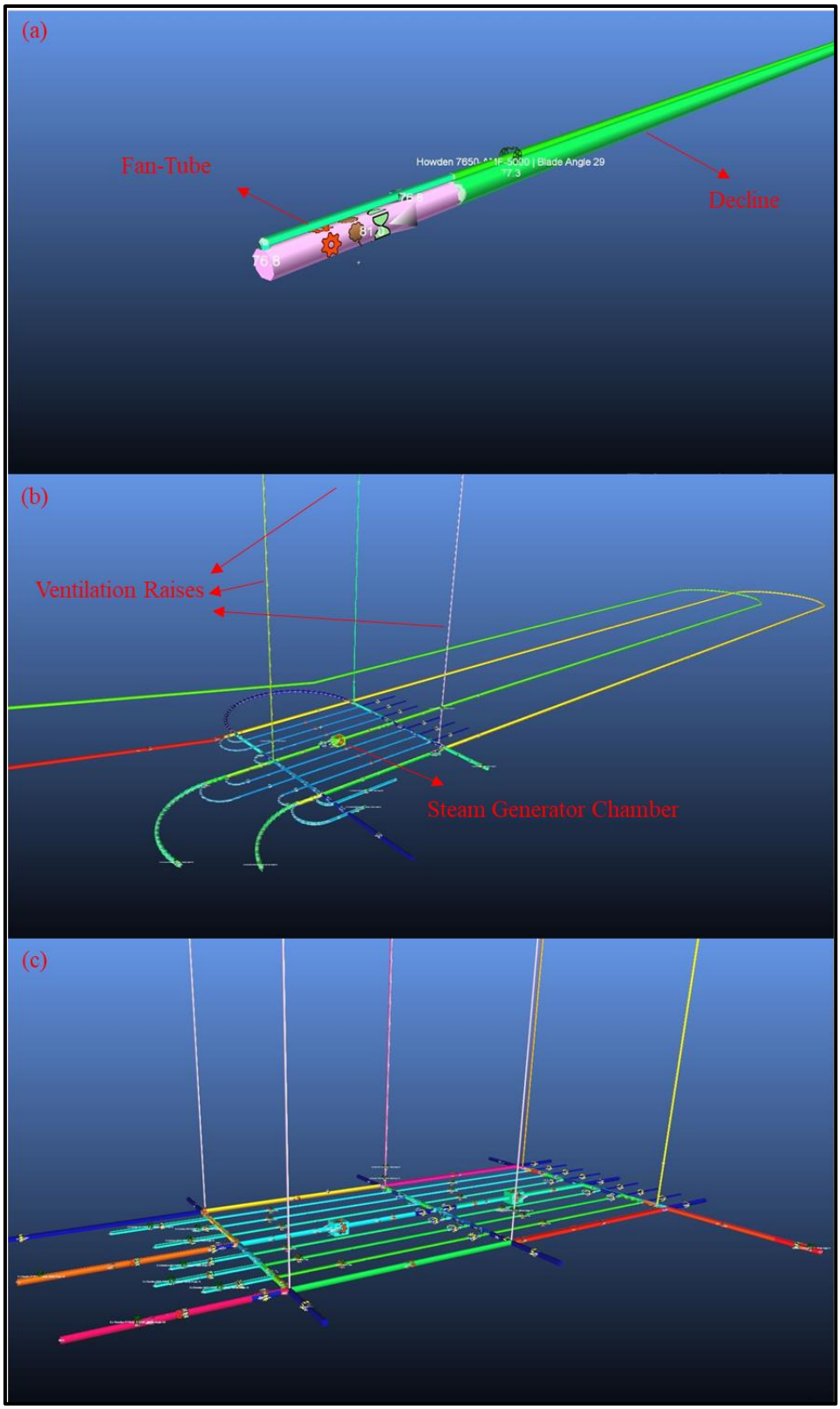

Figure 29 Cases Used for Mine Ventilation

In Figure 29 (a), an almost 2750-meter-long decline with a 15 percent gradient is created for the ventilation simulation. In this case, from the above calculations, the required fresh air which is 75 m^3/s, is supplied to the excavation face. As with all the TBM excavations which will be done in the Bati Raman Reservoir, the system explained in the literature review is used. Therefore, fresh air is blown into face the, and the exhaust which is air directly taken away with the help of two 1.5-meter diameter fan tubes. In order to represent the TBM operation in the decline, the resistance of the last 50 meters of the opening. Additionally, in this part of the opening, 13.65 mg/m^3 dust concentration is applied to test the ventilation system. The system resistance is directly calculated by the program as 0.21 Ns^2/m^8. To ventilate this section, an exhaust-type fan that supplies almost 80 m^3/s with 2,27 kPa is selected and operated at 78.2% efficiency.

In the second case (Figure 29 (b)), P7 from Figure 24 is simulated. To directly supply the fresh air from the surface and use natural ventilation, 10-meter diameter production openings are utilized. The openings that are not ventilated in that instance are blocked by the ventilation doors and the fresh air that comes from the declines is directed into the panel and the excavation locations. Similarly, in this case, the required fresh air is mostly decided by the dust dilution process. According to those calculations, 300 m^3/s of air is expected to ventilate the whole panel. However, due to the length of the openings and the mine resistance, an additional air fresh air supply that comes from one ventilation raise that is close to the excavation area is directed. Hence, the supplied fresh air amount is taken as almost 400 m^3/s. Unlike the decline ventilation, generally because of the expected methane in the openings, the air that comes from the panel is directed to one of the exhaust ventilation raises and fresh air that comes from other ventilation raise is used to ventilate excavations. It should be stated that the steam generator chambers are created in this scenario, but the exhaust air related to the steam generators did not implement in this simulation because the exhaust air that is created from the steam generators will be separated from the main ventilation system in order not to spread exhaust air to the working areas. Additionally, the production galleries that are used for the MAHOP

production, should be well-ventilated not only for methane dilution but also for mine cooling purposes. Therefore, while the ventilation system is being created, the velocity of the air in these openings is defined to be higher than 1 m/s.

The details of this simulation can be described as follow: 5 different fan types are used to ventilate the panel except for auxiliary ventilation fans. A total of 21 fans are located in 13 different locations with an average efficiency of 75.5%. The power consumption of the system is calculated as 9,854 kW without a cooling system. In this design, mine resistance and pressures are simulated and found as approximately 0.7 Ns^2/m^8 and 18.2 kPa, respectively.

In the last case, like the previous case, the isolation of the modular system is done after the ventilation raise location is selected. In this case, the production location was purposely selected as remote as possible to the declines to cover almost every possible ventilation case that can be seen in the Bati Raman Underground Mine. In this case, the calculated 375 m^3/s is directly supplied from the 4 ventilation raises. Unlike the second case, the ventilation raises that are used for the exhaust air are located closest to the excavation areas to be able to suck and direct the sufficient amount of air in the excavation areas. Additionally, each panel ventilation tried to be separated from each other for safety purposes. Except for the above-mentioned changes, the rest of the simulation is created according to the same principles that are used in the second case.

According to this last simulation, a total of 37 fans are located in 25 different positions. The number of fans that are used in this case is higher than in the other cases due to the auxiliary fans that are located in almost each production galleries to distribute the fresh air evenly. The required energy that is needed to work properly for the 80.5% efficient ventilation system is calculated as 5,979 kW. The mine pressure and resistance of this system are almost 0.56 Ns^2/m^8 and 11 kPa, respectively.

In this part of this chapter, 3 different cases that represent almost every possible case in terms of ventilation are detailly investigated. In the next part, the same ventilation

cases are simulated for the mine cooling operations and the adjustment of the systems will be depicted.

4.2 Bati Raman Underground Mine Cooling

Another sub-topic that should be discussed in the MAHOP implementation of Bati Raman Reservoir is the mine cooling operation. As known from the literature review, the reservoir temperature is expected to be around 65.5 ^{o}C. Hence, the implementation of this heat should be done before the cooling operations are utilized. In order to, increase the reservoir temperature, the thermal gradient is increased to 6.9 ^{o}C/ 100m. Although this approach is unrealistic for the excavation which is not located in the reservoir, the only excavation done above the reservoir are declines. Therefore, this approach has negligible impact on the heat simulations done in the reservoir.

Except for the heat that is transferred from the surrounding rock, there are several heat sources related to the production of MAHOP that should be taken into consideration. These heat resources are decided to be heat transfer related to equipment usage, broken rocks, MAHOP production, and auto-compression. Among these heat sources, auto-compression is directly calculated in the simulation program, but for the other heat sources, an additional calculation is required.

Generally, the heat transfer related to equipment usage is mostly related to internal combustion engines. Nevertheless, electrical-powered equipment such as TBM and the continuous miner has an undeniable effect on heat transfer to the atmosphere. To calculate the heat transfer from these two pieces of equipment, a TBM excavation case which is taken place 3000 meters below the surface is investigated (von Glehn & Bluhm, 2000). According to this study, a 4-meter diameter TBM that has 2000 kW power consumption, creates 1040 kW of heat while working. If the heat created is taken as directly proportional to the power consumption, 4160 kW of heat creation is expected for the 10-meter diameter TBM which is going to be used in Bati Raman Reservoir. Additionally, due to a lack of information related to the continuous

miners, the same proportionality is used to estimate the heat created from the continuous miners and found as 416 kW.

For the other types of equipment which use diesel for fuel, heat transfer values to the mine environment are directly calculated by the ventilation program by multiplying the engine power with diesel efficiency and diesel load factor. Thus, the diesel-powered equipment is implemented into the simulations by adding the engine power values to the related section of the mine. In addition to the diesel-powered equipment, the steam generators for the required capacity for MAHOP production are expected to work with organic fuels. Therefore, another heat transfer calculation should be done. In order to calculate the heat transfer, the efficiency of the 20,000 kg/hr steam generators efficiency and the power consumption values should be known. According to the ICI Caldaie product catalog (*ICI Caldaie GX12 Bar Industrial Steam Generator Catalogue*, n.d.), the power consumption and efficiency for the required steam generator are 13963 kW and 90%, respectively. From this information, the utilized heat transfer to the implemented into the simulation is calculated as 1396,3 kW.

One of the other heat resources expected to affect mine air temperature is the heat that comes from the broken material. To be able to calculate it, the specific heat of reservoir rock, the amount of broken material that is going to be transferred to the surface, and the temperature of broken material at the surface should be known. The specific heat of the reservoir rock is unknown. Thus, the specific heat of limestone is taken as 1,03 kJ/(kg·K) from a study conducted by Kravcov et al. (2020). The excavation rate is calculated for a single TBM as 25 kg/s (Appendix II) and the temperature of broken rock at the surface is assumed as 40 ^{o}C. From these calculations and assumptions, the heat transfer from the broken rock is estimated as 625.6 kW for one TBM. To implement this as point heat in the simulations, the heat is added to the openings that come right after the TBM or continuous miners.

Lastly, the heat that comes from the steam and oil transportation in the mine is considered for the heat simulations. To estimate the heat transfer, a series of

calculations have been done by using specific heat of the piping material, diameter and cross-sectional area of piping, and temperature difference of steam (Appendix II). To calculate the pipe cross-sectional area and piping diameter, a steam velocity in the piping is assumed as 10 m/s from an example calculation made by the piping company, and the steam flow rate is calculated as 2222,22 kg/h from the hourly steam production. From these calculations, the diameter of the pipe that is to be utilized for steam transportation is selected as almost 5.85 cm. Also, to calculate the heat transfer, the piping material is selected as carbon steel pipe A53/A106 Gr. With a thermal conductivity of 51 W/m·K. By using this information, the heat transfer for the farthest distance that steam travels in a panel is calculated as 555,43 kW. For the worst case, the heat transfer that comes from the piping is taken as equal on each production galleries and implemented into simulations.

After the heat sources were added to the simulation, in some regions wet bulb temperature reached 75 ^{o}C. It should be noted that in the Yarega mine which is the closest petroleum production to the MAHOP implementation are cooled the mining environment to 28 ^{o}C wet-bulb temperature(Zakirov D. R. et al., 2019). Therefore, in most of the openings refrigeration systems are utilized to decrease the wet bulb temperature to 28 ^{o}C like in the Yarega mine. Starting from the decline ventilation case similar to the ventilation part, the fresh air amount that is blown to the face is sufficient to cool down the 27.7 ^{o}C wet-bulb temperature.

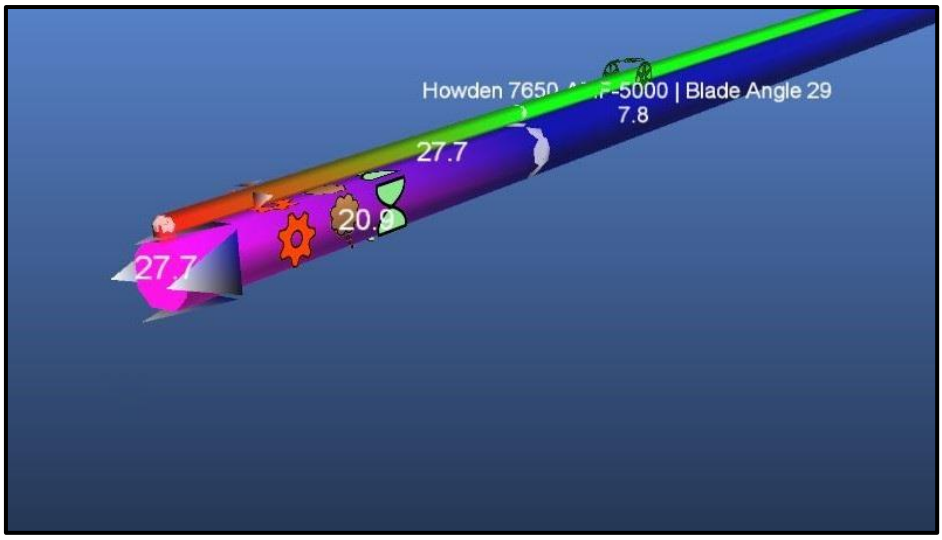

Figure 30 Decline Heat simulation results

On the other hand, for the panel cases, the temperature in some regions increased without a refrigeration system to 75 ^{o}C. To cool down the temperature to a sufficient level, mostly two types of refrigeration systems are used. These are chilled water spraying and a refrigeration pocket and are detailly investigated in the literature review. The chilled water spray system is used on almost all of the production galleries to decrease the wet-bulb temperature and compensate for the heat coming from the steam piping. According to the need of the refrigeration system, the water amount that is sprayed into the environment will be changed and this will directly affect the refrigeration system capacity as kWR (kilowatts of refrigeration). Thus, mostly the refrigeration capacity of 500 kWR, is used for both panel cases. In addition, in some regions where the excessive heat comes from the steam generators, TBM, and continuous miners, refrigeration pockets that are excavated parallel to the openings are used to cool down the air (Figure 31). In Figure 31, As can be seen, the cooling pocket is placed right after the steam generation and cooled down the air from 29 ^{o}C to an acceptable level of 26.4 ^{o}C. In this illustration, the red gear icon represents the heat input while the gray one illustrates the refrigeration system.

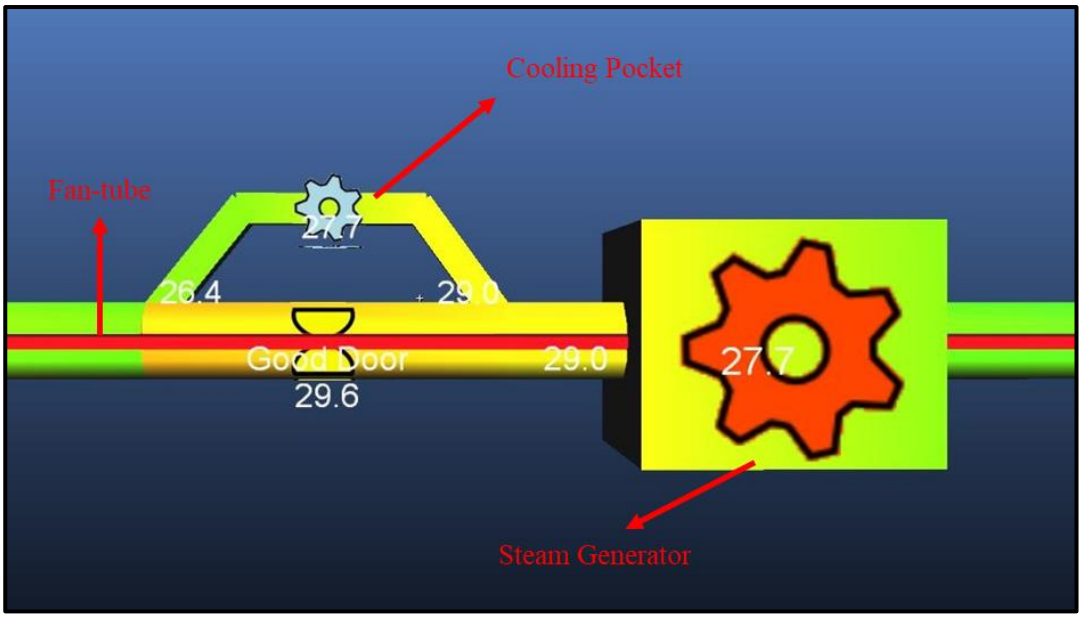

Figure 31 Cooling Pocket Implementation into Simulation

After all the refrigeration systems are utilized in the one-panel case, a total of 17 refrigeration systems with an 8,174.1 kWR are used to cool down the panel. While two of the refrigeration systems from 17 is cooling pockets with a cooling capacity of 2,300 kWR, 15 chilled water spray system with an average capacity of 400 kWR is selected. Figure 32 depicts the comprehensive ventilation system in accordance with the wet-bulb temperature. The only places where the wet-bulb temperature is over 28 ^{o}C are the places where no excavation or production occurs. Furthermore, although the wet-bulb temperature exceeds the threshold in the excavation faces, the hotter air is promptly channeled into the fan tube. Consequently, the heat generated by TBM excavations will not impact any individuals.

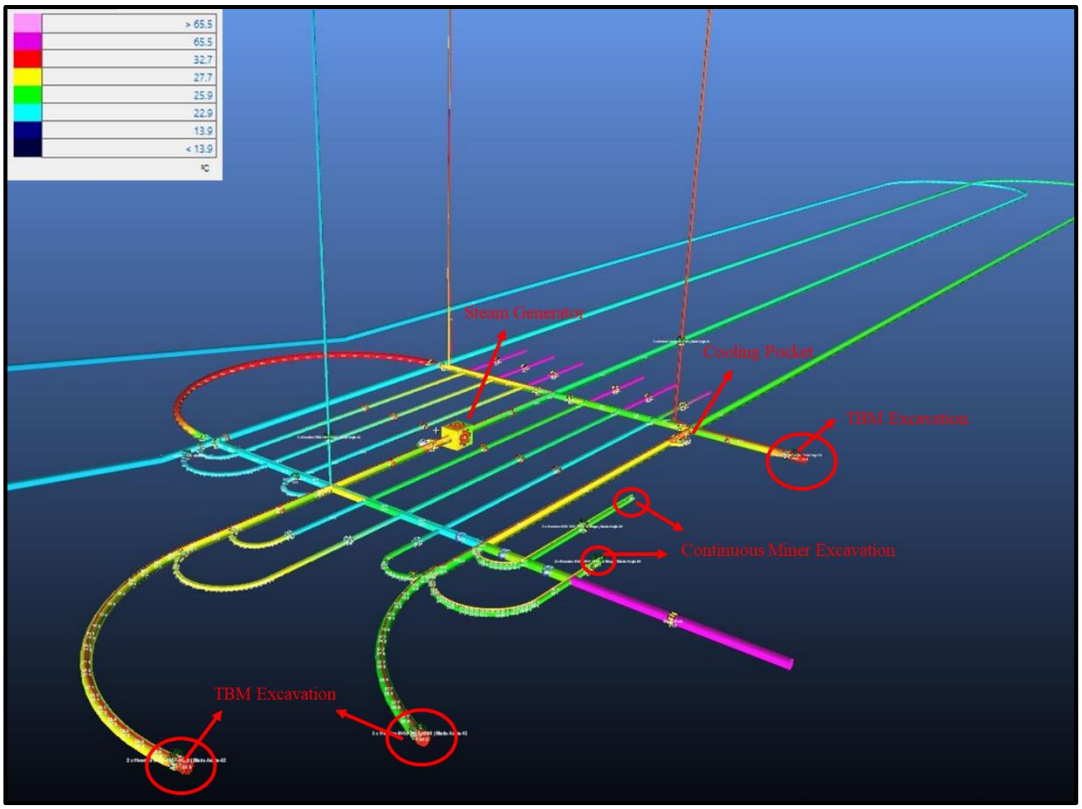

Figure 32 One-panel Ventilation Simulation by the Wet-bulb Temperature

Lastly, for the two-panel ventilation case, 34 refrigeration sources are added in this case. Among them, 10 cooling pocket with 5,900 kWR refrigeration capacity and 24 chilled water spray system with an average 500 kWR capacity is used. A total of 17900 kWR refrigeration is used to cool down the two consecutive panel productions. The ventilation system is depicted below according to the wet-bulb temperature (Figure 33). The threshold limit for the wet-bulb temperature did not exceed in any regions where the excavation and MAHOP production activities occur.

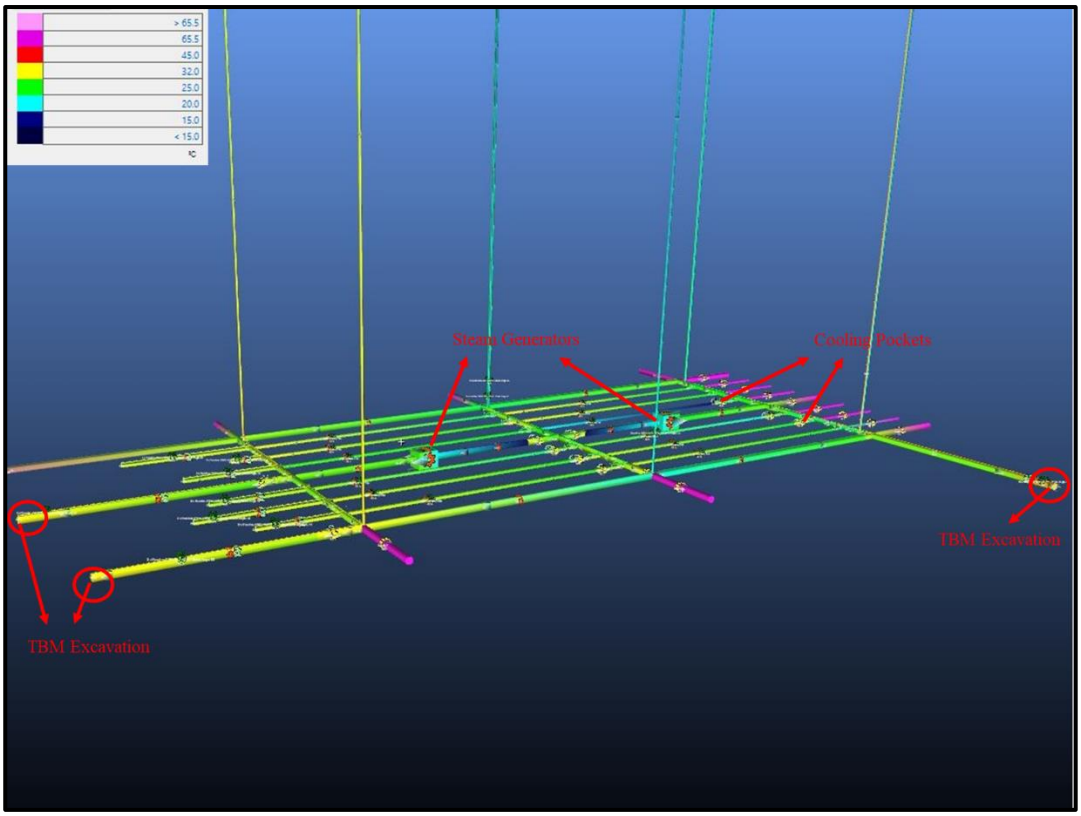

Figure 33 Two-panel Ventilation Simulation by the Wet-bulb Temperature

In this chapter, the ventilation system and its simulations together with the heat simulations are investigated in detail. In addition, the ventilation and cooling costs are calculated by the program and utilized in Chapter 5 economic evaluation of Bati Raman Reservoir's MAHOP implementation.

CHAPTER 5

ECONOMIC EVALUATION OF BATI RAMAN

In this chapter, the MAHOP implementation of Bati Raman Reservoir will be investigated economically. Firstly, a capital cost estimation using the component cost ratio method will be evaluated. Then a detailed operational cost estimation will be incorporated into this study. Finally, in order to determine the feasibility of the project, the Net Present Value (NPV) and Internal Rate of Return (IRR) values fro various recovery percents shall be computed for a potential MAHOP implementation at the Bati Raman Reservoir.

5.1 Capital Cost Estimation

After the major parameters and the designs are completed for the implementation of MAHOP in Bati Raman Reservoir, an economic evaluation can be done based on the conceptual design. To start, the capital investment required to initiate the underground operations should be taken into account. As mentioned in the literature review part, there are several capital investment prediction methods that can be used based on the available data and knowledge. According to the available data and the knowledge related to the Bati Raman Reservoir, the component cost ratio method is selected to be used to estimate capital cost.

In this method, the overall equipment cost is multiplied by a coefficient (Table 12) that is created from the mining project data to estimate the expenses that cannot be calculated without an additional such as an auxiliary building, site enhancement works, process buildings, etc. Therefore, to start with the capital cost estimation, the pieces of equipment that are going to be used for this project should be decided. For the major operations like the excavation of the openings and steam injection, the piece of equipment is already selected in Chapters 3 and 4, therefore the rest of the

additional required vehicles and machinery should be investigated. According to the calculations that have been done in Appendix III, the list of equipment is represented in Table 11.

Table 11 List of Equipment with Cost Calculations

Type	Number of Machines	Cost per item ($) (2019)	Cost per item ($) (2023)	Total Cost ($)
TBM	9	36,000,000	42,480,549	382,324,937
Continuous Miner	18	2,603,300	3,071,934	55,294,806
Raise Borer (Fan-shaped Boreholes)	48	4,619,845	5,451,487	261,671,400
Rock Bolter	3	100,600	118,710	356,129
Underground Truck	73	800,600	944,720	68,964,575
Raise Borer (Ventilation Raises)	6	2,139,840	2,525,044	15,150,263
Transmixer	18	381,000	449,586	8,092,544
Shotcrete Machine	18	421,000	496,786	8,942,155
Scissors Lift	18	384,000	453,126	8,156,265
Maintenance Vehicle	3	x	60,000	180,000
Heavy-Duty Pickup	12	x	60,000	720,000
Personnel Carrier	10	286,600	338,192	3,381,924
Fans (Main)	64	173,200	204,379	13,080,233
Fans (Auxiliary)	28	24,800	29,264	819,403
Pumps (Oil)	3	x	400,000	1,200,000
Pumps (Water Drainage)	12	22,700	26,786	321,436
Pumps (Water for Steam Generators)	15	12,100	14,278	214,173
Pumps (Concrete)	18	160,000	188,802	3,398,444
Pumps (Refrigerant)	85	35,500	41,891	3,560,696
Pumps (Fuel)	5	4,800	5,664	28,320
Conveyor belt (8.5 km)	3	8,923,607	10,529,992	31,589,977
5 m^3 Cap. Loader	3	1,037,600	1,224,384	3,673,151
Surface Truck (25 m3)	30	755,800	891,856	26,755,665
Waste Dump	1	x	4,997,502	4,997,502
Heat Exchanger	22	809,500	955,222	21,014,891
Steam Boilers	5	1,250,000	1,475,019	7,375,095
	Total			**931,263,984**

The cost of these vehicles and machinery is estimated by using an estimation guide published by InfoMine USA (2019). From this guide, the cost per item for all of the equipment that is used in the Bati Raman Reservoir is estimated in terms of 2019 dollar value. In order to find the estimated value at present, the yearly average inflation between 2019 to 2023 is 4.225.

After all the machinery cost is calculated, the purchased equipment cost can be implemented into the component cost ratio method. Table 12, represents the calculation related to the component cost ratio. According to the calculations, the estimated initial investment is approximately 5.36 billion dollars. However, all the equipment that is going to be purchased will not be operated until the decline excavation is done. Hence, based on the calculations done by the advancement rate of TBMs, the majority of the initial capital expenses will be spent in the second year. To decide the first and second-year initial capital expenses a basic proportionality is used related to the equipment required for the first and second years. So, in accordance with this proportionality, the first-year capital investment is calculated as almost 2.2 billion dollars. The rest of the capital expenditure which is approximately 3.2 billion dollars, is planned to be spent on the second year of the excavations.

Additionally, the development cost in the mining industry is specified as an initial capital investment it involves activities such as land acquisition, exploration, feasibility studies, and the construction of necessary infrastructure. These activities require financial resources and lay the foundation for future mining operations. The money spent during mine development is not immediately recoverable or revenue-generating but is important for establishing an operational mine.

While implementing the mine development cost to capital cost calculations, most of the activities which is stated above are neglected because of the completion of land acquisition and exploration. Therefore, the main cost that should be added to the initial investment is the excavation of declines to reach the reservoir. In order to

calculate, the hourly TBM operational cost which is 3426,49 $ is multiplied by the working hour to excavate declines and found as 473,934,553 $ (Appendix III).

Table 12 Component Cost Ratio Method for Bati Raman Reservoir

Component Cost Ratio Method			
No	**Operation**		**Cost ($)**
I	Purchased Equipment Cost		**931,263,984**
II	Delivered Equipment Cost	1.03 x I	959,201,904
III	Equipment Installation	0.20 x II	186,252,797
IV	Piping, material, and labor, excluding service piping	0.20 x II	186,252,797
V	Electrical, material, and labor, excluding building lighting	0.20 x II	186,252,797
VI	Instrumentation	0.10 x II	93,126,398
VII	Process buildings, including mechanical services and lighting	0.40 x II	372,505,594
VIII	Auxiliary building, including mechanical services and lighting	0.10 x II	93,126,398
IX	Plant services such as freshwater systems, sewers, compressed air, etc.	0.10 x II	93,126,398
X	Site improvements such as fences, roads, railroads, etc.	0.10 x II	93,126,398
XI	Field expenses related to construction management	0.11 x II	102,439,038
XII	Underground Development Cost	-	473,934,553
XIII	**Total Physical Cost**	**Σ (II,..., XI)**	**3,770,609,057**
XIV	Project management including eng. and construction	0.30 x II	279,379,195
XV	**Direct plant cost**	**XIII + XIV**	**4,049,988,252**
XVI	Contingency	0.15 x XV	607,498,238
XVII	**Total fixed capital cost**	**XV + XVI**	**4,657,486,490**
XVIII	Working capital	0.15 x XVII	698,622,974
XIX	**Total capital cost**	**XVII + XVIII**	**5,356,109,464**

In addition to the initial capital expenditures, the replacement capital cost should be considered to properly evaluate this project. Generally, every piece of equipment has a working life span, and if the operation that equipment conduct is not finished, a replacement will be required. In most cases, the whole machinery will not be replaced by the new one, but a considerable number of parts going to be replaced. Thus, the replacement cost will not be the same as the newly purchased equipment. To estimate the replacement cost of each piece of equipment same estimation guide that is used for estimating the capital cost (InfoMine USA, 2019).

To implement the replacement cost into the economic model of Bati Raman Reservoir, the working life span of each piece of equipment that is used should be known. According to the guide, the life span of each type of equipment is mostly different (Table 13). Hence, replacement capital investments will be implemented in the economic model based on the life span of the equipment.

Table 13 Average Life Span of Machinery (InfoMine USA, 2019)

Equipment	**Average Life Span (hr)**
TBM, Continuous Miner, Conveyor	10,000
Raise borer, Rock bolter	18,000
Trucks, pick-ups, Personnel carriers, etc.	25,000
Shovels	37,500
Pumps	12,000

With this information, TBMs, continuous miners, conveyor belts, and pumps will be replaced almost every year, Trucks, pick-ups, personnel carriers, and transmixers will be replaced every 3 years. On the other hand, shovels will be replaced every 5 years and the other machinery which is not represented in Table 13 has a life span higher than the mine life which is calculated in Chapter 3.

5.2 Operational Cost Estimation

The estimation of operational cost for Bati Raman Reservoir is separated into 6 major parts. These are, operation costs related to the excavation, ventilation, water treatment, steam generator, overhead cost, and surface processing cost.

Mostly for the operational cost that is expected from the excavation is estimated with the help of the cost estimation guide published by InfoMine USA (2019). In this guide, overhaul, maintenance, fuel, electric consumption lube, tires, and wear parts together with the labor costs are estimated from the previous mining operations. For every piece of equipment's hourly operational cost that is going to be used in MAHOP implementation is calculated and tabulated (Table 14). However, in order to predict the annual operational cost, the daily operational hour for each piece of equipment should be evaluated. After assumptions are made, the annual operational cost for every piece of machinery is found by multiplying by the annual working hour and hourly operational cost.

However, certain equipment like TBMs, a linear regression should be used to estimate both for capital (Appendix III) and operational expenses for specific diameters. From the known data, the relation between the diameter of the TBMs diameter and hourly operational cost is expressed as 373.06x-304.11=y with a 97.48% R^2 value. where x is the diameter of TBM and y is the hourly operational cost in the expression. Based on the regression model, 3426.5 $ is predicted to be the hourly operating cost of a 10-meter diameter TBM (Figure 34).

Table 14 Operating Cost of Equipment of Bati Raman

Type	Number of the Machine	Hourly Operational Cost ($) (2023)	Working Hours a Day (h)	Yearly Operational Cost ($)
TBM	9	3,486	23.0	310,841,681
Continuous Miner	18	249	23.0	44,408,629
Raise Borer (Fan-shaped Boreholes)	18	226	23.0	40,384,125
Rock Bolter	3	20	8.0	205,188
Underground Truck (Electrical)	73	73	20.0	46,168,707
Raise Borer (Ventilation Raises)	6	420	16.0	17,368,529
Transmixers	18	40	20.0	6,158,745
Shotcrete Machine	18	30	8.0	1,842,662
Scissors Lift	18	53	20.0	8,160,492
Maintenance Vehicle	3	29	20.0	757,439
Heavy-Duty Pickup	12	23	20.0	2,357,855
Personnel Carrier	10	25	12.0	1,307,105
Pumps (Oil)	3	x	24.0	775,270
Pumps (Water Drainage)	12	x	24.0	793,876
Pumps (Water for Steam Generators)	15	25	24.0	755,113
Pumps (Concrete)	18	6	24.0	1,040,102
Pumps (Refrigerant)	85	5	24.0	11,764,981
Pumps (Fuel)	5	6	24.0	31,528
Conveyor belt (8.5 km)	3	13	24.0	20,439,219
Loader (5m3 bucket cap.)	3	1	24.0	3,860,535
Surface Truck (25 m3)	30	659	20.0	14,081,488
Waste Dump	1	124	20.0	473,776
			Total	**568,031,974**

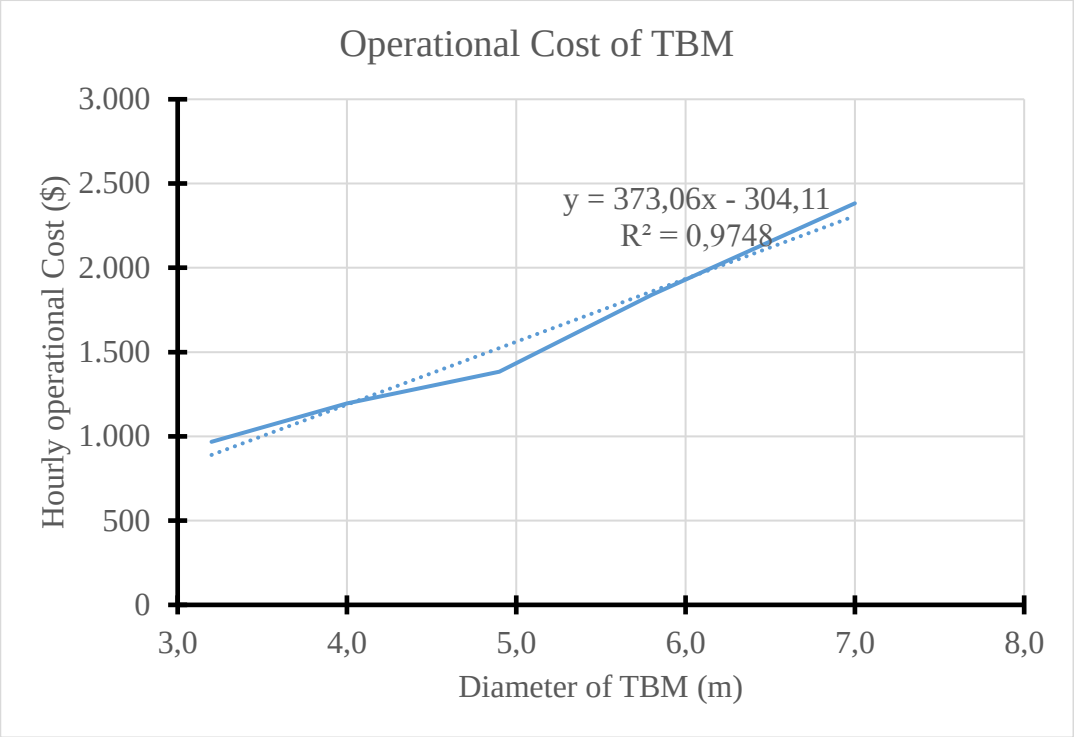

Figure 34 Linear Regression Graph of Operational Cost of TBM

The annual ventilation and cooling costs are calculated by the simulation program. According to the Ventsim, yearly 34,055,230 $ should be spent to ventilate and cool down the operations that occurred underground. It should be stated that, the calculations made by the program only electrical consumption of fans and cooling systems and unit power cost ($ 0.1/ kWh). Hence, additional overhead costs should be added to the operating cost after all the items are discussed.

Unlike the ventilation and cooling costs, the operating cost of steam generators cannot be estimated by a specific program. While it is true that most of the components associated with the steam generator, such as water and fuel pumps, have been included in the operating cost presented in Table 14, it is important to note that fuel consumption has not been taken into consideration. The details related to the calculations are represented in another table below (Table 15).

Table 15 Diesel Requirement of Steam Generators

Steam Generators	
Number of Steam Generators	5.0
Diesel Consumption (kg/h)	1,307.1
Diesel Density (kg/l)	0.7
Diesel Specific Volume (l/kg)	1.4
Diesel Consumption (l/h)	1,802.9
Diesel Consumption (l/annual)	14,214,036.4
Diesel Cost (in Türkiye) ($/l)	1.1
Diesel Cost for a Steam Generator ($/annual)	15,635,440.1
Average Diesel Cost for MAHOP ($/annual)	**76,262,404**

The other operational cost related to the MAHOP production in Bati Raman Reservoir is the water treatment cost. As the steam is injected through the reservoir, cooled-down steam converts into liquid and comes from the production boreholes after some point. The treatment of that water is required to continue the oil production operations underground. To estimate the water treatment cost, the unit cost of water treatment ($/barrel) is taken as $ 3 / barrel (oil) from Nguye et al. (2014) study. Based on the yearly production of Bati Raman, the expected water production and the annual water treatment cost is depicted in Table 16.

Table 16 Water treatment Cost of Bati Raman

Water Treatment Cost	
Water Treatment Cost ($/barrels oil)	3
Annual Average Oil Production (Barrels)	62,050,118
Annual Average Water Treatment Cost ($)	**186,150,354**

Although the excavation cost mostly consists of equipment cost, another major expense which is supporting cost is not included in this calculation. Therefore, according to InfoMine USA (2019), the supporting cost per meter values are taken as 2000 $/meter. The related supporting cost for each year is estimated by the yearly excavation amount and implemented in the economic evaluation in Chapter 5.3.

Lastly, the processing cost of excavated material from the reservoir should be added to the annual operational cost of Bati Raman. The unit cost of the process is anticipated to be closer to the shale retorting process. Thus, it is taken as 15 $/barrel (Qian & Wang, 2006). The table related to the surface process operating cost can be seen below.

Table 17 Surface Processing Cost of Bati Raman

Surface Processing Cost	
Processing Cost ($/barrel)	15.0
Total Production from Excavation (Barrels)	11,128,655
Total Processes Cost ($) (Surface)	**166,929,820**

It should be noted that the overhead cost is not included in the above operating cost calculations. Therefore, an additional table that estimates the laboring cost that is not included in Table 14 is created (Table 18). Additionally, the overhead cost are calculated from the cost estimation guide as $ 1,153,714 for very year.

After all operating costs are summed up, the yearly anticipated operational cost of Bati Raman is calculated as 1,240,662,395 $/year when excavation continues and MAHOP is operational. If the operating cost is divided by the produced oil from Bati Raman, the unit cost of oil production can be found as 32.32 $/barrel (Table 19). From this point, the economic evaluation of Bati Raman can be conducted in the next part of this chapter.

Table 18 Laboring Cost

Job Description	Number	Salary (Loaded) ($/person/month)	Salary ($/year)
Labor (Piping, waste dumps, etc.)	980	1,300	15,288,000
Foreman	98	1,430	1,681,680
Mining Engineer	15	1,950	351,000
Geologist	8	1,690	162,240
Petroleum Engineer	15	1,950	351,000
Process Engineer	15	1,690	304,200
Mechanical Engineer	5	1,690	101,400
Electrical Engineer	2	1,690	40,560
Control Engineer	10	1,690	202,800
Health and Safety Manager	1	2,210	26,520
Health and Safety Engineer	6	1,560	112,320
Chief Engineer	3	2,210	79,560
HR Manager	1	1,950	23,400
Deputy Manager	4	2,340	112,320
Mine Manager	1	2,600	31,200
Process Manager	1	2,600	31,200
General Manager	1	3,640	43,680
Doctor	1	1,950	23,400
Nurse	2	1,300	31,200
Lab Technician	10	1,300	156,000
Private Security	35	1,040	436,800
		Total	**19,590,480**

Table 19 Operational Cost Summary

Operational Cost Summary	
Mining Cost ($/barrel)	10.52
Ventilation Cost ($/barrel)	0.55
Steam ($/barrel)	1.23
Water Treatment ($/barrel)	5.02
Processing ($/barrel)	15.00
Total ($)	**32.32**

5.3 Economical Evaluation of Bati Raman Reservoir

The economic evaluation of Bati Raman is conducted starting from 2023 to the end of the life of the project, which is 2036. For each year the capital cost is calculated by the replacement time and replacement cost of the equipment as stated above. As known from the mining projects, these capital costs are depreciated with a method to reduce taxes that are paid at the end of each year. Although, there are several depreciation methods, straight-line depreciation (normal amortization) is the most commonly used depreciation method in Türkiye (Aksoylu, 2013). Therefore, in this study, straight-line depreciation is used to anticipate the depreciation for every year. To calculate every equipment depreciation, the capital investments including replacement costs are divided by the lifespan of each equipment (Table 20).

Table 20 Depreciation value of Bati Raman

Depreciation			
Years	**Initial Depreciation**	**Replacement depreciation**	**Total Depreciation**
2023	-77,181,471	0	-77,181,471
2024	-77,181,471	-5,465,594	-82,647,065
2025	-80,803,463	-5,465,594	-86,269,057
2026	-80,803,463	-11,120,987	-91,924,450
2027	-80,803,463	-6,665,433	-87,468,896
2028	-80,803,463	-6,999,861	-87,803,324
2029	-80,803,463	-11,120,987	-91,924,450
2030	-80,803,463	-12,632,286	-93,435,749
2031	-80,803,463	-5,465,594	-86,269,057
2032	-80,803,463	-11,432,447	-92,235,910
2033	-80,803,463	-13,353,833	-94,157,296
2034	-80,803,463	0	-80,803,463
2035	-5,432,988	-5,655,392	-11,088,380
2036	-5,432,988	0	-5,432,988

In addition to depreciation, income tax, and royalty are implemented in the economic study of Bati Raman with respect to the 6491 Turkish Petroleum Law. According to the law, 12.5% of production and 25% of the income will be subjected to royalty and taxation, respectively. After these considerations are implemented into the study, the payback period of this project is expected to be 6.5 years (Figure 35) with an almost 3.5 billion dollars net income. The net present value according to the 15 years of average interest rate (10%) is calculated as $ 6,519,530,246 with a 23% IRR value. The IRR of this project indicates that the investment required for Bati Raman will be economical unless the interest rate reaches 23%. Therefore, this project can be specified as investible. The cumulative net income vs years graph, the yearly economic evaluation table, and cumulative net income over years are depicted below.

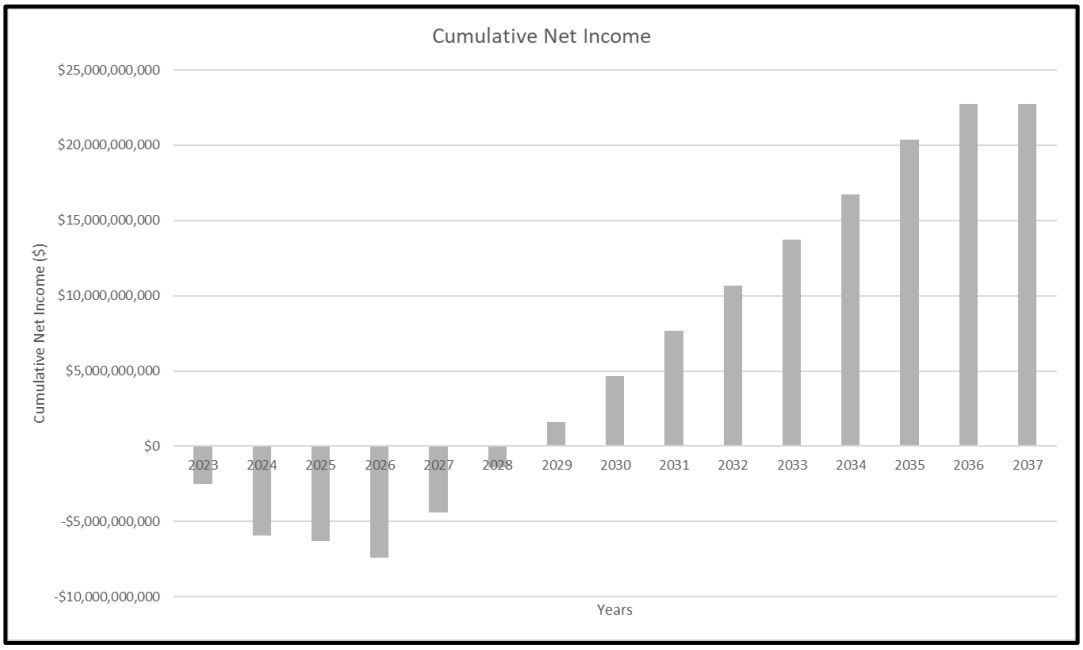

Figure 35 Cumulative Net Income vs Years Graph

Table 21 Yearly Economic Evaluation

Years	Investment ($)	Income ($)	Operational Cost ($)	Total Annual Cost ($)	Depreciation ($)	Royalty ($)	Income Tax ($)	Salvage ($)	Net Income ($)
2023	-2,190,223,426	0	-297,459,808	-2,487,683,234	-77,181,471	0	0	0	-2,487,683,234
2024	-3,172,309,519	0	-297,459,808	-3,469,769,327	-82,647,065	0	0	192,704	-3,469,576,623
2025	-6,423,482	0	-339,844,759	-346,268,241	-86,269,057	0	0	192,704	-346,075,537
2026	-14,410,995	46,847,780	-1,158,147,084	-1,172,558,078	-91,924,450	-5,855,973	0	432,330	-1,131,133,941
2027	-9,948,780	6,300,000,000	-1,240,662,395	-1,250,611,176	-87,468,896	-787,500,000	-1,240,479,982	298,463	3,021,707,306
2028	-13,203,770	6,300,000,000	-1,240,662,395	-1,253,866,165	-87,803,324	-787,500,000	-1,239,582,628	396,113	3,019,447,320
2029	-14,410,995	6,300,000,000	-1,240,662,395	-1,255,073,390	-91,924,450	-787,500,000	-1,238,250,540	432,330	3,019,608,400
2030	-18,594,535	6,300,000,000	-1,240,662,395	-1,259,256,930	-93,435,749	-787,500,000	-1,236,826,830	557,836	3,016,974,076
2031	-6,423,482	6,300,000,000	-1,240,662,395	-1,247,085,877	-86,269,057	-787,500,000	-1,241,661,266	192,704	3,023,945,561
2032	-15,069,236	6,300,000,000	-1,240,662,395	-1,255,731,632	-92,235,910	-787,500,000	-1,238,008,115	452,077	3,019,212,331
2033	-22,494,309	6,300,000,000	-1,240,662,395	-1,263,156,704	-94,157,296	-787,500,000	-1,235,671,500	674,829	3,014,346,625
2034	0	6,300,000,000	-1,240,662,395	-1,240,662,395	-80,803,463	-787,500,000	-1,244,633,535	21,351,275	3,048,555,344
2035	-7,987,513	6,300,000,000	-457,372,131	-465,359,644	-11,088,380	-787,500,000	-1,455,887,994	239,625	3,591,491,988
2036	0	4,062,267,790	-205,627,898	-205,627,898	-5,432,988	-507,783,474	-962,801,726	1,680,306	2,387,734,998
								NPV	**$6,519,530,246.37**

Table 22 Cumulative Net Income Over Years

Years	**Cumulative Net Income ($)**
2023	-2,487,683,234
2024	-5,957,259,857
2025	-6,303,335,394
2026	-7,434,469,335
2027	-4,412,762,029
2028	-1,393,314,709
2029	1,626,293,691
2030	4,643,267,767
2031	7,667,213,328
2032	10,686,425,659
2033	13,700,772,284
2034	16,749,327,628
2035	20,340,819,616
2036	22,728,554,614
IRR	**23%**

After the yearly economical evaluation is done, another crucial component of economic project evaluation, which is sensitivity analysis, should be discussed. In an ever-changing and uncertain business environment, projects face various risk factors that can affect their economic viability. In this case, these factors mostly consist of oil prices, capital expenditure, operational expenditures, and interest rate. Therefore, a sensitivity analysis that investigates these parameters within a positive and negative 20% error margin is conducted (Figure 36).

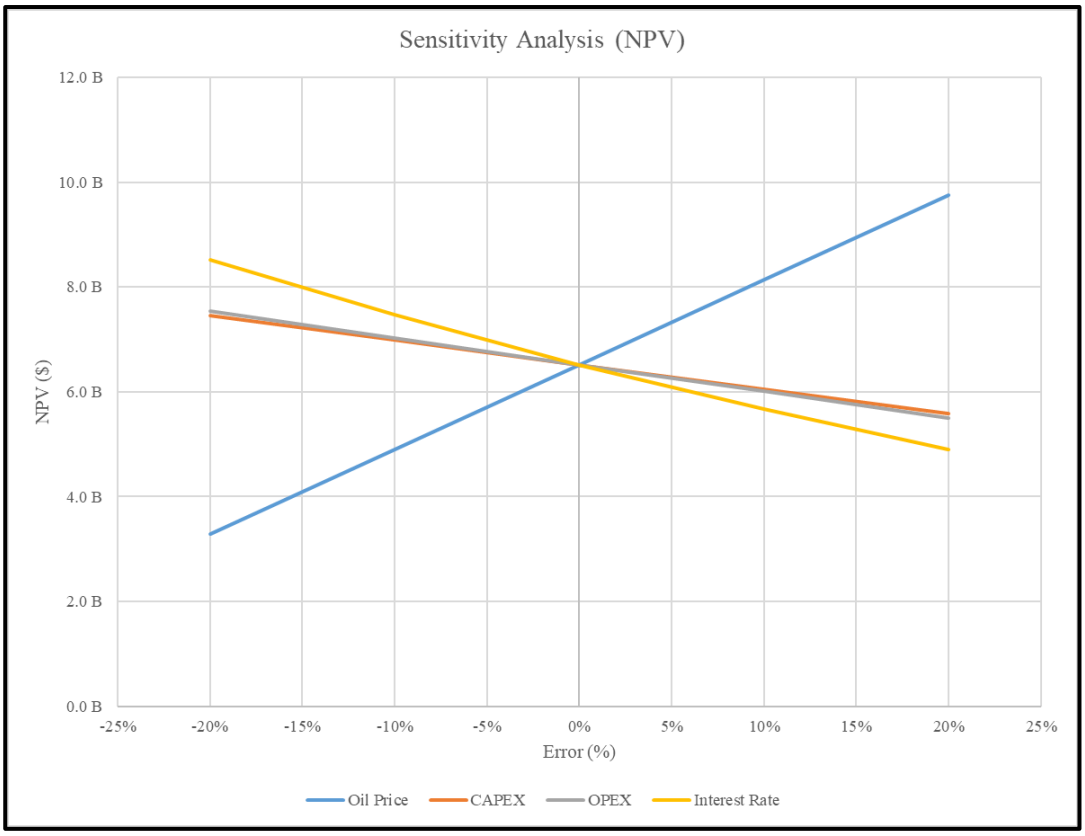

Figure 36 NPV Sensitivity Analysis of Bati Raman

As can be seen in Figure 36, the parameter that affects the most NPV value is the oil prices. The 10% change in oil prices has an effect on the project NPV value is almost a 24% change. Therefore, if this project is considered to be implemented in Bati Raman Reservoir, the oil prices on those days will play a highly important role in the future of this project. It should be noted that, for this study, the oil price is taken as 70 $/barrel from the present-day (May 2023) value.

Another parameter that affects the NPV value of this project is the Interest rate applied on Bati Raman. The interest value is taken from other oil production projects (Galvão et al., 2014; Nguyen et al., 2014). The 10 and 20% change in the interest rate of Bati Raman will result in a change in the NPV values of almost 14% change.

The changes in the CAPEX and initial OPEX are the parameters that affect the NPV value of the project less compared to the oil price and interest rate. The 10% change in both CAPEX and OPEX results in almost equal to 8%.

At the end of the sensitivity analysis, the project's economic evaluation showed that the possible implementation of MAHOP in Bati Raman Reservoir has economic potential for investors with a 23% IRR value and almost 6.5 B $ NPV value. According to the operational cost investigation, the 32.32 $ cost per barrel production can be considered as inexpensive compared to today's oil prices. However, the required initial capital investment which is approximately 5.36 B $ can be seen as high compared to the usual mine initial investment values due to the excessive amount of excavations.

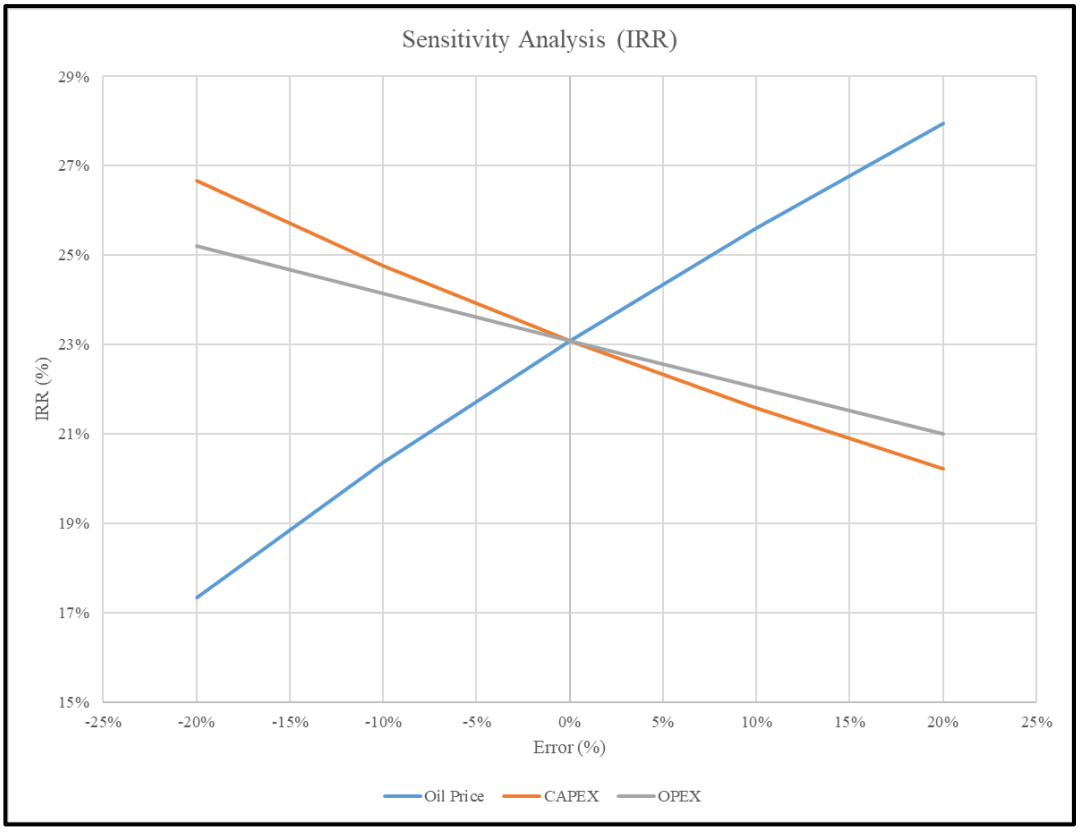

Figure 37 IRR Sensitivity Analysis of Bati Raman

A Similar sensitivity study is adapted to the IRR values (Figure 37). In this case, unlike the NPV sensitivity analysis, oil price, CAPEX, and OPEX were investigated in terms of IRR. The interest rate is not considered while calculating the IRR values, hence there is no observable change in IRR while evaluating the change in interest rate. According to the graph above, the influence of the three parameters is almost similar. For capital investment and operational expenses, 10% of the change will result in a 1.5% change in IRR. However, the 10% change in oil price effects the IRR value by almost 3%.

In addition to the sensitivity analysis, similar economic evaluations have been done for different recovery percentages. For the above-mentioned yearly economic evaluation has been done according to the 70 % of oil recovery. These recovery values are taken from Canbolat's et al. (2023) MAHOP experiment 3 model which is the highest recovery values. However, in similar SAGD implementations, the recovery values can be seen as lower than 70% of the recovery. Therefore, a series of economic evaluations covering the 80, 60, 50, and 40% recovery have been done. The table that contains the NPV and IRR values is depicted below. As expected, while the recovery of the production is decreased the NPV and IRR values are decreased (Table 23). In almost every case, the required steam generator specifications are adapted to a point where the MAHOP production ends 3 months later the excavation works end. This approach is utilized to increase the NPV values as high as possible by decreasing the production life. However, even with this method, recoveries that are below 50 % might be stated as risky for the investment.

Table 23 Sensitivity Analysis Based on the Recovery of MAHOP Production

Sensitivity Analysis (Recovery)		
Recovery	**NPV ($)**	**IRR (%)**
80%	7,772,578,444	24%
70%	6,519,530,246	23%
60%	5,172,608,913	22%
50%	3,277,185,278	18%
40%	1,170,291,019	13%

Lastly, a break-even analysis for the oil prices is conducted. According to the analysis, when the oil prices reach values below $ 41.8 / barrel, oil production from the MAHOP implementation in Bati Raman becomes non-profitable. With this break-even value, the internal rate of return value reaches the discount rate that is used to evaluate NPV value which is 10% (Figure 38).

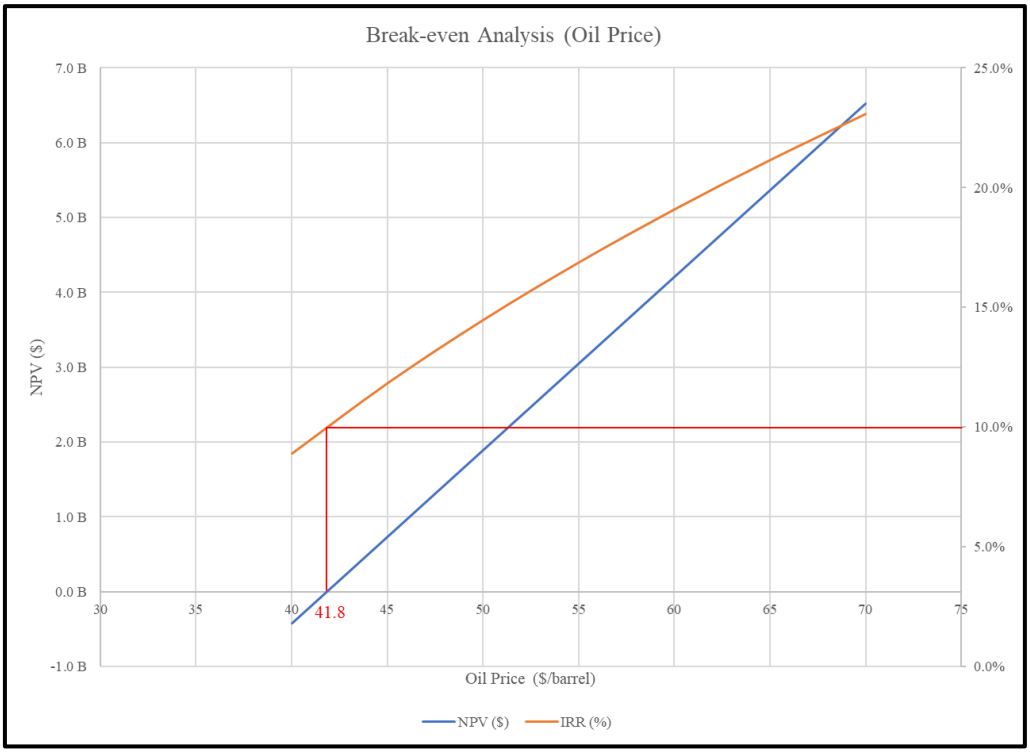

Figure 38 Break-even Analysis for Oil Price

CHAPTER 6

CONCLUSIONS AND RECOMMENDATIONS

- The MAHOP method involves an underground steam injection process similar to Steam Assisted Gravity Drainage (SAGD) to overcome challenges associated with reservoir depth heterogeneity. Fan-shaped boreholes drilled at the roof of production galleries facilitate steam injection and oil production beneath the surface. The collected oil in sumps within the production galleries is then pumped to the surface. Additionally, surface processing of excavated materials follows an oil shale retorting process.
- The study begins by creating a 3D model of the Bati Raman reservoir using drill hole data from TPAO. The orientation of production openings and their optimal production levels are determined based on reservoir shape and efficiency calculations of the fan-shaped boreholes. The mine layout considers the connection of nested production galleries, cross-cut locations, and declines.
- To enhance overall recovery, two different excavation operations are planned, utilizing both Tunnel Boring Machines (TBM) and continuous miners. The mine layout results in an expected excavation length of approximately 463.5 km. The MAHOP production is isolated in specific panels to ensure safety and ventilation requirements.
- The excavation with the TBM creates challenges to overcome especially at 1450-meter depth. The structure of the geology of the excavation area with geological logging, rock mass characterization, hydraulic test, and seismic profiles between holes and probe drilling for deep TBM excavation should be assessed before and during the excavation. After the geological structure is described, the strength of the rock mass with pre-grouting and an umbrella-shaped rock bolting ahead of the TBM might be used where there is no option to change the location of the tunnel.

- Additional to tunneling challenges, the TBM application in a gassy environment can be expected in the Bati Raman Reservoir. Therefore, solutions such as compartmentalization of TBM, using explosion-proof equipment, implementing a special forced ventilation system design, using continuous monitoring, and assessing particular procedures for excavations are underlined.
- A production schedule is developed, dividing the Bati Raman reservoir into three major production areas northern and southern parts of the western section and the eastern section. A total of 88 panels are assigned for MAHOP production, with five panels operating simultaneously. The average excavation time for a panel is calculated as 118 days, determining the required capacity of a 20,000 kg/h steam generator.
- Ventilation and cooling cases are addressed by implementing modular sections and considering decline ventilation, single-panel ventilation, and consecutive panel ventilation. Ventilation simulations determine the required intake of fresh air, accounting for factors like diesel engine emissions, dust dilution, harmful gas dilution, and breathing. For the heat challenges, cooling systems such as cooling pockets and chilled water spray methods, are employed to maintain temperatures below the wet-bulb threshold of 28 °C.
- Capital cost estimation utilizes the component cost ratio method, considering the cost estimation guide and machinery required for the project. The total initial investment is calculated as 5.36 billion dollars, accounting for mine development excavations. Operational costs per barrel (32.32$) encompass machinery, vehicles, steam generation, ventilation and cooling, water treatment, surface processing, and overhead expenses. The annual economic evaluation yields a net present value (NPV) of 6.5 billion dollars and an internal rate of return (IRR) of 23%.
- Sensitivity analysis explores the influence of varying oil prices, production rates, interest rates, and initial investments on NPV and IRR. The analysis reveals that NPV is highly sensitive to oil prices and production rates. The sensitivity analysis for IRR demonstrates consistent changes across all three parameters, unlike the

NPV values. This change is related to the time of initial capital investment and the huge difference between expenditure and revenue values.

- Break-even analysis showed that the oil price below $ 41.8 /barrel resulted in non-profitable oil production in Bati Raman Oil Reservoir.
- The overall study indicates that the MAHOP implementation in the Bati Raman reservoir is highly profitable, as evidenced by the positive NPV and robust IRR values.

Although the projects seem highly profitable, some parts of this study should be investigated further. These areas can be explained as follows;

- In this study, the mine layout is mostly affected by the 3D model of Bati Raman due to the restricted knowledge about the structure of the reservoir. With detailed drillhole data and a structural map, the mine layout can be improved and changed.
- Even a previous work investigated the MAHOP implementation in Bati Raman, additional rock stability evaluations should be done based on the mine layout that is completed in Chapter 3.
- The challenges related to the steam generator usage underground are not within the scope of this study. However, the usage of steam generators underground can pose a safety issue. Hence a detailed investigation in terms of safety should be assessed.
- The coefficients that are used in the method that is used to estimate the initial investment, are mostly based on the previous mining operations. Therefore, detailed estimation similar to the equipment cost estimation can be done for piping, processing facilities, field expenses, etc.

REFERENCES

Aksoylu, S. (2013). Finansal Raporlama Standartları Kapsamında Maden İşletmelerinde Amortisman Uygulamasının Değerlendirilmesi. *Eskişehir Osmangazi Universitesi IIBF Dergisi*, *8*(3), 137–156.

Ala, M. A., & Moss, B. J. (1979). Comparative Petroleum Geology of Southeast Turkey and Northeast Syria. In *Journal of Petroleum Geology* (Vol. 1, Issue 4).

Al-Dahhan, W. H., & Mahmood, S. M. (2019). Classification of Crude Oils and its Fractions on the Basis of Paraffinic, Naphthenic and Aromatics. *Journal of Science*, *22*(3), 35–42. https://doi.org/10.22401/ANJS.22.3.05

Alsharhan, A. S., & Nairn, A. E. M. (1997). *Sedimentary Basins and Petroleum Geology of the Middle East* (Second Impression). Elsevier.

Anon. (1972). Threshold Limit Values for Chemical Substances and Physical Agents and Biological Exposure Indices. *American Conference of Governmental Industrial Hygienists*.

Ayhan, M., Aydın, D., İmamoğlu, M. Ş., Çoğalan, M., & Karakuş, A. (2019). Investigation of a methane flare during the excavation of the Silvan irrigation tunnel, Turkey. *Bulletin of Engineering Geology and the Environment*, *78*(4), 2641–2652. https://doi.org/10.1007/s10064-018-1265-y

Bandini, A., Berry, P., Cormio, C., Colaiori, M., & Lisardi, A. (2017). Safe excavation of large section tunnels with Earth Pressure Balance Tunnel Boring Machine in gassy rock masses: The Sparvo tunnel case study. *Tunnelling and Underground Space Technology*, *67*, 85–97. https://doi.org/10.1016/j.tust.2017.05.001

Barla, G., Janutolo, M., & Zhao, K. (2011, March 10). Open issues in tunnel boring machine excavation of deep tunnels. *14th Australasian Tunnelling Conference*. https://www.researchgate.net/publication/288554918

Barla, G., & Pelizza, S. (2000). TBM tunnelling in difficult ground conditions. *An International Conference on Geotechnical & Geological Engineering*. https://www.researchgate.net/publication/228680502_TBM_tunnelling_in_difficult_ground_conditions

Barton, N. R. (2000). *TBM tunnelling in jointed and faulted rock*. Crc Press.

Barton, N. R. (2004, January). Risks and risk reduction on TBM. *ARMS Asian Rock Mechanics Symp.*

Barton, N. R. (2013). Hybrid TBM and Drill-and-Blast from the start. *Tunnel Journal*, 22–32.

Belle, B., & Biffi, M. (2010). Cooling pathways for deep Australian longwall coal mines of the future. *Mine Ventilation Conference*, 94–104.

Belle, B., & Foulstone, A. (2015). Explosion Prevention in Coal Mine TBM Drifts – An Operational Safety Knowledge Share. *Procedia Earth and Planetary Science*, *11*, 15–28. https://doi.org/10.1016/j.proeps.2015.06.004

Bilgin, N., Copur, H., & Balci, C. (2016). Effect of methane and other gases on TBM performance. In *TBM Excavation in Difficult Ground Conditions* (pp. 273–292). Wiley-VCH Verlag GmbH & Co. KGaA. https://doi.org/10.1002/9783433607190.ch13

Blank, L. T., & Tarquim, A. J. (1989). *Engineering Economy* (3rd edition). Mc-Graw Hill.

Bluhm, S., Moreby, R., von Glehn, F., & Pascoe, C. (2014). Life-of-mine ventilation and refrigeration planning for Resolution Copper Mine. *Journal of South African Institute of Mining and Metallurgy*, *114*, 497–503.

Board, M. P. (1994). *Numerical examination of mining-induced seismicity*. University of Minnesota.

Boldt, H., & Hennek, J. (1981). Tunnel boring under coal mining conditions. *Rapid Excavation and Tunneling Conference*, 722–737.

Borg I.Y. (1982). *OIL MINING: A REVIEW WITH RECOMMENDED R&D IN THE FEDERAL SECTOR*.

Brox, D. (2013). Technical considerations for TBM tunneling for mining projects. *Transactions of the Society for Mining, Metallurgy and Exploration*, *334*, 498–505.

Bullock, R. L. (2018). Introduction to Cost Estimating for Feasibility Projects. In R. L. Bullock & S. Mernitz (Eds.), *Mineral Property Evaluation: Handbook for Feasibility Studies and Due Diligence* (pp. 351–401). SME.

Butler, R. M. (1982). *Method for continuously producing viscous hydrocarbons by gravity drainage while injecting heated fluids* (Patent No. 4,344,485).

Butterworth, M. (1999). Controlled Recirculation in Deep South African Gold Mines. *Proceedings of the 8th US Mine Ventilation Symposium*, 697–704.

Canbolat, S., Ozturk, H., & Akin, S. (2020). Economics of Mining Assisted Heavy Oil Production (MAHOP) Method for Ultimate Recovery. *Türkiye IV. Bilimsel ve Teknik Petrol Kongresi*.

Canbolat, S., Ozturk, H., & Akin, S. (2022). Exploitation of Bati Raman field using advanced thermal methods: MAHOP VS. CSHP. *Journal of Petroleum Science and Engineering*, *208*. https://doi.org/10.1016/j.petrol.2021.109802

Canbolat, S., Ozturk, H., & Akin, S. (2023). Experimental and numerical investigation of mining assisted heavy oil production for the Bati Raman field, Turkey. *Geoenergy Science and Engineering*, *223*, 211497. https://doi.org/10.1016/J.GEOEN.2023.211497

Chertenkov, M. V. , S., Mulyak, V. V. , L., & Konoplev, Y. P. , P. branch of L. E. (2012). *RUSSIA'S YAREGA HEAVY OIL FIELD*.

http://onepetro.org/JPT/article-pdf/64/04/153/2206530/spe-0412-0153-jpt.pdf/1

Cigla, M., Yagiz, S., Cigla, M., Yagiz, S., & Ozdemir, L. (2001). *Application of tunnel boring machines in underground mining development Application of Tunnel Boring Machines in Underground Mine Development*. https://www.researchgate.net/publication/280233359

Cinar, M., & Feridunoglu, C. (1994). Tünel açma makineleri. *Uaşımda Yeraltı Kazıları I. Sempoziyumu*, 343–367.

Copur, H., Cinar, M., Okten, G., & Bilgin, N. (2011). A case study on the methane explosion in the excavation chamber of an EPB-TBM and lessons learnt including some recent accidents. *Tunnelling and Underground Space Technology*. https://doi.org/10.1016/j.tust.2011.06.009

De Souza, E. M., & Katsabanis P.D. (1991). On the prediction of blasting toxic fumes and dilution ventilation. *Mining Science and Technology*.

Dimension and Weights per metre for Iso 2448. (n.d.). Retrieved May 15, 2023, from http://entech.rs/PDF-ENG/B2.4.6.pdf

Doyle, B. R. (2001). *Hazardous gases underground : applications to tunnel engineering*. Marcel Dekker.

Emci, M. E., & Ozturk, H. (2021). Numerical analysis of deep twin excavations and boreholes for heavy oil production. *IOP Conference Series: Earth and Environmental Science*, *833*(1). https://doi.org/10.1088/1755-1315/833/1/012185

Engineering ToolBox. (2003). *Gases - Explosion and Flammability Concentration Limits*. https://www.engineeringtoolbox.com/explosive-concentration-limits-d_423.html

Epiroc. (2020). *Minetruck MT42 Battery: Technical Specification Manuel*. https://www.epiroc.com/en-us/products/loaders-and-trucks/electric-trucks/minetruck-mt42-battery

Fang, Y., Fan, J., Kenneally, B., & Mooney, M. (2016). Air flow behavior and gas dispersion in the recirculation ventilation system of a twin-tunnel construction. *Tunnelling and Underground Space Technology*, *58*, 30–39. https://doi.org/10.1016/J.TUST.2016.04.006

Forbes, J. J., & Grove, G. W. (1954). *Mine gases and methods for detecting them* (Vol. 33). US Bureau of Mines.

Galvão, E. R. V. P., Rodrigues, M. A. F., Dutra, T. V., & Da Mata, W. (2014). Economic Evaluation of Steam and Solvent Injection for Heavy-Oil Recovery. *SPE Latin American and Caribbean Petroleum Engineering Conference*, *3*, 2070–2084. https://doi.org/10.2118/169442-MS

Gentry, D. W., & O'Neil, T. J. (1984). *Mine Investment Analysis*. Society of Mining Engineers of American Institute of Mining, Metallurgical and Petroleum Engineers (AIME).

Goch, D. C., & Patterson, H. S. (1940). The Heat Flow into Tunnels. *J. Chem., Met. Mng. Soc. S. Afr.*, *41*(3), 117–128.

Gong, Q., Yin, L., Ma, H., & Zhao, J. (2016). TBM tunnelling under adverse geological conditions: An overview. *Tunnelling and Underground Space Technology*, *57*, 4–17. https://doi.org/10.1016/j.tust.2016.04.002

Grandori, R. (2006). Abdalajis east railway tunnel (Spain) – double shield universal TBM cope with extremely poor and squeezing formations. *Tunnelling and Underground Space Technology*, *21*(3–4), 268. https://doi.org/10.1016/j.tust.2005.12.128

Grave, D. F. H., & Stroh, R. M. (1972). The planning of Ventilation and Refrigeration requirements in Deep Mines. *Journal of the South African Institute of Mining and Mettalurgy*, 171–186.

Grothen, B. (2018). *Case studies in challenging geology: Gerede water tunnel & Deleware aqueduct repair*. https://nff.no/wp-content/uploads/sites/2/2020/04/05-Grothen.pdf

Halim, A. (2016). Ventilation requirements for diesel equipment in underground mines-Are we using the correct values? In J. F. Brune (Ed.), *16th North American Mine Ventilation Symposium*. Society of Mining, Metallurgy and Exploration.

Handewith, H. J. (1980). Mine applications of tunnel boring machines. *CIM Bull.*, *73*(823), 133–136.

Handewith, H. J. (1983). TBM tunnels in the western hemisphere - an overview. *Tunneling Technology Newsletter*, *41*, 1–8.

Hardcastle, S. G., Kocsis, C., Hardcastle, S. G., & Kocsis, C. K. (2004). The ventilation challenge. *CIM Bulletin*. https://www.researchgate.net/publication/295574832

Harding, D. (2019). *Rebuilding TBMs: Are Used TBMs as Good as New?*

Hartman, H. L., Mutmansky, J. M., Ramani, R. V., & Wang, Y. J. (1997). *Mine Ventilation and Air Conditioning* (3rd ed.). Kohn Wiley & Sons.

Hoek, E. (1994). Strength of rock and rock masses. *ISRM News Journal*, *2*(2), 4–16.

Hoek, E., & Martin, C. D. (2014). Fracture initiation and propagation in intact rock - A review. In *Journal of Rock Mechanics and Geotechnical Engineering* (Vol. 6, Issue 4, pp. 287–300). Chinese Academy of Sciences. https://doi.org/10.1016/j.jrmge.2014.06.001

Home, L., & Askilsrud, O. G. (2011). Tunnel Boring Machines in Mining. In P. Darling (Ed.), *SME Mining Engineering Handbook* (3rd ed., pp. 1255–1270). Society for Mining, Metallurgy, and Exploration (SME).

Howden Group Limited. (2019). *Ventsim Design 5* (5.2.9.5). www.ventsim.com

Huber, B. (2004). *Stress-induced Fractures in the Deep-seated Bedretto Tunnel: Their Geological and Geomechanical Reasons*. ETH Zurich.

Hutchins, J. S., Bond, E., & Bass, D. M. (1978). *MINING FOR PETROLEUM: FEASIBILITY STUDY*.

ICI Caldaie GX12 Bar Industrial Steam Generator Catalogue. (n.d.). Retrieved May 4, 2023, from https://www.icicaldaie.com/en/catalog/gamma/GAM/MOD_GX_12_bar_WEB

InfoMine USA. (2019). *Mine and Mill Equipment Cost: an Estimator Guide*. www.costmine.com

ISRM. (1981). *Rock Characterization Testing and Monitoring* (E. Brown, Ed.). Pergamon Press.

Kamyar, A., Mostafa Aminossadati, S., Leonardi, C., & Sasmito, A. (2016). Current Developments and Challenges of Underground Mine Ventilation and Cooling Methods. *Coal Operators' Conference*, 277–287. https://ro.uow.edu.au/coalhttps://ro.uow.edu.au/coal/615

Kantar, K., Petroleum Corp Karaoguz, T. D., & Petroleum Corp, T. K. (1985). *Design Concepts of a Heavy-Oil Recovery Process by an Immiscible CO 2 Application*. http://onepetro.org/JPT/article-pdf/37/02/275/2242854/spe-11475-pa.pdf

Kidd, J. (1995). Slurry ice Production in gold mining. *South African Mechanical Engineer*, *45*, 11–14.

Kissel, F. N. (2006). *Handbook for Methane Control in Mining*. Niosh. www.cdc.gov/niosh

Komery, D. P., Luhning, R. W., & O'rourke, J. G. (1999). Towards Commercialization of the UTF Project Using Surface Drilled Horizontal SAGD Wells. *Journal of Canadian Petroleum Technology*, *38*(9), 36–43. http://onepetro.org/JCPT/article-pdf/38/09/36/2170554/petsoc-99-09-03.pdf/1

Kravcov, A., Cherepetskaya, E., Svoboda, P., Blokhin, D., Ivanov, P., & Shibaev, I. (2020). Thermal infrared radiation and laser ultrasound for deformation and water saturation effects testing in limestone. *Remote Sensing*, *12*(24), 1–14. https://doi.org/10.3390/rs12244036

Laughton, C. (2005). Geotechnical problems encountered by tunnel boring machines mining in sedimentary rocks. *International World Tunnel Congress and the 31st ITA General Assembly*, 857–863.

Li, T., Cai, M. F., & Cai, M. (2007). Earthquake-induced unusual gas emission in coalmines - A km-scale in-situ experimental investigation at Laohutai mine. *International Journal of Coal Geology*, *71*(2–3), 209–224. https://doi.org/10.1016/J.COAL.2006.08.004

Liu, Q., Nie, W., Hua, Y., Jia, L., Li, C., Ma, H., Wei, C., Liu, C., Zhou, W., & Peng, H. (2019). A study on the dust control effect of the dust extraction system in TBM construction tunnels based on CFD computer simulation technology. *Advanced Powder Technology*, *30*(10), 2059–2075. https://doi.org/10.1016/j.apt.2019.06.019

Loew, S., Barla, G., & Diederichs, M. (2010). Engineering geology of Alpine Tunnels: Past, present and future. *11th IAEG Congress*. https://www.researchgate.net/publication/259762406_Engineering_geology_of_Alpine_Tunnels_Past_present_and_future_keynote_lecture

Macias, J., & Bruland, A. (2014, May). D&B versus TBM: Review of the parameters for a right choice of the excavation method. *ISRM European Rock Mechanics Symposium (EUROCK)*.

Maden İşyerlerinde İş Sağlığı ve Güvenliği Yönetmeliği. (2013, September 19). Legal Gazette. https://www.mevzuat.gov.tr/mevzuat?MevzuatNo=18858&MevzuatTur=7&MevzuatTertip=5

Maidl, B., Schmid, L., Ritz, W., & Herrenknecht, M. (2008). *Hardrock Tunnel Boring Machines*. Wiley. https://doi.org/10.1002/9783433600122

Mamaghani, A. S., Erdogan, T., Dogan, E., & Bilgin, N. (2016). Evaluation of the Performance of a Raise Boring Machine in Pb-Zn Underground mine, Balya, Turkey. *World Tunnel Conference*.

Martin, C. D., Kaiser, P. K., & Mccreath, D. R. (1998). Hoek-Brown parameters for predicting the depth of brittle failure around tunnels. *Canadian Geotechnical Journal*.

McPherson, M. J., Eng, C., Aime, M., & Ashrae, M. (1993). *Subsurface Ventilation Engineering*. http://www.mvsengineering.com/

Metropolitan Water Reclamation District of Greater Chicago. (n.d.). *Metropolitan Water Reclamation District of Greater Chicago Fact Sheet*. Retrieved May 9, 2023, from https://www.robbinstbm.com/projects/chicagos-tunnel-reservoir-plan-tarp/

Micromine Pty Ltd. (2022). *Micromine Origin & Beyond* (22.0.508.3). https://www.micromine.com

Miller, E. C. (1946). OIL MINING IN PENNSYLVANIA. In *History: A Journal of Mid-Atlantic Studies* (Vol. 13, Issue 3). https://www.jstor.org/stable/27766717

Mohutsiwa, M., & Musingwini, C. (2015). Parametric estimation of capital costs for establishing a coal mine: South Africa case study. *Journal of South African*

Institute of Mining and Metallurgy, *115*, 789–797. https://www.saimm.co.za/Journal/v115n08p789.pdf

Nguyen, X. H., Bae, W., Gunadi, T., & Park, Y. (2014). Using response surface design for optimizing operating conditions in recovering heavy oil process, Peace River oil sands. *Journal of Petroleum Science and Engineering*, *117*, 37–45. https://doi.org/10.1016/J.PETROL.2014.02.012

Nie, X., Wei, X., Li, X., & Lu, C. (2018). Heat Treatment and Ventilation Optimization in a Deep Mine. *Advances in Civil Engineering*, *2018*. https://doi.org/10.1155/2018/1529490

Nord, G. (2006). TBM versus Drill and Blast, the choice of tunneling method. *International Conference and Exhibition on Tunnelling and Trenchless Technology*, 7–9.

Nord, G., & Stille, H. (1988). Bore-and-blast techniques in different types of rock: Sweden's experience☆. *Tunnelling and Underground Space Technology*, *3*(1), 45–50. https://doi.org/10.1016/0886-7798(88)90032-6

Nourali, H., & Osanloo, M. (2019). Mining capital cost estimation using Support Vector Regression (SVR). *Resources Policy*, *62*, 527–540. https://doi.org/10.1016/J.RESOURPOL.2018.10.008

O' Hara, A. T., & Suboleski, S. C. (1992). Costs and Cost Estimation. In *SME mining engineering handbook* (Vol. 1, pp. 405–424).

O' Hara, T. A. (1980). Quick guides to the evaluation of orebodies. *CIM Bulletin*, *73*(814), 87–89.

Ostwald, P. F. (1992). *Engineering Cost Estimating* (3rd ed.). Prentice Hall.

Paltrinieri, E., Sandrone, F., & Zhao, J. (2016). Analysis and estimation of gripper TBM performances in highly fractured and faulted rocks. *Tunnelling and Underground Space Technology*, *52*, 44–61. https://doi.org/10.1016/J.TUST.2015.11.017

Pipes and Pipe Sizing | Spirax Sarco. (n.d.). Retrieved May 15, 2023, from https://www.spiraxsarco.com/learn-about-steam/steam-distribution/pipes-and-pipe-sizing

Qian, J., & Wang, J. (2006). World Oil Shale Retorting Technologies. *International Conference on Oil Shale* .

Ramsden, R., Branch, A., & Wilson, R. (2007). Factors influencing the choice of cooling and refrigeration systems for mines. *Journal of the Mine Ventilation Society of South Africa*, *60*, 92–98.

Rice, G. S. (1932). A Study of Methods Used in France and Germany and Possible Application to Depleted Oil Fields under America Conditions. In *Mining Petroleum by Underground Methods*. United States Goverment Printing Office.

Robbins, R. J. (1984). Future of mechanical excavation in underground mining. *Mining Engineering*, *36*(6), 617–627.

Rodríguez, R., & Lombardía, C. (2010). Analysis of methane emissions in a tunnel excavated through Carboniferous strata based on underground coal mining experience. *Tunnelling and Underground Space Technology*, *25*(4), 456–468. https://doi.org/10.1016/j.tust.2010.02.010

Rudenno, V. (2009). *The mining valuation handbook: mining and energy valuation for investor and mangment* (3rd ed.). Milton.

Sahin, S., Kalfa, U., Celebioglu, D., Duygu, E., & Lahna, H. (2012). *SPE 157865 A Quarter Century of Progress in the Application of CO 2 Immiscible EOR Project in Bati Raman Heavy Oil Field in Turkey*.

Sahin, S., Kalfa, U., Uysal, S., Kilic, H., & Lahna, H. (2014). *SPE-169035-MS Design, Implementation and Early Operating Results of Steam Injection Pilot in already CO 2 Flooded Deep-Heavy Oil Fractured Carbonate Reservoir of Bati Raman Field, Turkey*. http://onepetro.org/SPEIOR/proceedings-pdf/14IOR/All-14IOR/SPE-169035-MS/1517720/spe-169035-ms.pdf/1

Sanlav, M., Tolgay, M., & Genca, F. (1963, June 19). Geology, Geophysics, and Production History of the Garzan-Germik Field, Turkey. *6th World Petroleum Congress*. http://onepetro.org/WPCONGRESS/proceedings-pdf/WPC06/All-WPC06/WPC-10042/2078221/wpc-10042.pdf/1

Shafiee, S., & Topal, E. (2012). New approach for estimating total mining costs in surface coal mines. *Transactions of the Institutions of Mining and Metallurgy, Section A: Mining Technology*, *121*(3), 109–116. https://doi.org/10.1179/1743286312Y.0000000011

Sinanoğlu, D. (2021). Systematic and biostratigraphic evaluation of the Late Cretaceous benthic foraminiferal assemblages of southeastern Batman BULLETIN OF THE MINERAL RESEARCH AND EXPLORATION CONTENTS Research Articles. *Bull. Min. Res. Exp*, *165*, 267–293. https://doi.org/10.19111/bulletinofmre.809914

Smith, M. E., Parra, D., & Sac, A. (2014). Leach pad cost benchmarking. In *Proceedings of Heap Leach Solutions*.

Stacey, T. R., Ortiepp, W. D., & Kirsten, A. D. (1994). Energy-absorbing capacity of reinforced shotcrete, with reference to the containment of rockburst damage. *Journal of the Southern African Institute of Mining and Metallurgy*, *95*(3), 137–140. https://doi.org/https://doi.org/10.10520/AJA0038223X_2330

Stack, B. (1982). *Handbook of Mining and Tunneling Machinery*. J. Wiley.

Steingrimsson, J. H., Grøv, E., & Nilsen, B. (2002). The significance of mixed-face conditions for TBM performance. *World Tunneling*, *15*(9), 435–441.

Streeter, W. S., Hutchinson, T. S., Ameri, S., Wasson, J. A., & Aminian, K. (1991). Recovery of oil from underground drill sites. *Energy Sources*, *13*(4), 417–431. https://doi.org/10.1080/00908319108908999

Suorineni, F. T., Kaiser, P. K., & Henning, J. G. (2008). Safe rapid drifting – Support selection. *Tunnelling and Underground Space Technology*, *23*(6), 682–699. https://doi.org/10.1016/j.tust.2008.01.002

Tang, B. (2000). *Rockburst Control Using Destress Blasting*. McGill University.

Taylor, J. G., Taylor, R. N., & Hall, A. E. (1978). The introduction of a tunnel borer into a South African gold mine. *Journal of the South African Institute of Mining and Metallurgy*, 188–198.

TBM STAFF. (2017, May 31). *Tunnel Update – June 2017*. https://tunnelingonline.com/tunnel-updates-2/

Thakur, P. (2019). Origin of Gases in Coal Mines. *Advanced Mine Ventilation*, 213–226. https://doi.org/10.1016/B978-0-08-100457-9.00013-4

TMRG. (2020, October 17). *L&T Begins Assembling India's Largest TBM for Mumbai's Coastal Road - The Metro Rail Guy*. https://themetrorailguy.com/2020/10/17/lt-begins-assembling-indias-largest-tbm-for-mumbais-coastal-road/

Toraño, J., Torno, S., Menendez, M., Gent, M., & Velasco, J. (2009). Models of methane behaviour in auxiliary ventilation of underground coal mining. *International Journal of Coal Geology*, *80*(1), 35–43. https://doi.org/10.1016/J.COAL.2009.07.008

Tóth, Á., Gong, Q., & Zhao, J. (2013). Case studies of TBM tunneling performance in rock–soil interface mixed ground. *Tunnelling and Underground Space Technology*, *38*, 140–150. https://doi.org/10.1016/j.tust.2013.06.001

TPAO. (2022). *Annual Report (2021)*.

Tucker, H. S. G. (1968). The Thermal Conductivity of Rock. *J. Mine Vent. Soc. S. Afr.*, *21*(10), 179–181.

Turton, R., Bailie R. C., Whiting W. B., & Shaeiwitz J. A. (2009). Estimation of capital cost. In *Analysis, Synthesis, and Design of Chemical Processes* (3rd ed.). Pearson Education. https://edisciplinas.usp.br/pluginfile.php/5897970/mod_resource/content/1/Mat%20complementar.pdf

Van Der Walt, J., & Whillier, A. (1978). Considerations in the design of integrated systems for distributing refrigeration in deep mines. *Journal of the South African Institute of Mining and Metallurgy*, 109–124.

von Glehn, F. H., & Bluhm, S. J. (2000). Practical aspects of the ventilation of high-speed developing tunnels in hot working environments. *Journal of South African Institute of Mining and Metallurgy*, 445–448.

Vost, K. R. (1973). In Situ Measurements of the Surface Heat Transfer Coefficient in Underground Airways. *The Journal of South African Institute of Mining and Metallurgy*, *73*(8), 269–272.

White, S. B. (1978). The use of a tunnel boring machine on a coal mine decline. *Australian Tunnelling Conference, 3rd*, 66–70.

Yilmaz, O. (2023). Drilling and blasting designs for parallel hole cut and V-cut method in excavation of underground coal mine galleries. *Scientific Reports*, *13*(1), 2449. https://doi.org/10.1038/s41598-023-29803-6

Zakirov D. R., Fayzrakhmanov R. A., Mukhamedshin M. A., & Zakirov G. D. (2019). Problems and ways of improving thermal oil recovery efficiency in the Yarega field. *Gornyi Zhurnal*, *12*. https://doi.org/10.17580/gzh.2019.12.17

Zare, S., Bruland, A., & Rostami, J. (2016). Evaluating D&B and TBM tunnelling using NTNU prediction models. *Tunnelling and Underground Space Technology*, *59*, 55–64. https://doi.org/10.1016/j.tust.2016.06.012

Zhang, C., Feng, X., Zhou, H., Qiu, S., & Wu, W. (2012). A Top Pilot Tunnel Preconditioning Method for the Prevention of Extremely Intense Rockbursts in

Deep Tunnels Excavated by TBMs. *Rock Mechanics and Rock Engineering*, *45*(3), 289–309. https://doi.org/10.1007/s00603-011-0199-5

Zhao, J., Gong, Q. M., & Eisensten, Z. (2007). Tunnelling through a frequently changing and mixed ground: A case history in Singapore. *Tunnelling and Underground Space Technology*, *22*(4), 388–400. https://doi.org/10.1016/j.tust.2006.10.002

Zheng, Y. L., Zhang, Q. B., & Zhao, J. (2016). Challenges and opportunities of using tunnel boring machines in mining. *Tunnelling and Underground Space Technology*, *57*, 287–299. https://doi.org/10.1016/j.tust.2016.01.023

APPENDICES

A. Appendix I

Production Openings Diameter Selection

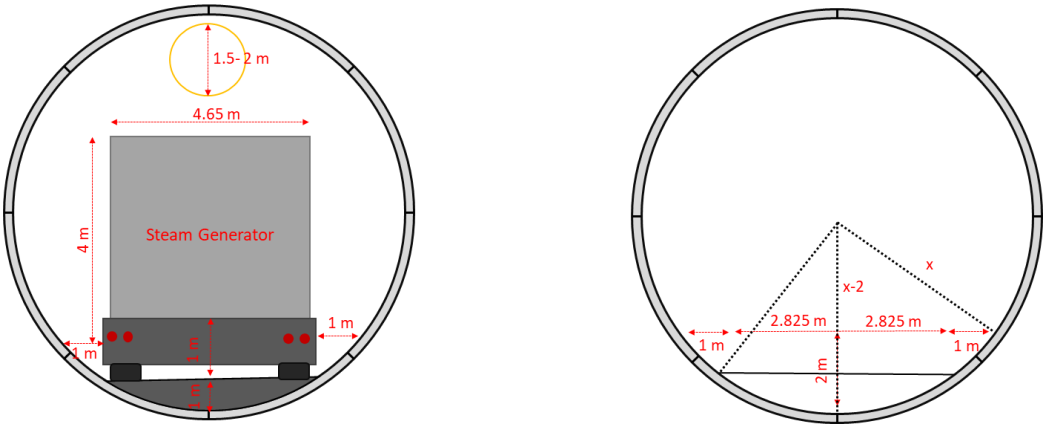

Figure APX I - 1 Radius calculation illustration

Where x is the radius of the inner circle

$$(x)^2 = (2.825 + 1)^2 + (x - 2)^2$$

$$x = 4.65\ meter$$

$$2x = 9.30\ meter$$

If the concrete supports and the TBM gripper are taken into account 10-meter diameter TBM will be sufficient.

Table APX I - 1 Borehole Efficiency, Recovery, and Tunneling Below the Eastern Part Reservoir Data

Sections Elevations (m)	Total Fan Shape Borehole Length (m)	Fan Shape Borehole Length in Reserve (m)	Borehole Efficiency (%)	Producible Reserve (m^3)	Produced Reserve (m^3)	Production Recovery (%)	Total Tunnel Surface Area (m^2)	Tunnel Surface Area in Clay (m^2)	Tunneling in Clay (%)
-496	737	528	71.66%	389,034,405	22,707,210	5.84%	1,383,913	1,086,674	78.52%
-506	1,775	1,434	80.78%	389,034,405	50,984,482	13.11%	1,383,913	837,236	60.50%
-516	3,681	3,114	84.60%	389,034,405	93,474,168	24.03%	1,383,913	588,572	42.53%
-526	6,108	5,190	84.96%	389,034,405	142,594,607	36.65%	1,383,913	468,771	33.87%
-536	9,061	7,531	83.11%	389,034,405	193,905,521	49.84%	1,383,913	460,275	33.26%
-546	12,222	9,863	80.71%	389,034,405	243,316,741	62.54%	1,383,913	519,274	37.52%
-556	15,595	12,046	77.25%	389,034,405	287,378,795	73.87%	1,383,913	634,114	45.82%
-566	18,909	13,627	72.07%	389,034,405	322,854,405	82.99%	1,383,913	807,396	58.34%
-576	21,981	14,528	66.09%	389,034,405	349,990,896	89.96%	1,383,913	1,006,743	72.75%
-586	24,464	14,416	58.93%	389,034,405	368,164,443	94.64%	1,383,913	1,158,495	83.71%
-596	26,390	13,345	50.57%	389,034,405	377,891,372	97.14%	1,383,913	1,281,220	92.58%
-606	27,621	11,414	41.32%	389,034,405	382,896,117	98.42%	1,383,913	1,340,333	96.85%
-616	28,908	9,445	32.67%	389,034,405	386,252,041	99.28%	1,383,913	1,365,323	98.66%

Table APX I - 2 Borehole Efficiency, Recovery, and Tunneling Below the Western Part Reservoir Data

Sections Elevations (m)	Total Fan Shape Borehole Length (m)	Fan Shape Borehole Length in Reserve (m)	Borehole Efficiency (%)	Producible Reserve (m^3)	Produced Reserve (m^3)	Production Recovery (%)	Total Tunnel Surface Area (m^2)	Tunnel Surface Area in Clay (m^2)	Tunneling in Clay (%)
-496	15,034	14,893	99.06%	1,501,721,108	377,269,136	25.12%	4,326,616	2,532,458	58.53%
-506	20,318	19,723	97.08%	1,501,721,108	486,173,038	32.37%	4,326,616	2,470,713	57.10%
-516	25,892	24,227	93.57%	1,501,721,108	597,449,491	39.78%	4,326,616	2,447,904	56.58%
-526	31,509	28,087	89.14%	1,501,721,108	709,442,560	47.24%	4,326,616	2,445,305	56.52%
-536	36,895	30,958	83.91%	1,501,721,108	820,218,624	54.62%	4,326,616	2,511,575	58.05%
-546	42,323	32,775	77.44%	1,501,721,108	927,499,988	61.76%	4,326,616	2,575,397	59.52%
-556	47,567	33,577	70.59%	1,501,721,108	1,035,146,06	68.93%	4,326,616	2,609,134	60.30%
-566	52,448	33,045	63.01%	1,501,721,108	1,135,692,14	75.63%	4,326,616	2,688,801	62.15%
-576	56,708	33,236	58.61%	1,501,721,108	1,219,833,41	81.23%	4,326,616	3,001,393	69.37%
-586	60,292	29,742	49.33%	1,501,721,108	1,286,397,67	85.66%	4,326,616	3,309,952	76.50%
-596	63,111	26,797	42.46%	1,501,721,108	1,331,145,08	88.64%	4,326,616	3,694,229	85.38%
-606	65,269	23,256	35.63%	1,501,721,108	1,356,794,63	90.35%	4,326,616	4,000,922	92.47%
-616	66,751	19,478	29.18%	1,501,721,108	1,369,597,80	91.20%	4,326,616	4,191,486	96.88%

Cycle Time Calculation for Cross-cut Distance Selection

For 250-meter distant cross-cuts haulage distance;

$$(number\ of\ cross-cut)x(62.5)+(28)+(number\ of\ section)x250$$

$$=7x62.5+28+6x250$$

$$=1965.5\ meters$$

For the path for 250-meter distant cross-cuts cycle time;

Average gradient for path = 0 % → 20 km/h for both empty and full travel speed

Path distance = 1965.5 meters → cycle distance = 3931 meters

Travel Time = 11.8 min → cycle time* = 15.13 min

*With 200 seconds of maneuvers, spot and dumping time

For 500-meter distant cross-cuts;

$$(number\ of\ cross-cut)x(62.5)+(28)+(number\ of\ section)x500$$

$$=7x62.5+28+3x500$$

$$=1965.5\ meters$$

For path for 500-meter distant cross-cuts cycle time;

Average gradient for path = 0 % → 20 km/h for both empty and full travel speed

Path distance = 1965.5 meters → cycle distance = 3931 meters

Travel Time = 11.8 min → cycle time* = 15.13 min

*With 200 seconds of maneuvers, spot and dumping time

For 1000-meter distant cross-cuts;

$$(number\ of\ cross-cut)x(62.5)+(528)+(number\ of\ section)x1000$$

$$=7x62.5+528+1x1000$$

$$=1965.5\ meters$$

For the path for 1000-meter distant cross-cuts cycle time;

Average gradient for path = 0 % → 20 km/h for both empty and full travel speed

Path distance = 1965.5 meters → cycle distance = 3931 meters

Travel Time = 11.8 min → cycle time* = 15.13 min

*With 200 seconds of maneuvers, spot and dumping time

The Required Number of Raise Borer Calculations

The average excavation rate of the pilot hole by raise borer: 1.54 m/h

The average borehole length (for vertical borehole): 53.15 m

The approximate drilling amount of a Raise borer to create fan-shaped boreholes:

$$53.15\ (m) + \frac{53.15}{\sin(80°)}\ x\ 2\ (m) + \frac{53.15}{\sin(70°)}\ x\ 2\ (m) = 274.2\ m$$

Daily advance rate: $1.54(\frac{m}{h})x\ 24(\frac{h}{d}) = 30.8(\frac{m}{d})$

Required day to drill a series of boreholes: $\frac{274.2\ (m)}{30.8\ (\frac{m}{d})} = 8.9 \sim 9\ days$

TBM advance in 9 days: 90 meters → 3 Fan-shaped boreholes can be created

Continuous Miner advance in 9 days: 67.5 meters→ 2 Fans-shaped boreholes can be created

For the production galleries opening by continuous 2 raises borer should work in order not to delay production operations. However, 2 raise borers for 10-meter diameter production galleries will be sufficient due to the waiting time to return TBM for the last production opening of the panel.

Production Scheduling Calculations

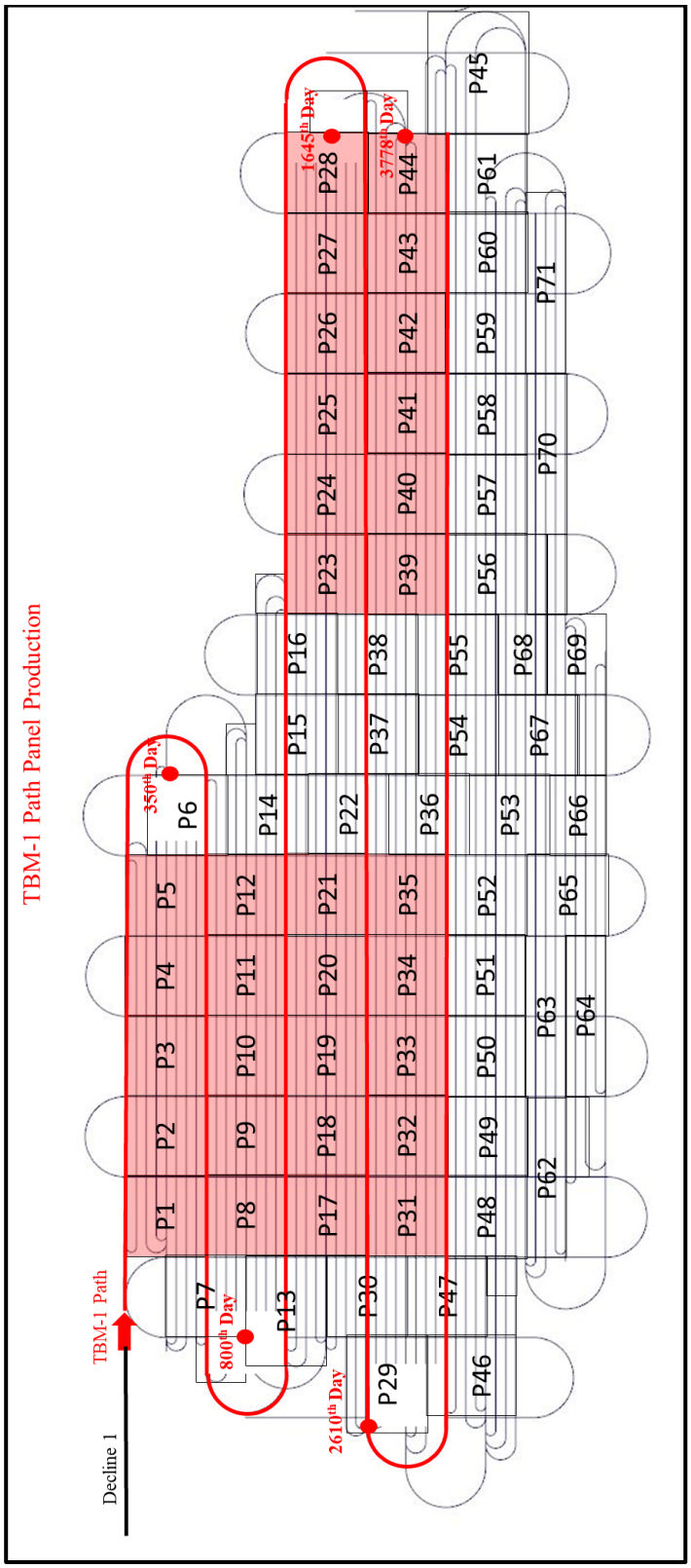

Figure APX I - 2 TBM-1 Path Panel Production Illustration

The day when the excavation is completed for each panel represented in Figure APX I – 2 are tabulated below.

Panel ID	The day excavation ends	Panel ID	The day excavation ends
P1	678.5	P24	2,035.5
P2	628.5	P25	1,985.5
P3	578.5	P26	1,935.5
P4	528.5	P27	1,885.5
P5	478.5	P28	1,835.5
P8	957.0	P31	2,814.0
P9	1,007.0	P32	2,864.0
P10	1,057.0	P33	2,914.0
P11	1,107.0	P34	2,964.0
P12	1,157.0	P35	3,014.0
P17	2,485.5	P39	3,214.0
P18	2,435.5	P40	3,264.0
P19	2,385.5	P41	3,314.0
P20	2,335.5	P42	3,364.0
P21	2,285.5	P43	3,414.0
P23	2,085.5	P44	3,464.0

Table APX I - 3 Panel Production with the day excavation ends

For the first-row panel calculations;

$$(the\ day\ excavation\ ends\ for\ the\ last\ panel)/(number\ of\ panel\ that\ excavated)$$

$$= 678.5/5$$

$$= 135.7\ days$$

For the second-row panel calculations;

$$(the\ day\ excavation\ ends\ for\ the\ last\ panel\ on\ the\ row)$$
$$/(number\ of\ panel\ that\ excavated)$$

$$= 1157/10$$

$$= 115.7\ days$$

For the third-row panel calculations;

$$(the\ day\ excavation\ ends\ for\ the\ last\ panel\ on\ the\ row) \\ /(number\ of\ panel\ that\ excavated)$$

$$= 1835.5/21$$

$$= 87.4\ days$$

For the fourth-row panel calculations;

$$(the\ day\ excavation\ ends\ for\ the\ last\ panel\ on\ the\ row) \\ /(number\ of\ panel\ that\ excavated)$$

$$= 3464.5/32$$

$$= 108.25\ days$$

On the other hand, for the production galleries that were excavated by the continuous miners, the day the excavation ends are illustrated in Figure APX I – 2 as a red dot. According to that calculation. 32nd panels excavation will end on the 3778th day. According to this, the average excavation time for panels will be calculated as follows:

$$(the\ day\ excavation\ ends\ for\ the\ last\ panel\ on\ the\ row) \\ /(number\ of\ panel\ that\ excavated)$$

$$= 3778/32$$

$$= 118.06\ days$$

The MAHOP Production Initiation Day Calculation;

$$\frac{(the\ average\ length\ of\ declines)}{(average\ advance\ rate\ of\ TBM)} + (the\ day\ to\ start\ production\ of\ panel\ P5)$$

$$= \frac{8500}{10} + 478.5$$

$$= 1328.5\ days = 3.6\ years$$

The Total Excavation Time Calculation;

$$\frac{(The\ time\ to\ excavate\ one\ panel)x(number\ of\ panels)}{(Number\ of\ simultaneous\ excavation)}$$

$$= \frac{118.06x88}{3}$$

$$= 3465\ days = 9.5\ years$$

The Mine Life Calculation;

$$Producible\ Panel\ Volume\ (m^3)$$
$$= (Length\ of\ the\ Panel)x(Width\ of\ the\ Panel\ )x(Average\ thickness\ of\ producible\ reservoir)$$

$$= 562.5x500x53.15$$

$$= 14{,}948{,}437.5\ m^3$$

$$Producible\ oil\ from\ Panel\ (m^3)$$
$$= (Producible\ Panel\ Volume)x(Porocity)x(Percentage\ of\ Oil\ in\ Pore\ )x(MAHOP\ Recovery)$$

$$= 14{,}948{,}437.5x0.2x0.75x0.8$$

$$= 1{,}793{,}813\ m^3 = 11{,}281{,}840\ barrels$$

$$Total\ Recoverable\ oil\ from\ Bati\ Raman\ Reservoir\ (m^3)$$
$$= (Producible\ oil\ from\ a\ Panel)x(number\ of\ Panels)$$

$$= 11{,}281{,}840x88$$

$$= 981{,}520{,}047\ barrels$$

$$Aproximate\ Production\ Life\ of\ Bati\ Raman\ with\ MAHOP\ (m^3)$$
$$= \frac{(Total\ Recoverable\ oil\ From\ Bati\ Raman)}{(Required\ Daily\ Production) * 360}$$
$$+ (The\ Time\ to\ reach\ required\ daily\ production)$$

$$= \frac{981{,}520{,}074}{250{,}000x360} + 1.4$$

$$= 12.3\ years$$

$$Mine\ Life\ of\ Bati\ Raman\ (years)$$
$$= (Aproximate\ Production\ Life\ of\ Bati\ Raman\ with\ MAHOP$$
$$+ (MAHOP\ production\ initiantin\ time)$$

$$= 12.3 + 3.6$$

$$= 15.9\ years$$

B. Appendix II

The Fresh Air Requirement Calculations

Decline Ventilation;

- Breathing

20 personnel are expected to be working there with moderate activity. Oxygen consumption and Carbon dioxide production of a moderately working person are 1.96 l/min/man and 1.764 l/min/man, respectively. The lowest oxygen concentration in the air is taken as 20 % and the threshold limit value of carbon dioxide is 0.5%.

Oxygen Consumption:

$$(0.21)Q_{intake} - (1.96x20) = (0.2)Q_{intake}$$

$$Q_{intake} = 3920\ lt/\min = 0.065\ m^3/s$$

Carbon dioxide Production:

$$(0.0003)Q_{intake} + (1.764x20) = (0.005)Q_{intake}$$

$$Q_{intake} = 7506\ lt/\min = 0.1251\ m^3/s$$

- Dust Dilution

According to Liu et al. (2019), the required air to dilute the 6.35-diameter TBMs excavation is 28 m^3/s. From this study, the required air for a 10-meter diameter TBM excavation is estimated by taking directly proportional to the excavation cross-section.

The cross-section area for a 6.35-meter diameter TBM is:

$$= 6.35^2 x\ \pi\ x0.25$$

$$31.67\ m^2$$

The cross-section area for a 10-meter diameter TBM is:

$$= 10^2 x\ \pi\ x0.25$$

$$84.13\ m^2$$

$$\frac{84.13}{31.67}\ x\ 28 = 74.38\ m^3/s$$

Panel Ventilation Calculations;

- Breathing

Oxygen Consumption:

$$(0.21)Q_{intake} - (1.96x137) = (0.2)Q_{intake}$$

$$Q_{intake} = 2{,}700\ lt/\min = 0.45\ m^3/s$$

Carbon dioxide Production:

$$(0.0003)Q_{intake} + (1.764x137) = (0.005)Q_{intake}$$

$$Q_{intake} = 52{,}200\ lt/\min = 0.87\ m^3/s$$

- Dust Dilution

The cross-section area for a 6.35-meter diameter TBM is:

$$= 6.35^2 x\ \pi\ x0.25$$

$$31.67\ m^2$$

The cross-section area for an almost 4x4 Continuous Miner is:

$$15.97\ m^2$$

$$\frac{15.97}{31.67}\ x\ 28 = 15\ m^3/s$$

- Methane Dilution

  The methane spreading from the excavation openings is taken as 40 l/s which is equal to 2.4 m^3/s. The maximum allowable concentration for methane is 1%

$$Q_{intake} = 2.4\frac{(1-0.01)}{(0.01-0.001)}$$

$$Q_{intake} = 24\ m^3/s$$

$$(Total\ number\ of\ excavation)\ x\ 24m^3/s = 216\ m^3/s$$

- Diesel Engine fresh air requirement

  As the table states in Chapter 4, the required air for the diesel engines in P7 is 185.56 m^3/s. To explain the calculations done a single equipment fresh air requirement is stated below:

  6 Raise borer with 155 kW will be used in the panel. The availability of this equipment is assumed to be 0.6.

$$6\ x\ 155x0.6 = 558\ kW$$

$$\frac{558\ kW\ x\ 7}{100} = 39.06\ m^3/s$$

Additionally, a contingency coefficient which is 20% is multiplied by the overall power consumption and added to the total fresh air requirement.

- CO_2 dilution

In-place CO_2 0.8 bscf → 22,656,000 m^3

The pore volume of Bati Raman: $(volume\ of\ Bati\ Raman)\ x\ (porosity)$

$$= 1{,}927{,}352{,}112\ x\ 0.2 = \ 385{,}470{,}422\ m^3$$

CO_2 concentration: $\frac{22{,}656{,}000}{385{,}470{,}422} = 0.059\ \rightarrow 6\%$

Carbon Dioxide emission for TBM

$$S\ (specific\ emission) = \frac{5.9}{100} x \frac{75x3600x24}{785.4} = 486.78$$

$$q(P) = PxS = 785.4\ x\ 486.78 = 382{,}320\frac{m^3}{day} \rightarrow 4.43\ \frac{m^3}{s}$$

To dilute CO_2:

$$Q_{intake} = 4.425\frac{(1-0.5)}{(0.5-0.0003)}$$

$$Q_{intake} = 4.43\ m^3/s$$

Carbon Dioxide emission for Continuous Miner

$$S\ (specific\ emission) = \frac{5.9}{100} x \frac{25x3600x24}{120} = 1062$$

$$q(P) = PxS = 120\ x\ 1062 = 127{,}440\frac{m^3}{day} \rightarrow 1.475\ \frac{m^3}{s}$$

To dilute CO_2:

$$Q_{intake} = 1.475\frac{(1-0.5)}{(0.5-0.0003)}$$

$$Q_{intake} = 1.476\ m^3/s$$

Total required fresh air to dilute CO_2: $4.43\ x\ 3 + 1.476\ x\ 6 = 22.14\ m^3/s$

Heat Transfer Calculations

TBM and Continuous Miner's Heat Calculations;

The heat created from the 2000kW TBM is 1040 kW.

The heat created from the 8000 kW 10-meter diameter TBM is:

$$\frac{8000}{2000}\ x\ 1040 = 4160\ kW$$

The heat created from the 800 kW Continuous Miner is:

$$\frac{800}{2000}\ x\ 1040 = 416\ kW$$

Steam Generator's Heat Calculations;

The power requirement of a 20 tph steam generator: 13963 kW

The efficiency of the steam generator: 90%

$$0.1\ x\ 13963 = 1396{,}3\ kW$$

Broken Material's Heat Calculations;

Unit weight of Limestone: 2.75 tonnes/m^3

Specific Heat of Limestone: 1,03 kJ/kg·K

The temperature of the broken rock right after fragmentation: 65.5 ^oC

The temperature of the broken rock at the surface: 40 ^oC

Daily advance rate of TBM: 10 m/day

Cross-sectional Area of openings: 78,54 m^2

Hourly production rate:

$$10\ (\frac{m}{day})/\ 24\ \left(\frac{hr}{day}\right)$$

$$0.4167\ m/hr$$

$$0.4167\ x\ 78.54 = 32.73\ \ m^3/hr$$

$$32.73\ \frac{m^3}{hr}\ x\ 2.75\ \frac{tonnes}{m^3}\ = 90\frac{tonnes}{hr} = 25\frac{kg}{s}$$

$$mC(\theta_1 - \theta_2) = 25x1.03x(65.5 - 40)$$

$$656.6\ kW$$

Steam piping's Heat Calculations;

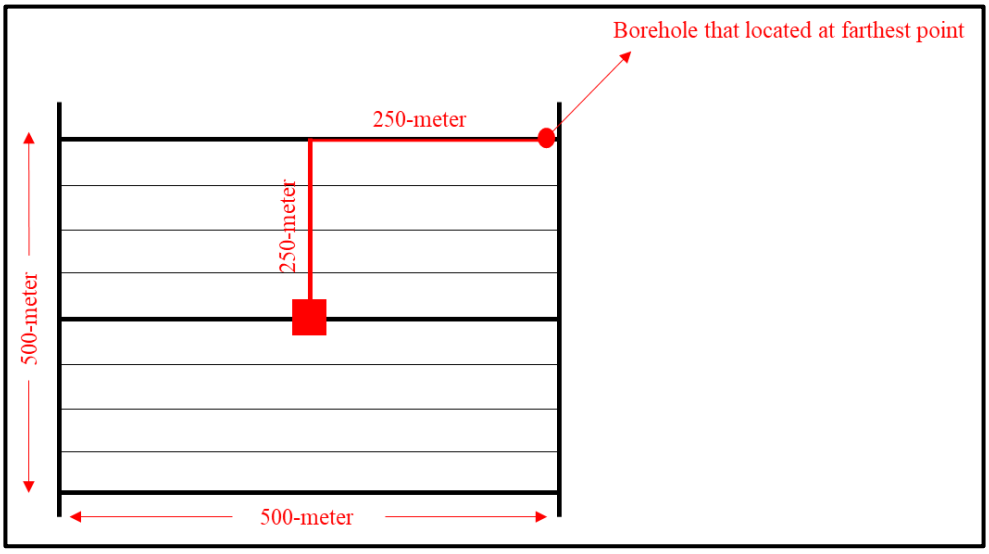

Figure APX II - 1 Illustration of Travel Distance of Steam

According to the farthest borehole that steam will be traveled, the piping length will be approximately 500 meters. Additionally, the number of boreholes that pumps steam to the reservoir, in a panel system is 90, and hourly steam production from the steam generator is 20,000 kg/hr. İf steam created from the steam generator is uniformly distributed to these 90 boreholes, each borehole will reach 222,22 kg/hr. For the systems investigated in this case, 10 boreholes will pump 2222,22 kg/hr steam to the reservoir.

As stated in Chapter 4, 10 m/s velocity will be used for the steam's traveling speed. According to the steam velocity function from the Spiral Sarco company (*Pipes and Pipe Sizing | Spirax Sarco*, n.d.):

$$Steam\ Velocity$$

$$= \frac{steam\ flowrate\ \left(\frac{kg}{h}\right) x\ v_g \left(\frac{m^3}{kg}\right) x\ 4}{3600\ \left(\frac{s}{h}\right) x\ \pi\ x\ D^2(m^2)}\ (\frac{m}{s}) \qquad (16)$$

$$10 = \frac{2222.22 \left(\frac{kg}{h}\right) x\ 0.34759 \left(\frac{m^3}{kg}\right) x\ 4}{3600\ \left(\frac{s}{h}\right) x\ \pi\ x\ D^2(m^2)}\ (\frac{m}{s})$$

$$= 0.058425756\ m = 5.84\ cm$$

From the table (*Dimension and Weights per Metre for Iso 2448*, n.d.), the thickness of the cylindrical wall is taken as 0.045 m. Then heat transfer from the steam piping is calculated by using equation 15 as 555.43 kW.

$$Q = kA(\frac{\Delta T}{\Delta r}) \qquad (17)$$

C. Appendix III

Equipment Selection for Capital Cost Estimation

The Number of Truck Calculations for TBMs;

The hourly excavation of TBMs in place (m^3/h): $10\frac{m}{day} \div 24\frac{hr}{day}\ x\ 5^2 x\ \pi$

$$= 32.72\ m^3/h$$

Swell factor: 1.6

The volume of excavated material to be hauled: $32.75\ m^3/h\ x\ 1.6 = 52.35\ m^3/h$

To calculate the required number of underground trucks for TBMs a travel length for cycle time estimation is required. To represent the worst case, the travel length for both empty and full is taken as 7900 meters.

The Tramming speed of the truck (full and empty): 5,56 m/s

Haulage time: 7900 /5.6 = 1420.86 sec

Maneuver time: 60 sec

Spotting time: 60 sec

Filling time: $53.35\ m^3/h \div 23\ m^3(Truck\ Capacity) = 0.44\ hr = 1581.6\ sec$

Cycle Time: $60\ \text{sec} + 60\ \text{sec} + 1420.86\ sec + 1581.6\ \text{sec} = 3122.52\ sec$

Truck output: $\frac{3600x23x0.8}{3122.52} = 21{,}21\ m^3/h$

The required number of trucks for one TBM: $\frac{52.35}{21.21} = 2.46\ \rightarrow \mathbf{3\ trucks}$

The Number of Truck Calculations for Continuous Miners;

A similar approach will be used to calculate the required number of trucks for a single continuous miner.

The hourly excavation of continuous miners in place (m^3/h):

$$7.5\frac{m}{day} \div 24\frac{hr}{day}\ x\ 16x$$

$$= 5\ m^3/h$$

The volume of excavated material to be hauled: $5\ m^3/h\ x\ 1.6 = 8\ m^3/h$

The travel length (empty and full): 7780 meters

The Tramming speed of the truck (full and empty): 5,56 m/s

Haulage time: 7780 /5.6 = 1400 sec

Maneuver time: 60 sec

Spotting time: 60 sec

Filling time: $8\ m^3/h \div 23\ m^3(Truck\ Capacity) = 2.8\ hr = 10080\ sec$

Cycle Time: $60\ \text{sec} + 60\ \text{sec} + 1400\ sec + 10080\ \text{sec} = 11600\ sec$

Truck output: $\frac{3600x23x0.8}{11600} = 5.71\ m^3/h$

The required number of trucks for one Continuous Miner: $\frac{8}{5.71} = 1.4\ \rightarrow \mathbf{2\ trucks}$

<u>For the whole operation:</u>

$$3\ trucks/TBM\ x\ 9\ TBMs = 27\ trucks$$

$$2\ trucks/Continuous\ miner\ x\ 18\ Continous\ Miner = 36\ trucks$$

$$Total: 36 + 27 = 63\ truck + 10\ spare$$

$$= \mathbf{73\ Trucks}$$

These calculations are based on the electrical truck produced by Epiroc (2020).

Conveyor Belt Capacity Calculation;

From single decline:

TBM Excavations → 32.72 m^3/h x 3 = 98.16 m^3/h

Continuous Miner Excavations → 5 m^3/h x 6 = 30 m^3/h

Total Excavations → 98.16 + 30 ~ 108 m^3/h

The Number of Truck Calculations for Surface Operations;

Hourly excavated material reaches the surface: 3 x 108 = 312 m^3/h

Cycle time of shovel: 35 sec

$$C_d(Dipper\ Capacity) = \frac{312x35x1.6}{3600x1x0.8x0.9x1.3} = 5.18\ m^3$$

The approximate distance of the surface facility to declines: 12 km

Tramming speed: 50 km/s → 13.8 m/s

Travel time: $24000\ m\ /13.88\ m/s\ \rightarrow 1728\ sec$

Maneuver time: 60 sec

Dumping time: 60 sec

Loading time: 6 (number of dippers) x 35 (shovel cycle time) = 210 sec

Cycle time: $60\ \text{sec} + 60\ \text{sec} + 210\ sec + 1728\ \text{sec} = 2058\ sec$

Truck output: $\frac{3600x30x0.8}{2058} = 35\ m^3/h$

The required number of trucks for surface operations: $\frac{312}{35}$

$$= 8.9\ \rightarrow 9 + 1\ spare = \mathbf{10}\ \boldsymbol{trucks}$$

For the whole surface operation:

The haulage operations will be started from 3 different locations (declines) therefore 3 shovels will be required.

$$10\ trucks/shovel\ x\ 3\ shovel = \mathbf{30\ trucks}$$

Pump Calculations:

Pumps that are going to be used in the Bati Raman Reservoir can be categorized by the fluid which will be pumped to the surface. The expected categories are oil, water drainage, water for steam generators, concrete for shotcrete works, fuels, and refrigerant pumps.

Oil Pumps:

The expected average production from one panel daily: 50,000 barrels = 7950 m^3/day

The hourly production from one panel: 331.25 m^3/h

In the western part, two consecutive panels are expected to work simultaneously in the southern and northern parts of the reservoir. Therefore, the hourly production for the one working site is calculated as 662.5 m^3/day. To compensate for the hourly production from three different working areas, an example heavy-duty oil pump from Ruhrpumpen is selected for an approximately 1500-meter head with a high efficiency is selected. In addition, due to the distance between the working areas, 3 pumps will be working in the area simultaneously.

Water Pumps for Steam Generators:

The water requirement for 20,000 kg/h steam generators is approximately 29250 l/hr according to the ICI Caldaie catalog (*ICI Caldaie GX12 Bar Industrial Steam Generator Catalogue*, n.d.).

While selecting the pumps for the steam generator water requirement, the worst case where there is no groundwater coming from the strata to be used is selected. According to the worst case, most of the water will be pumped from the surface until the water production from the MAHOP production starts. When the water travel path

is considered, most of the pumps are required to pump water at the production level (horizontally). Hence, 3-series connected 10 m^3/h capacity pumps for each steam generator with a total of 15 pumps are expected to be sufficient.

Groundwater Drainage Pumps:

In this case, the groundwater condition of Bati Raman Reservoir is unknown, but 4-series connected 1000 gpm (227 m^3/h) 1200 ft head for 3 working areas is expected to be sufficient for most of the cases.

Fuel Pumps:

Most of the fuel consumption of MAHOP will be required by the steam generators. The fuel needed for a single 20,000 kg/h steam generator is 1802.9 l/h, but while selecting the pumps for fuel 2000 l/h capacity pumps are considered to be on the safe side. Similar to the water pumps for steam generators, fuel that comes from the surface, will be required to be pumped after it reaches the production level. Thus, the pumps that have at least 250 meters of distance capacity been selected for each steam generator.

Refrigerant Pumps:

The refrigerant that is going to be used for cooling pockets is needed to be pumped from the surface. The location where the refrigerants reach the production levels will be close to the ventilation raises. Due to the horizontal distance that refrigerants to be pumped is expected to be small, the number of pumps that are going to be used for the heat exchanger is restricted by two for each cooling pocket. Based on this assumption, the required number of pumps for 38 cooling pockets is estimated as 76.

Waste Dump Calculations:

The waste dump for the MAHOP implementation on Bati Raman Reservoir is anticipated to be similar to the leach pads that are used for the heap leach operation in mostly gold mines. Although, the excavated material which is processed will have a small portion of oil in it. Therefore, dumping the processed material directly into

the ground will violate some environmental considerations and laws, the specific dumping site similar to the leaching pad is designed. While estimating the capacity of the dumping site, backfilling operations can take place underground where the production ended is considered. According to the first two years of excavation, the required volume is calculated as 6,739,200 m^3 after the compaction in the dump site.

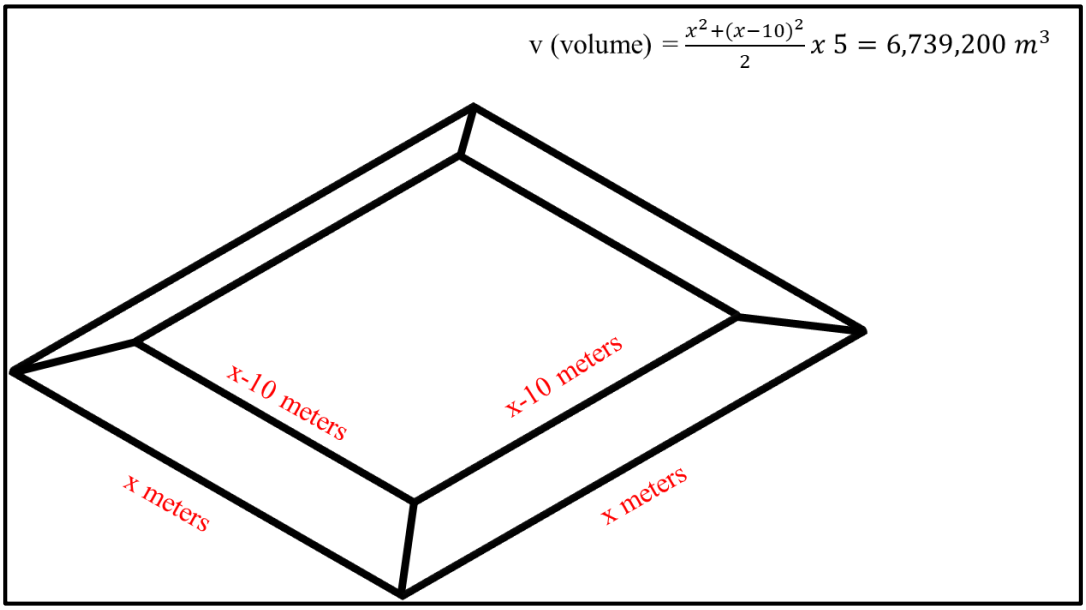

Figure APX III - 1 Representative Square Dump Site

From the above calculation, 372 meters long square dump site with 138,511.7 m^2 base area is required. According to Smith et al. (2014), the meter squire cost of a leach pad in 2014 in Türkiye is around 28.41 $. With an average yearly interest rate of 2.74%, today's cost is expected to be around 36.08 $/$m^2$. From this assumption, the waste dump cost that is going to be added to the mine development cost is calculated as 4,997,502.72 $.

TBM Capital Cost Estimation:

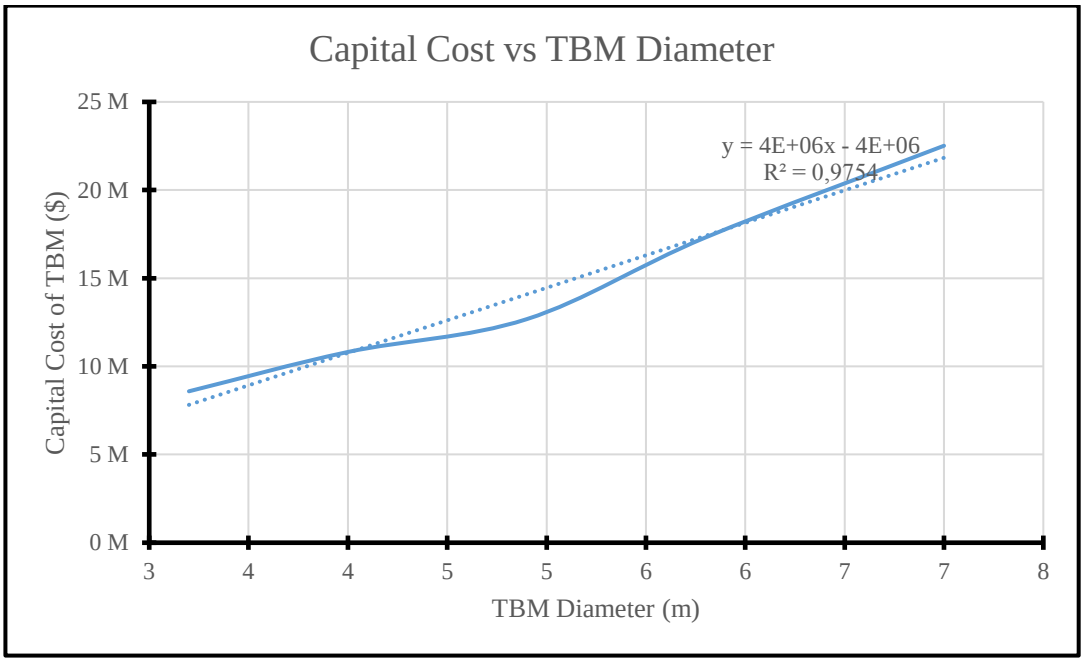

Figure APX III - 2 Capital Cost vs TBMs Diameter Graph

Based on the linear regression that shows a relation between the TBM diameter and capital cost is depicted above. According to the regression model with an R^2 value of 97.54%, the capital cost of TBM changes with this equation stated below.

$$y = 4x10^6\boldsymbol{x} - 4x10^6$$

Where x is the diameter of TBM and y is the capital cost of TBM.

For 10-meter diameter TBM: $4x10^7 - 4x10^6 = 36{,}000{,}000\ \$$

Operational Cost Estimation Calculations:

Steam Generator Diesel Consumption:

The hourly diesel consumption of the 20,000 kg/h steam generator: 1307.1 kg/h

The diesel unit weight: 0.7-0.75 kg/l

$$1307.1/0.725 = 1802.9\ l/h$$

$$24\ hr/day\ x365\ day/year\ x0.9(availability)x\ 1802.9\ l/h$$
$$= 14{,}214{,}036.41\ l/year$$

The unit cost of Diesel in Türkiye: 1.1 $/l

$$= 14{,}214{,}036.41\ l/year\ x\ 1.1\ \$/l = 15{,}618{,}614.37\ \$/year$$
$$\rightarrow for\ one\ steam\ generator$$

$$= 15{,}618{,}614.37\ \$/year\ x\ 5 = \mathbf{78{,}093{,}071.83}\ \$/year \rightarrow for\ total\ mine$$

Surface Processing Cost:

Oil Shale Retorting unit operational cost: 10-20$/tonne

The average excavation volume in the reservoir:

$$9{,}132{,}495.9\ m3/year\ \rightarrow\ 21{,}917{,}990.16\ tonnes/year$$

$$21{,}917{,}990.16\ \text{tonnes/year}\ x\ 15\ \$/tonne = \mathbf{328{,}769{,}852.4}\ \$/year$$

Water Treatment Cost:

Water Treatment Cost = $ 3 / barrel of oil

The average yearly production: 62,050,118 barrels/year

$$62{,}050{,}118\ \frac{barrels}{yearx}\ 3\ \$/barrel = \mathbf{186{,}150{,}354}\ ^{\$}/_{years}$$